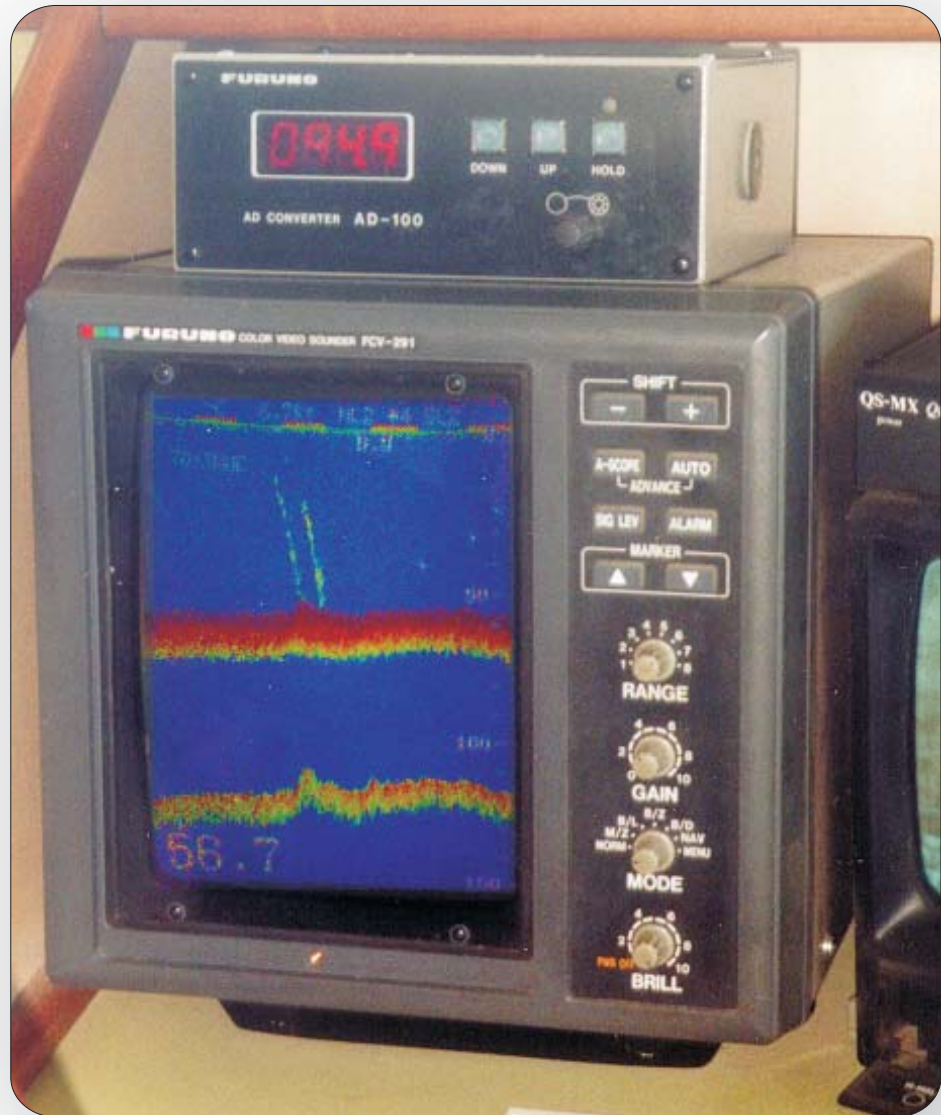


Technical report produced for  
Strategic Environmental Assessment - SEA6

## Gas-Related Seabed Structures in the Western Irish Sea (IRL-SEA6)



by P.F. Croker, M. Kozachenko & A.J. Wheeler

Technical report produced for  
Strategic Environmental Assessment – SEA6

## Gas-Related Seabed Structures in the Western Irish Sea (IRL-SEA6)

by P.F. Croker<sup>1</sup>, M. Kozachenko<sup>2</sup> & A.J. Wheeler<sup>3</sup>

<sup>1</sup> Petroleum Affairs Division, Department of Communications, Marine and  
Natural Resources, Dublin, Ireland

<sup>2</sup> Coastal & Marine Resources Centre, University College Cork, Cork, Ireland

<sup>3</sup> Department of Geology, University College Cork, Cork, Ireland

January 2005

This document was produced as part of the UK Department of Trade and Industry's offshore energy Strategic Environmental Assessment programme. The SEA programme is funded and managed by the DTI and coordinated on their behalf by Geotek Ltd and Hartley Anderson Ltd.

Crown Copyright, all rights reserved

## **Table of contents**

<b>1. Introduction</b>	3
1.1 Study aims and general introduction	3
1.2 Seabed and sub-seabed evidence for shallow gas	5
1.2.1 <i>Definition and types of shallow gas</i>	5
1.2.2 <i>Shallow gas accumulation and its evidence</i>	7
1.2.3 <i>Gas-related seabed structures</i>	8
1.2.4 <i>Identification of gas seepage</i>	12
1.3 Setting of IRL-SEA6	14
1.3.1 <i>Geographical setting</i>	14
1.3.2 <i>Geological setting</i>	14
1.3.3 <i>Hydrodynamic conditions and sediment transport</i>	16
<b>2. Materials and Methodology</b>	19
2.1 Data overview	19
2.2 Seismic data 1965-2004	19
2.3 Exploration wells 1977-2004	21
2.4 Route survey data 1986-2004	21
2.5 Overview of research cruises 1995-2002	23
2.5.1 <i>RV Lough Beltra cruise 1995</i>	25
2.5.2 <i>RV Lough Beltra cruise 1996</i>	26
2.5.3 <i>RV Lough Beltra cruise 1997</i>	27
2.5.4 <i>RV Celtic Voyager cruise 1998</i>	29
2.5.5 <i>RV Celtic Voyager cruise 1999</i>	30
2.5.6 <i>RV Celtic Voyager cruise 2000</i>	32
2.5.7 <i>RV Celtic Voyager cruise 2001</i>	32
2.5.8 <i>RV Celtic Voyager cruise 2002</i>	33
2.6 GIS approach to data visualisation	34
<b>3. Distribution of Methane Sources</b>	35
3.1 Source rocks	35
3.1.1 <i>General distribution of methane sources</i>	35
3.1.2 <i>Exploration well data</i>	35
3.1.2.1 <i>Kish Bank Basin</i>	37
3.1.2.2 <i>Central Irish Sea Basin</i>	39
3.1.2.3 <i>Conclusions</i>	40
3.1.3 <i>Evidence from seismic data</i>	40
3.2 Gas-bearing sediments	46
<b>4. Gas Migration Pathways</b>	48
4.1 Major faults	48
4.2 Faults observed on conventional seismic data	50
4.3 Multidisciplinary mapping of the Codling Fault	57
4.3.1 <i>General setting</i>	57
4.3.2 <i>Multibeam mapping</i>	61
<b>5. Shallow Gas Accumulations</b>	67

<b>6. Gas Escape Structures and their Distribution</b>	79
6.1 Pockmarks	79
6.2 Seabed doming	79
6.3 Mounds	79
6.4 Mud diapirs	82
6.5 Trenches	82
6.6 Abnormal sand waves	89
6.7 Summary of distribution of gas accumulations and gas escape structures.	93
<b>7. Evidence of Gas Seepage</b>	95
7.1 Acoustic evidence	96
7.2 Ground-truthing evidence	98
7.2.1 <i>Methane-derived Authigenic Carbonate (MDAC)</i>	98
7.2.1.1 <i>Video evidence</i>	99
7.2.1.2 <i>Seabed sample data</i>	99
7.2.1.3 <i>Evidence from fishermen</i>	99
7.2.2 <i>Unusual benthic biology</i>	102
7.3 Evidence from aerial video survey	103
<b>8. Discussion and Conclusions</b>	109
<b>9. Recommendations for Further Work</b>	113
<b>10. References</b>	116

## **1. Introduction**

### **1.1 Study aims and general introduction**

The aim of this report is to present an up-to-date overview of all relevant data concerning methane-derived authigenic carbonate and features associated with shallow gas and seabed fluid flow in the Irish sector of the western Irish Sea (Fig. 1.1). It presents a detailed assessment of potential gas sources and migration pathways, shallow gas, gas-related seabed structures and evidence of present day gas seepage in the study area. In doing so, this report mainly analyses datasets held by the Petroleum Affairs Division (PAD) of the Irish Department of Communications, Marine and Natural Resources. It also makes use of some previously published data.

Using a GIS-based data integration approach this study produces a number of thematic and interpretative maps, including maps showing the:

- distribution of potential methane source rocks;
- distribution of sediment types;
- distribution of potential gas migration pathways;
- distribution of sub-surface gas accumulations;
- distribution of evidence for gas seepage

In addition, this report presents a comprehensive overview of all relevant data held by the PAD for the western Irish Sea collected from 1965 to present, illustrated in a number of maps and summarised in tables.

A number of data examples are also presented to visually illustrate gas-related seabed structures, sub-seabed gas accumulations and migration pathways. The latter includes images collected by seismic, acoustic and video surveying techniques.

The study area dealt with in this report is referred to below as the IRL-SEA6 area and includes all of the Irish Sea that falls within Irish Jurisdiction. The report is intended to complement a similar study of UK waters in the Irish Sea being undertaken as part of the

UK Government's Strategic Environmental Assessment (SEA6) (Judd, 2005). The primary purpose of these studies is to evaluate the distribution and extent of methane-derived authigenic carbonate ('submarine structures formed by leaking gas') which has been identified by the European Commission's '*Habitats Directive*' (Directive 92/43/EEC; see European Commission, 1997) as a habitat worthy of protection.

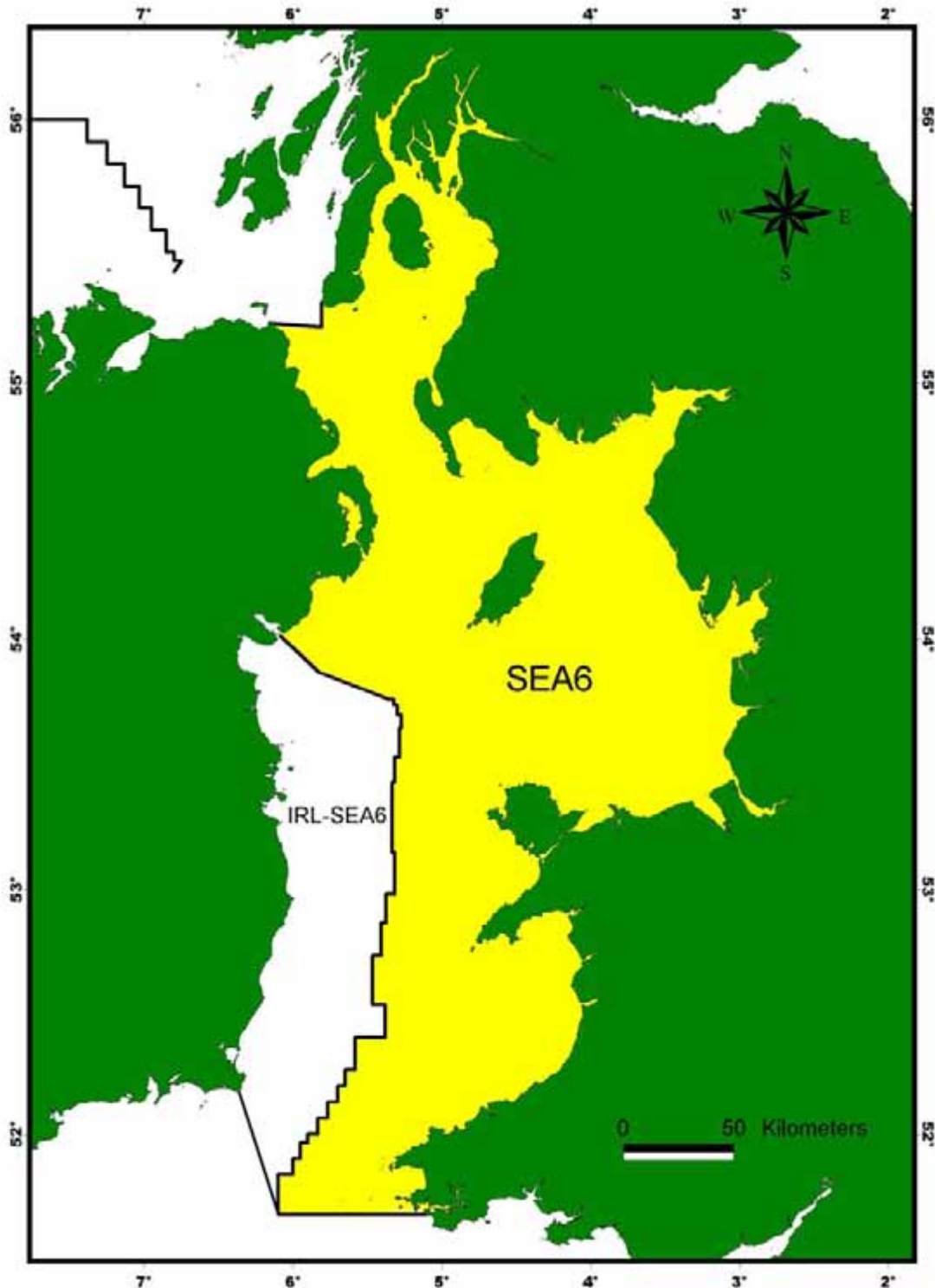


**Figure 1.1:** Location map of SEA6 and IRL-SEA6 areas.

## **1.2 Seabed and sub-seabed evidence for shallow gas**

This section presents a concise overview of state-of-the-art knowledge related to the subject of shallow gas in marine sediments. This is performed in order to introduce the reader to the main subject of this report, and therefore provide a foundation for a comprehensive understanding of the following chapters.

### ***1.2.1 Definition and types of shallow gas***

Existing literature predominantly defines shallow gas as gas that is present within shallow marine sedimentary sequences down to 1000m below seabed (e.g. Davis, 1992). Using various surveying techniques it is possible to identify sub-seabed gas accumulations, gas escape structures and active seeps.

Shallow gas in offshore settings is dominated by methane (CH<sub>4</sub>) that is mainly of microbial or thermogenic origin (Floodgate & Judd, 1992). The gas is produced via recycling of organic material by microbial degradation in the case of microbial methane (sometimes referred to as biogenic gas), or under the influence of temperature and pressure at depth (thermal degradation) in the case of thermogenic methane. Thus, in the case of microbial gas, gas is produced within the shallow sedimentary sequence, whilst in the case of thermogenic gas, the gas is delivered to the shallow sediments from deeper sources via migration pathways (usually following faults or unconformities) or diffusion. Microbial production of methane can take place down to a few hundred meters below seafloor, although more commonly it occurs within a few meters of the seabed. Thermogenic methane-generating processes normally occur at depths greater than 1000m below the seafloor. The distinction between microbial and thermogenic methane can be performed on the basis of the following parameters (Schoell, 1980; Faber & Stahl, 1984; Floodgate & Judd, 1992; Whiticar, 1999):

- a) Methane to higher hydrocarbons ratio expressed by the formula:

$$C_{2+} = [1 - (C_1 / \sum C_{1-5})] \times 100;$$

where  $C_{2+}$  is the ratio of methane ( $C_1$ ) to higher hydrocarbon gases ( $C_{1-5}$  ethane, propane, butane, pentane);

for microbial gas  $C_{2+} < 0.05\%$ , for dry gas (thermogenic)  $C_{2+} < 5\%$ , and for wet gas (thermogenic)  $C_{2+} > 5\%$ .

b) Carbon stable isotope ratio:

for thermogenic methane  $\delta^{13}C$  (PDB<sup>1</sup>) is between  $-60$  and  $-20\%$ ;

for microbial methane  $\delta^{13}C$  (PDB) is between  $-60$  and  $-80\%$ .

However, during migration thermogenic gas may be subjected to microbial activity, affecting the isotopic signature, which progressively becomes closer to that of a microbial methane; the signature of the true origin thus might be unclear. Also, in some cases, methane in marine sediments might be of a mixed microbial-thermogenic origin.

c) Hydrogen stable isotope ratio:

hydrogen isotope abundances ( $\delta D^2$ ) are indicative of maturity and origin. Carbon and hydrogen isotope ratios together show distinctions between methane origins (thermogenic and microbial).

Moreover, deep seabed structures underlying the gas escape features (observed on seismic data) might aid the interpretation of the origin of the shallow gas. For instance, if seepage occurs in an area of seabed underlain by potential source rocks and contains pathways suitable for gas migration (e.g. faults), then at a given location gas with microbial gas signatures may more likely to be of thermogenic origin. However, the unambiguous definition of the origin of shallow gas in reality is normally complicated due to the mixture of gases of different origins.

---

<sup>1</sup> PDB: relative to the Pee Dee Belemnite, a recognised international standard.

<sup>2</sup> Quoted as ‰ relative to the SMOW (Standard Mean Ocean Water) standard.

### ***1.2.2 Shallow gas accumulation and its evidence***

The subsurface accumulation of shallow gas may only occur if the seabed or one of the sub-seabed sedimentary layers is relatively impermeable. Otherwise, gas will constantly flow through the seabed into the water column and probably never reach concentrations sufficient to form noticeable gas accumulations.

Over the years, geophysical exploration has established that sub-surface accumulations of shallow gas may be identified via distinctive signatures observed on seismic data. This is due to the fact that even a small quantity of gas bubbles within marine sediments (~0.1% of sediment volume) can influence the speed of sound, reducing it by as much as one third in comparison to the speed of sound in gas-free sediments (Schubel, 1974). Typical evidence for shallow gas accumulations, reviewed by Judd & Hovland (1992), is summarised below:

1) **Acoustic turbidity.** This signature appears on seismic profiles as areas of chaotic reflection and sound absorption. Areas of acoustic turbidity might be of regional or localised extent, and appear correspondingly as extensive areas or localised plumes (e.g. Taylor, 1992; Yuan et al., 1992). The required minimum gas content within marine sediments for acoustic turbidity to occur can be as little as 1% (Fannin, 1980; Jones et al., 1986). The boundary between the area affected by acoustic turbidity and the surrounding or overlying unaffected area is known as the ‘gas front’. It was suggested by Judd & Hovland (1992) that this signature is most likely to occur when shallow gas is finely dispersed within impermeable clay-rich sediments. This supposition is supported in this study (see Ch. 5).

2) **Acoustic blanking.** This signature appears on seismic profiles as areas of weak or absent sub-surface reflection. It is thought to be caused by the disruption of sedimentary layers by migrating pore fluids, or by absorption of acoustic energy by overlying gas-charged sediments.

3) **Enhanced reflections.** This signature occurs in the form of strong reflections, and in places is documented extending laterally from zones of acoustic turbidity. It has been

suggested by Judd & Hovland (1992) that this signature might reflect the situation when shallow gas occurs in the form of accumulations within porous silt-sand sediment.

4) **Bright spots.** Often seen on industry seismic profiles, bright spots are strong (high amplitude) reflections, which indicate the marked change in acoustic impedance that occurs at the top of shallow gas accumulations; they are comparable to enhanced reflections. Current interpretation practice involves specialised processing of digital data in order to identify additional attributes (phase reversal, flat spots, signal starvation etc.), which are commonly associated with shallow gas.

5) **Columnar disturbances or gas chimneys.** This signature occurs in the form of vertically extended disturbances of sub-bottom reflectors that are thought to occur due to vertical migration of gas or other fluids, usually referred to herein as gas plumes. This seismic feature is frequently coincident with seabed doming or mounded relief caused by sub-surface gas pressure or may underlie pockmarks.

### ***1.2.3 Gas-related seabed structures***

This section presents a brief overview of seabed structures that can be formed due to the presence and migration of shallow gas in marine sediments. A proper understanding of such structures and the mechanisms of their formation is of particular relevance to this study. The type and size of gas escape structures is normally a function of sub-seabed pressure created by gas accumulation and the lithological properties of the sediments that comprise both seabed and sub-bottom layers. Moreover, the seabed expression of the majority of gas escape structures is highly influenced by regional and local hydrodynamic conditions and by the rate of sediment supply. For example, erosion by benthic currents or active sediment transport, for instance in the form of migratory waves, might remove or overwhelm the original surface morphology of the gas escape structures. The most typical gas escape structures that can be identified on remotely sensed datasets such as seismic profiles and side-scan sonar imagery include the following: seabed doming, mud diapirs, seep mounds, pockmarks and trenches, and abnormal sand waves. Underwater video surveying techniques may also identify features associated with gas seepage such as methane-derived authigenic carbonates (MDAC) and bacterial mats (see Ch. 1.2.4). The coexistence of the latter with gas escape structures (e.g. pockmarks, mounds)

provides strong evidence that gas seepage might have occurred in the past or is ongoing at present. Most of the above-named gas escape structures have been documented worldwide (e.g. Hovland & Judd, 1988; Hovland, 1992; Premchitt et al., 1992; Soderberg & Floden, 1992; Judd, 2001; Garcia-Gil et al., 2002) and, as is shown by the present study, also occur extensively in the western Irish Sea region.

Interpretation of the above-named seabed structures as evidence of gas escape based solely on their presence in the remotely sensed data can be ambiguous. Therefore, in the existing literature they are referred to as “indirect evidence” of gas escape (Judd & Hovland, 1992). However, when interpreted in conjunction with sub-bottom evidence of gas accumulations (see Ch. 1.2.2) and supported by the knowledge of the underlying solid geology as well as by direct observations (e.g. with an ROV) they become a powerful tool in mapping past and present processes related to the migration and escape of shallow gas.

The seabed structures that can be potentially formed by gas escape are described in more detail below.

**Pockmarks.** Pockmarks are circular or sub-circular seabed depressions that are formed due to the removal of seabed sediments by escaping fluid. Hovland and Judd (1988) proposed a conceptual model for pockmark formation, identifying three main stages:

- 1) the formation of a seabed dome due to excessive fluid pressure underneath the seabed;
- 2) discharge of fluid in a single event, lifting the sediment into the water column, winnowing fines and leaving lag deposits;
- 3) continuation of pockmark formation due to continuously or periodically occurring fluid seepage.

The imperative requirement for pockmark formation is a suitable lithological composition of the seabed sediments. Pockmarks can only be formed if the seabed is composed of fine-grained (clay/silt) sediments. They may vary in diameter from a few meters to hundreds of meters, and in depth from tens of centimetres to 20m or even more. In most cases the escaping fluid responsible for the pockmark formation is gas (e.g. in the North

Sea: Judd, 2001), but pore water may also be responsible (e.g. Eckernförde Bay, Germany: Whiticar, 2002; the northern Rockall Trough: Masson et al., 2003). Pockmarks occur in various settings from shallow continental shelves to the deep oceans. The seabed expression of pockmarks may vary depending on hydrodynamic activity and sediment supply. Normally, pockmarks will not be preserved if seabed erosion occurs. In the event of high sedimentation rates, pockmarks could become covered with sediment, thus buried pockmarks are not uncommon.

Pockmarks have been the subject of numerous scientific reports and publications (e.g. Dando et al., 1991; Hovland, 1992; Dando, 2001; Judd, 2001; Hovland, 2002; Whiticar, 2002; Hovland et al., 2003; Masson et al., 2003 etc.). The most comprehensive overview of pockmarks to date was presented by Hovland and Judd (1988).

**Trenches.** Trenches are seabed depressions that are relatively narrow in relation to their length and in most cases possess a rough seabed morphology of an erosional nature. It is believed that some of these trenches might be formed due to large-scale linear gas venting through the seabed (e.g. Croker, 1994; Boe et al., 1998), with the formation mechanism being rather similar to pockmark formation. A possible example of the early stages of this process is shown in Fig. 1.2. However, submarine trenches may be formed by various mechanisms e.g. erosional hydrodynamic activity without the assistance of shallow gas-related sediment destabilisation. Supporting evidence for the role of gas is therefore required.

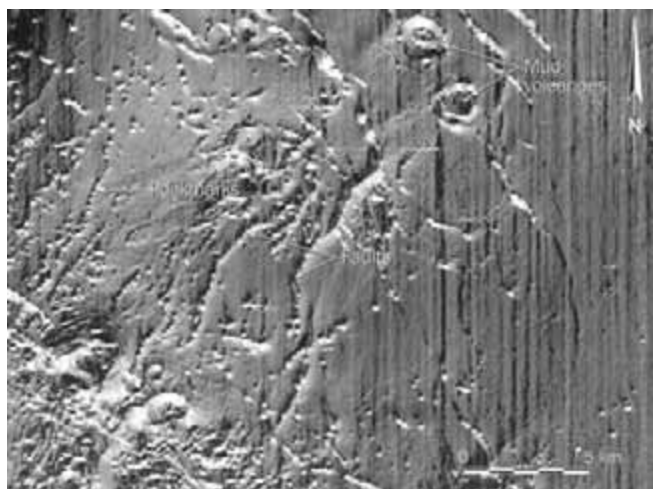


**Figure 1.2:** Azimuth map of the seafloor reflector from 3D seismic data showing the presence of pockmarks on the seabed, often aligned along fault lines (Nigerian continental slope). The pockmarks are probably caused by gas escape through the faults. Courtesy of Statoil (reproduced in TNO-NITG-INFORMATION, December 2004, p.3).

**Seabed domes.** Seabed doming can be associated with accumulations of shallow gas. These features are mainly documented on seismic profiles where seabed sediments are underlain by gas plumes. Seabed domes are generally characterised by a low profile (1-2m high) and relatively large lateral extent (from tens to hundreds of meters). One of the theories suggests that doming could occur due to the replacement of water in the pore spaces within the upper sediment layer with gas thus causing an increase in the sediment volume (Judd & Hovland, 1992). It is also plausible to assume that seabed doming might be the initial stage of pockmark formation (Hovland & Judd, 1988). The formation of seabed domes mainly occurs where the seabed is capped with fine-grained relatively impermeable sediments.

**Mud volcanoes and mud diapirs.** Mud diapirs occur when the gas charged layer of clay or mud rises through other sedimentary layers due to buoyancy effects. These structures are found worldwide within areas with defined hydrocarbon potential (e.g. Hovland & Curzi, 1989; Hovland, 1990) and may vary in size from a few meters to hundreds of meters across. Depending on the depth of the gas accumulation that triggers diapir formation and the depth of the clay horizon in relation to the seabed, diapirs can have a morphological expression on the seabed or may only exist as a sub-surface (buried) feature.

**Seep Mounds.** Seep mounds are mound-shaped bedforms generated by fluid seepage and sand ejection. In cases where the seeping fluid is pore water, the seep mound will possess the form of a sand volcano and will be composed of loose sand (e.g. Masson et al., 2003). If the seeping fluid is methane then cementation of sand grains may occur due to the formation of MDAC (methane-derived authigenic carbonates) (e.g. Dando et al., 1994b; Croker, 1997a), typically leading to slab formation within the mound.

**Giant (Abnormal) Sand waves.** Believed to be associated with gas seepage, Hovland (1993) suggested that the abnormal size of these bedforms could be explained by the assumption that gas seepage influenced the deposition of mobile sand grains in preferred locations which thus led to the development of their characteristic abnormal dimensions and being less mobile than the surrounding sand waves. However, the interpretation of such bedforms in terms of shallow gas seepage can be ambiguous if it is not supported

with other evidence that documents sub-seabed shallow gas accumulations or gas seepage in the water column.

#### ***1.2.4 Identification of gas seepage***

The identification of gas seepage may be conducted via direct or indirect methods. The direct methods include visual observations of potential seep localities with underwater video or still cameras deployed on ROVs, manned submersibles, deep-towed video systems or moorings (that may document gas bubbles escaping through the seabed) and near seabed measurements with methane-sensing equipment. Only such methods can confirm contemporary seep activity. Additionally, remotely sensed mapping techniques using echosounder or side-scan sonar equipment might indicate active seepage by documenting seepage plumes in the water column rising from apparent gas escape structures (e.g. pockmarks, mounds), and therefore may also be referred to as direct evidence. These plumes may rise vertically or be inclined depending on the local hydrodynamic conditions. However, as seepage may not be continuous but sporadic, direct evidence may not be obtained during once-off surveys as is often the case.

However, even if the seepage is not directly confirmed, indirect evidence indicating sporadic or recent seep activity might be present, for example methane-derived authigenic carbonates (MDAC), bacterial mats and typical seep-related biological assemblages.

The possibility of identifying gas seepage using direct methods depends on whether the seepage occurs in macro (large enough to be visible) or micro (micro-bubbles or dissolved gas) form (Judd & Hovland, 1992). A clear distinction between active seeps and those that were active in the past is only possible based on the combined interpretation of evidence derived from direct and indirect methods.

The presence of gas-related seabed structures (Ch. 1.2.3 above) may indicate that gas seepage has taken place at a given location, but does not necessarily imply that the seepage is ongoing at present. The same caveat relates to the presence of seep-associated bio-communities. This is due to the fact that gas escape might have occurred in the past but its consequences are still apparent.

The following are important indicators of gas seepage:

**Methane-derived Authigenic Carbonate (MDAC).** MDAC is a carbonate precipitate generally composed of high-magnesium calcite or aragonite ( $\text{CaCO}_3$  to  $\text{CaMg}(\text{CO}_3)_2$ ) (e.g. Jorgensen, 1992; Judd, 2001). This precipitation is linked to the anaerobic oxidation of methane as shown by Boetius et al. (2000):



The precipitation of carbonate causes cementation of seabed sediments so that MDAC normally results in the formation of carbonate blocks, chimneys, crusts or slabs, and is in some instances draped with a thin sediment layer. It can be detected by characteristic high backscatter on the side-scan sonar records. However, reliable identification is only possible in combination with video ground-truthing or seabed sampling.

The occurrence of MDAC can be used as evidence of gas seepage, but again does not necessarily imply that the seepage is ongoing.

**Bacterial mats.** Bacterial mats of the sulphide-oxidising bacterium *Beggiatoa*, *Thiothrix* and *Thioploca* sp. may occur as white patches on the seabed at active seep sites (e.g. Brooks et al., 1979; Spies & Davis, 1979; Grant et al., 1986; Hovland & Thomsen, 1989; Dando & Hovland, 1992; Judd, 2001). Bacterial mats can only be detected using video surveying techniques or via seabed sampling with grabs or box cores.

**Seep-specialist fauna.** The physical and chemical changes in the benthic environment arising from gas seepage have an impact on fauna and flora in the vicinity of the seeps (e.g. Dando & Hovland, 1992). Seep-specialist fauna may be represented by bivalves with endosymbiotic sulphide-oxidising bacteria (e.g. *Thyasira sarsi* – see Southward, 1987; Dando et al., 1991; Dando et al., 1994a; Dando, 2001), and particular species of tube worms (e.g. pogonophore species: Flugel & Langhof, 1983; Schmaljohann & Flugel, 1987; Dando & Hovland, 1992; Dando et al., 1994a). This fauna is largely absent from

areas unaffected by gas seepage and may therefore be tentatively used as evidence of hydrocarbon seepage.

### **1.3 Setting of IRL-SEA6**

This section describes IRL-SEA6 from a geographical, geological and hydrodynamic perspective.

#### ***1.3.1 Geographical setting***

IRL-SEA6 is bounded by the coast of Ireland to the west and by the Ireland/UK median line to the east and north (Fig. 1.1). The southern boundary of IRL-SEA6 was drawn from the south-western corner of the UK SEA6 area to Carnsore Point on the south-eastern coast of Ireland, thus roughly dividing the Irish and Celtic Seas. Although IRL-SEA6 is generally limited to Irish waters, the report also includes some data collected by PAD in what was at the time an undesignated area but is now included in the UK sector.

The water depth in the vicinity of the median line is c.100m; however, localised depressions down to 130-180m can also be observed. The BGS detailed bathymetry (10m contours) shows a number of linear seabed depressions or trenches (Fig. 1.3). This study will also test the probable association of these well-defined geomorphological structures with gas escape processes.

#### ***1.3.2 Geological setting***

The geology of the Irish Sea has been previously reviewed by Dobson & Whittington (1979), Naylor & Shannon (1982), Jackson & Mulholland (1993) and Jackson et al., (1995) and graphically presented by Croker et al. (1982), Martindale et al. (1982) and Ransome (1982) on the BGS 1:250,000 solid geology map series. The geology of the Kish Bank Basin was studied in more detail by Jenner (1981) and Naylor et al. (1993). Moreover, the solid geology of the western Irish Sea has been more recently revised by Croker & Power (1996b), and a new updated edition of the solid geology map is currently being prepared (Tappin & Croker, 1999).

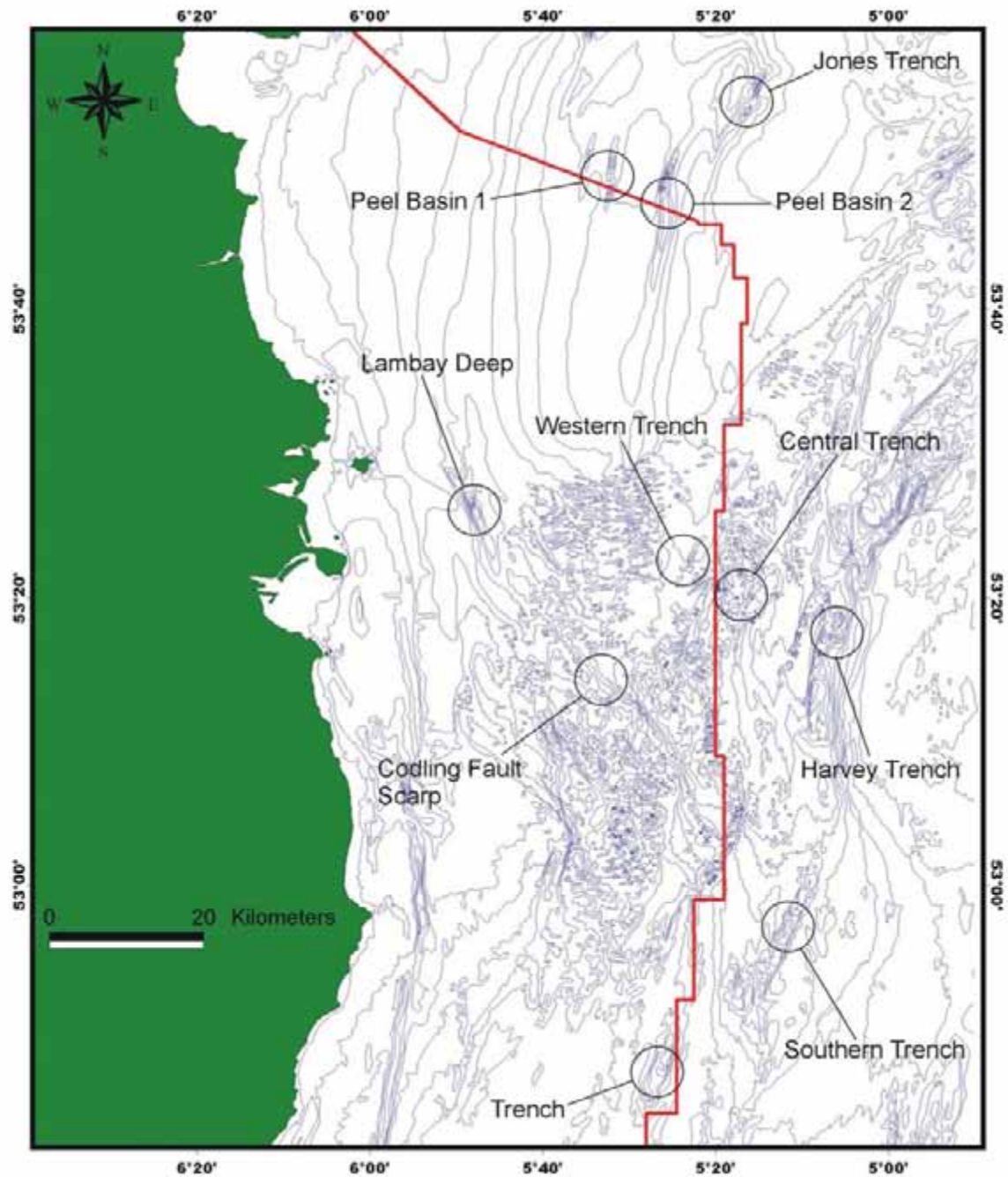


**Figure 1.3:** Location map of the western Irish Sea with the main areas containing gas-related seabed features labelled. The red line represents the boundary of the IRL-SEA6 study area. Bathymetric contours are at 10m intervals (courtesy of BGS).

The part of the Irish Sea that is relevant to IRL-SEA6 incorporates two Mesozoic sedimentary basins – the Kish Bank Basin and the south-western part of the Central Irish Sea Basin (see Fig. 3.3). The aspects of the solid geology of the western Irish Sea relevant to this report are discussed in Chapters 3 and 4.

### ***1.3.3 Hydrodynamic conditions and sediment transport***

Hydrodynamic conditions and seabed sediment types may have a direct impact on the type and appearance of gas seepage structures through seabed erosion and sediment transport. Particularly, structures formed by seeping gas and associated MDAC can be eroded by vigorous benthic currents or buried by active sediment transport.

Hydrographical surveys in conjunction with seabed mapping and video truthing (e.g. Wingfield et al., 1987; James, 1988; Orford, 1988; James, 1990; Wheeler et al., 2001; Croker et al., 2002) indicate active hydrodynamic conditions in IRL-SEA6 that facilitate both erosion and active sediment transport. Tidal currents heavily influence the hydrodynamics within IRL-SEA6, the strength of which changes from south to north (from approximately 120cm/sec to 20cm/sec respectively) (Fig. 1.4).

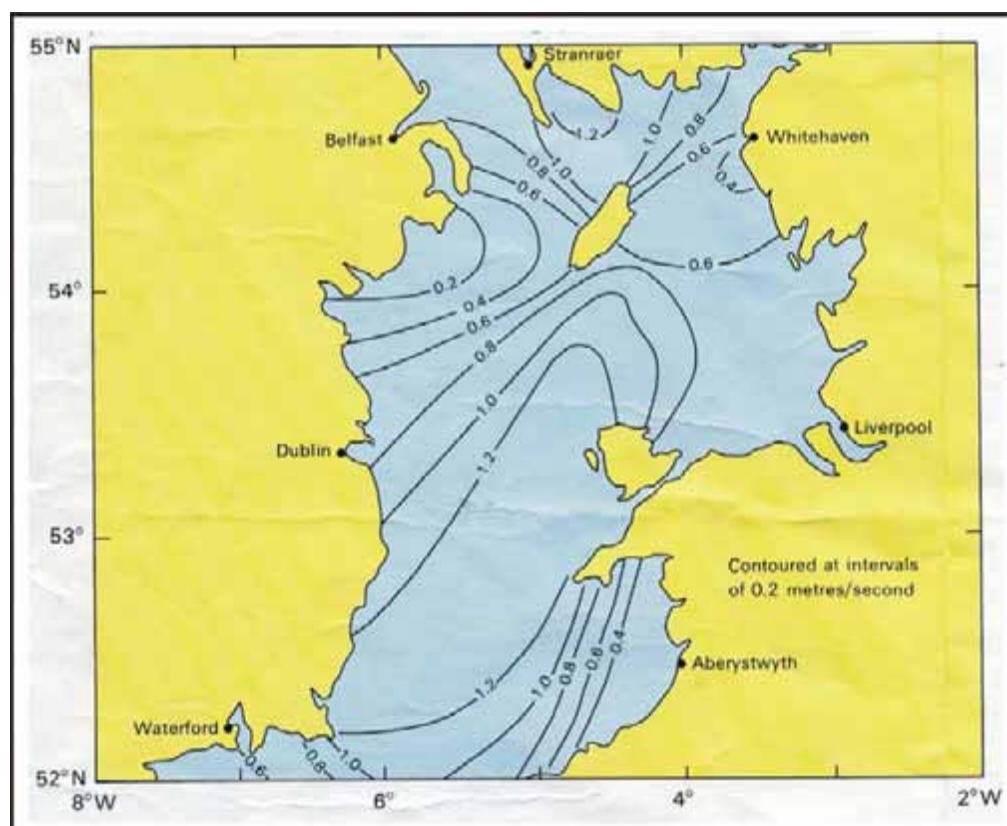


**Figure 1.4:** Tidal current speeds contoured at intervals of 0.2m/sec (courtesy of Institute of Oceanographic Science; source: James, 1990).

The change in hydrodynamic conditions throughout the area is reflected in the observed changes of sediment particle size and bedform distribution (Fig. 1.5).

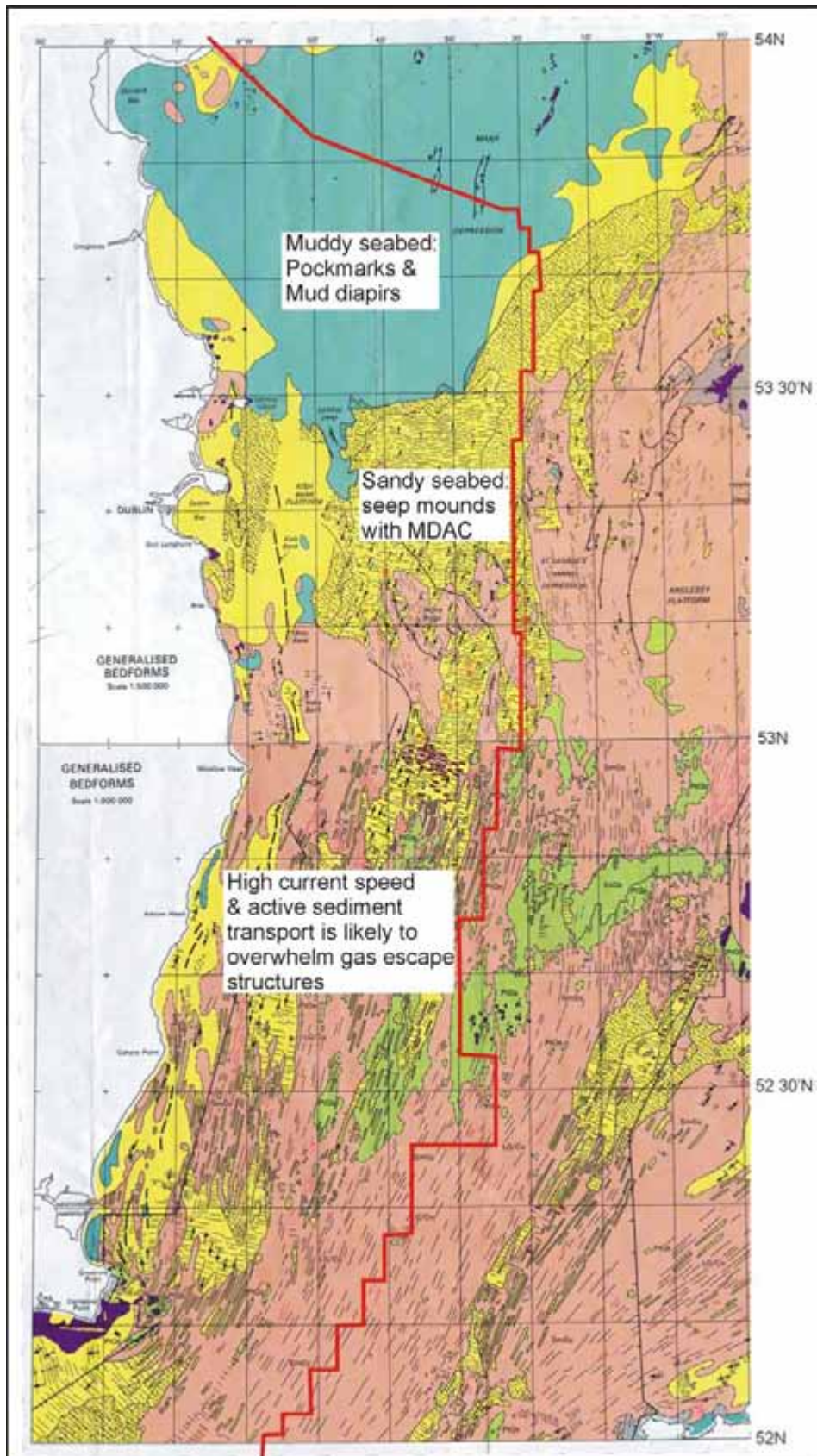


**Figure 1.5:** Generalised bedforms distribution map of the western Irish Sea (courtesy of BGS: James, 1988; 1990) overlain with comments regarding potential types of gas escape structures. The red line represents the limit of the IRL-SEA6 study area.

South of 53°10'N the IRL-SEA6 area is dominated by coarse deposits ranging from gravelly sands to cobble pavements. This part of IRL-SEA6 is typified by high-energy bedforms represented by sand streaks, sand ribbons, gravel furrows and high amplitude sand waves. In contrast, the area north of 53°10'N is characterised by weaker currents and shows generally finer particle size changing from sand to mud with consequent changes in the seabed morphology from sandy seabed typified by sand waves to a smooth muddy seabed. The generalised bedforms distribution map is shown on Figure 1.5. The original BGS map is overlain with comments relating to the potential distribution of gas escape structures. This distribution has been largely confirmed with data presented in the following chapters. This might suggest therefore that the distribution of gas-related seabed structures and MDAC (see Ch. 6) presented in this study could be potentially underestimated in the southern area.

## **2. Materials and Methodology**

### **2.1 Data overview**

Over the last 40 years the IRL-SEA6 area has been surveyed with a range of remote sensing and ground-truthing techniques providing information at various scales of resolution. The main driving factors for these investigations were exploration for hydrocarbons in the Kish Bank and the Central Irish Sea basins, as well as cable and pipeline route surveys. The existing data includes the following: seismic data including conventional seismic and high-resolution seismic (e.g. Sparker, Boomer, GeoChirp, etc.); echosounder; side-scan sonar and multibeam coverage over certain areas; video and photographic imagery of selected parts of the seabed, located based on remotely sensed data; and seabed samples collected with various techniques (e.g. gravity cores, dredge samples etc.).

This report is mainly based on the data that was made available for this study by the Petroleum Affairs Division (PAD) of the Department of Communications, Marine and Natural Resources, Ireland.

This data can broadly be subdivided into four groups:

- (1) Conventional seismic data (2D & 3D) collected during the period 1965-2004 (see Ch. 2.2);
- (2) Exploration wells drilled over the period 1977-2004 (see Ch. 2.3);
- (3) Route survey data obtained during 1986-2004 (see Ch. 2.4);
- (4) Multidisciplinary data collected during short annual research cruises by Peter Croker of the PAD during the period 1995-2002 (see Ch. 2.5).

### **2.2 Seismic data 1965-2004**

The IRL-SEA6 area has been surveyed with oil industry 2D conventional seismic surveys, particularly over the Mesozoic basins, during the period 1965 to 2004 (Fig. 2.1). A number of 3D seismic surveys have also been carried out, although these have generally been in the UK sector.

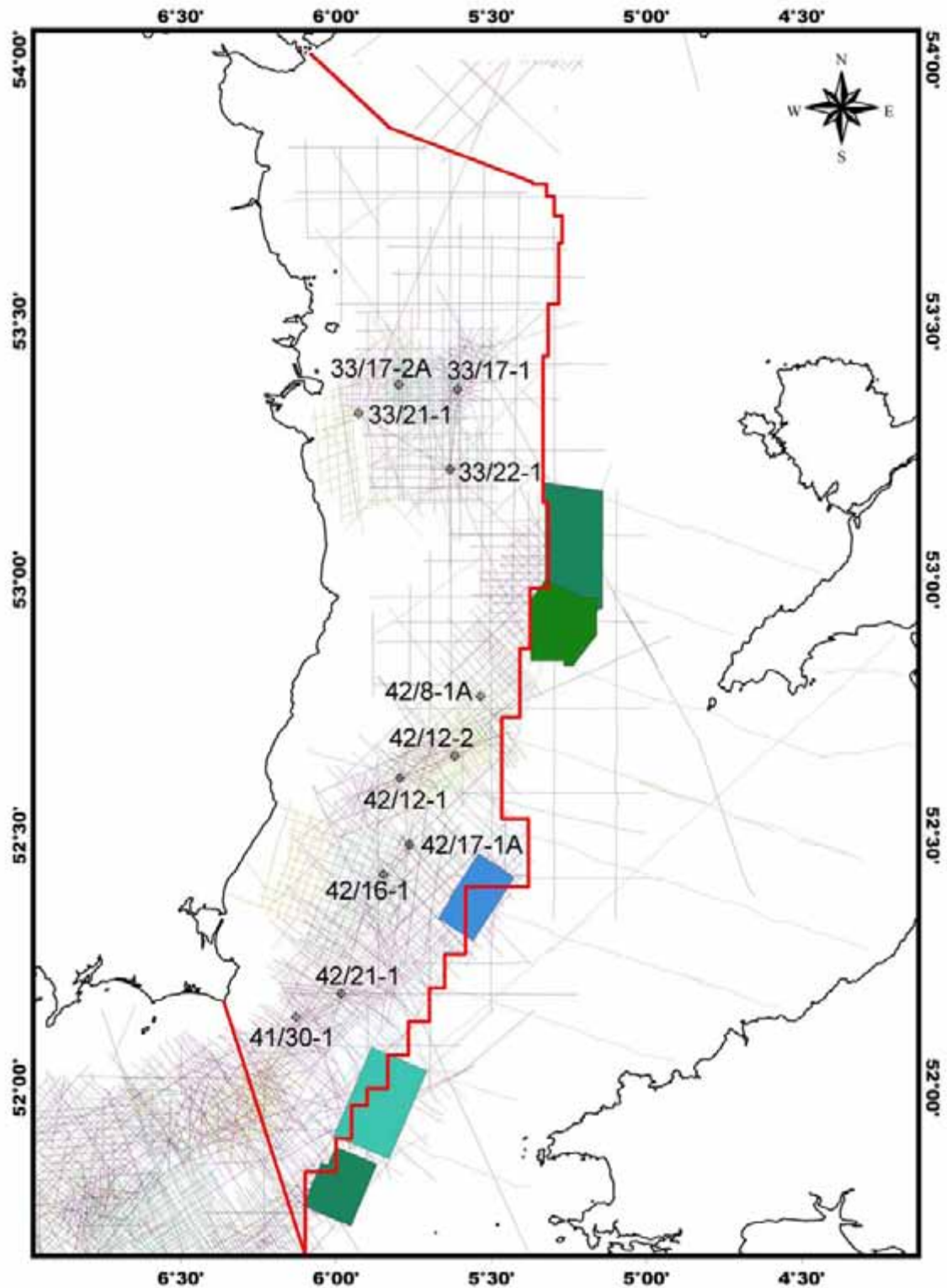


**Figure 2.1:** Location map of all oil industry 2D and 3D (solid colour) seismic surveys acquired in the western Irish Sea study area from 1965-2004. The position and reference numbers of all exploration wells within the IRL-SEA6 sector is also indicated. The red line represents the boundary of the IRL-SEA6 sector.

Industry seismic data, due to its low frequency, does not allow the identification of seismic artefacts characteristic of shallow gas accumulations (e.g. acoustic turbidity & gas blanking). The main purpose of including seismic data in this study was to identify the probable source rocks and document potential migration pathways for light hydrocarbons. Particularly, conventional seismic data was appraised to verify the existence of migration pathways or bedrock highs in relation to evidence for shallow gas observed on the high-resolution route survey (see Ch. 2.4) or site survey (see Ch. 2.5) data.

### **2.3 Exploration wells 1977-2004**

Table 2.1 lists all exploration wells that were drilled within IRL-SEA6. The location of these wells is shown on Figure 2.1. Exploration wells that are of particular relevance to the present study include the following: 33/22-1, 42/12-1, 42/12-2, 42/16-1 and 42/17-1A.

**Table 2.1: Exploration wells drilled within IRL-SEA6.**

Well Number	Latitude	Longitude	Area	TD (MD)	Rig Datum	Water Depth	Operator	Year	Well Result
33/22-1	53° 12' 51.081" N	05° 37' 57.094" W	KBB	3203	82	162ft	Amoco	1977	Dry Hole
42/17-1A	52° 28' 58.695" N	05° 45' 48.393" W	CISB	4968	83	247ft	Marathon	1978	Dry Hole
33/21-1	53° 19' 21.984" N	05° 55' 37.372" W	KBB	2338	35	18.5m	Shell	1979	Dry Hole
42/12-1	52° 36' 51.151"N	05° 47' 36.677"W	CISB	9265	108	206ft	Hydrocarbons Ireland	1986	Dry Hole
33/17-1	53° 22' 8.045"N	05° 36' 26.736"W	KBB	6660	110	236ft	Charterhouse	1986	Dry Hole
42/21-1	52° 11' 18.530"N	05° 59' 00.440"W	NCSB	6650	84	295ft	Gulf	1986	Dry Hole
42/16-1	52° 25' 25.510"N	05° 50' 45.450"W	CISB	4754	82	259ft	Conoco	1988	Dry Hole
42/12-2	52° 39' 27.815" N	5°37' 01.379"W	CISB	3800	98	238ft	Hydrocarbons Ireland	1990	Dry Hole
42/8-1A	52° 46' 28.542" N	05° 32' 00.216" W	CISB	8948	75	225ft	BHP	1994	Dry Hole
41/30-1	52° 08' 34.14" N	06° 07' 41.69" W	CISB	7343	85	248ft	Marathon	1995	Dry Hole
33/17-2A	53° 22' 40.291"N	05° 47' 46.79"W	KBB	1310	35.8	50.2m	Enterprise Oil	1997	Dry Hole

KBB = Kish Bank Basin  
 CISB = Central Irish Sea Basin  
 NCSB = North Celtic Sea Basin

### **2.4 Route survey data 1986-2004**

High-resolution route survey data was collected by Telecom Eireann, Bord Gais Eireann and the Electricity Supply Board over the period 1986-2004 (Fig. 2.2). Permission to use this data for shallow gas investigations was granted by these agencies to the PAD, which made the results of that study available for this report.

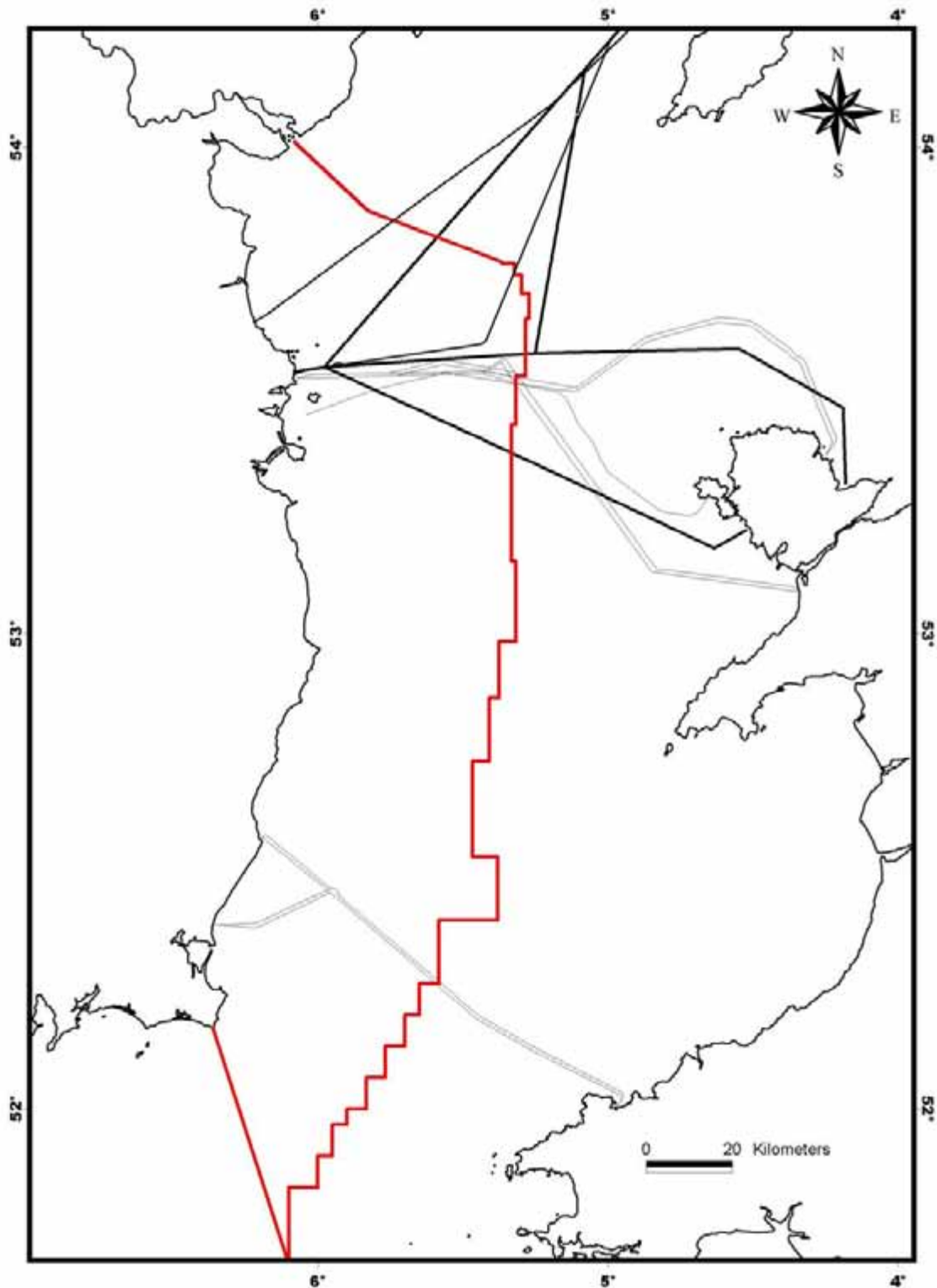


**Figure 2.2:** Location map of the route surveys in the Irish Sea, 1986-2004. The red line represents the boundary of the IRL-SEA6 sector.

Route survey datasets that provided valuable information with regards to shallow gas in marine sediments included the following types of seismic data:

- (1) 200J Boomer;
- (2) 300J Boomer;
- (3) Pinger – Seapro SBP 5.5kHz;
- (4) 5kHz Pinger;
- (5) 3.5kHz Pinger;
- (6) 1000J Sparker.

This data was analysed for visually identifiable evidence of shallow gas occurrences (see Ch. 1.2). Selected images from these surveys illustrating typical examples of shallow gas-related seabed and sub-seabed features are presented with interpretation later in this report.

### **2.5 Overview of research cruises 1995-2002**

Prompted by the extensive evidence of shallow gas occurrences observed on cable and pipeline route survey data (Ch. 2.4), the senior author organised eight short research cruises to the western Irish Sea in order to shed more light on the shallow gas and related features at particular study sites. These cruises were undertaken between 1995 and 2002 and collected multidisciplinary datasets including echosounder, GeoChirp, multibeam, side-scan sonar, Remote Operated Vehicle (ROV) video imagery and seabed sample data. The main sites investigated during these cruises included the following: Lambay Deep, Liassic outcrop, two sites within the Peel Basin, Jones Trench, Kish Bank Anomaly, Western Trench, Central Trench, and Codling Fault area (see Fig. 1.3).

These study sites were located based on pre-existing echosounder, side-scan sonar, pinger, sparker and conventional seismic profiles that were analysed in detail prior to the cruises.

These detailed site surveys, in conjunction with the high-resolution cable and pipeline route surveys, represent the crucial and most relevant datasets for this study. Figure 2.3 shows track lines of the cruises undertaken over the period 1995-2002. Details of each particular cruise including extent and type of data collected are outlined below (Ch. 2.5.1-2.5.8).

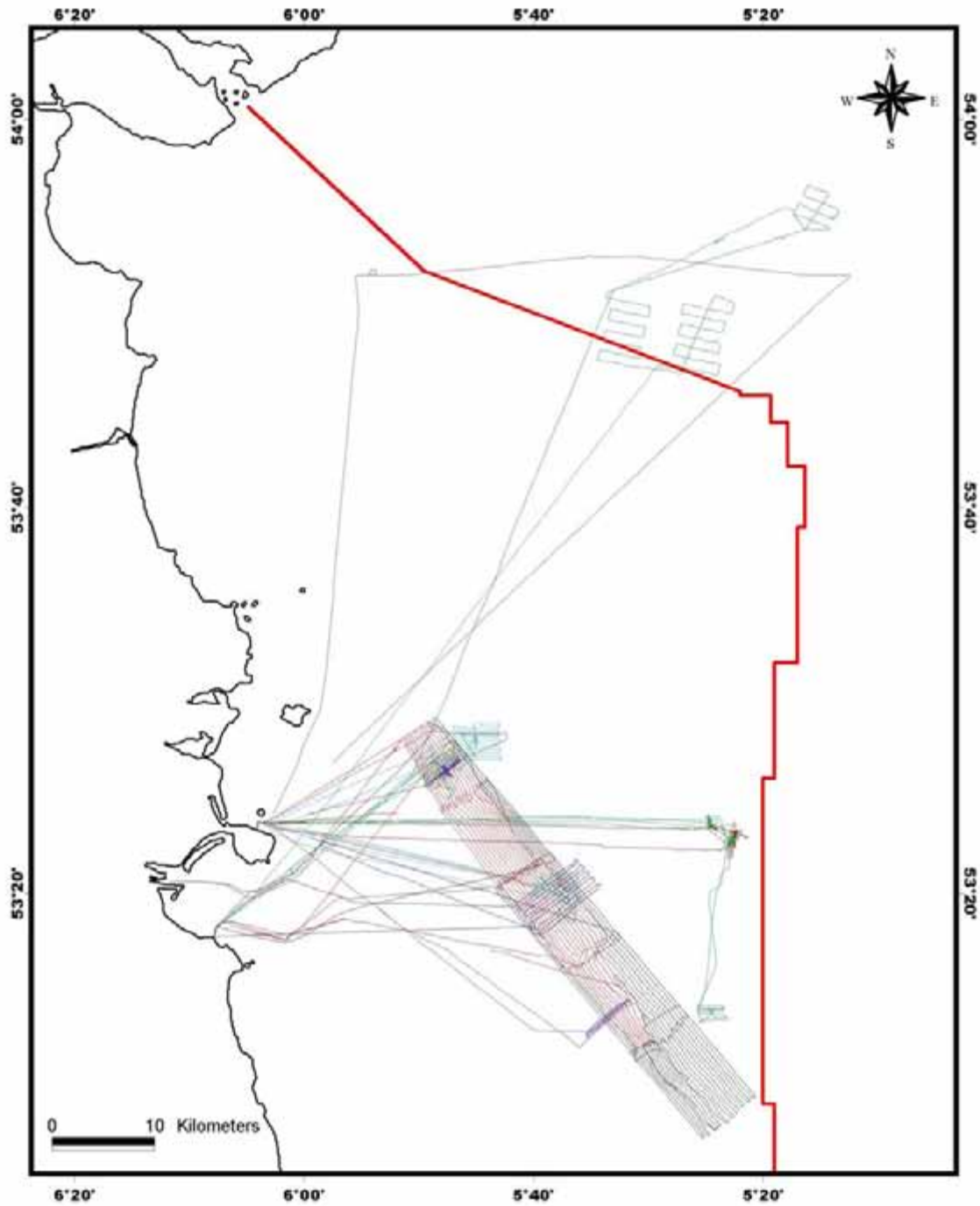


**Figure 2.3:** Location map showing tracklines of research cruises to the western Irish Sea study area undertaken by PAD during 1995-2002. The red line represents the boundary of the IRL-SEA6 sector.

### ***2.5.1 RV Lough Beltra cruise 1995***

The RV Lough Beltra 1995 cruise was undertaken from 23<sup>rd</sup> to 25<sup>th</sup> April 1995 (Croker & Power, 1995) and was devoted to investigation of the Western Trench (Lat 53°23'08"N Lon 5°22'20"W) and Kish Bank Anomaly (Lat 53°23'46"N Lon 5°24'38"W) (Fig. 2.4). However, out of three days ship time, productive work was possible only on one of these days. The study sites were located based on previously studied echosounder, side-scan sonar, pinger, sparker and conventional seismic profiles, which had suggested active gas seepage at these locations. Therefore, the aim of this cruise was to investigate present day seep activity from the geochemical and geobiological perspective using the ROV-mounted video and still cameras. The onboard equipment included the following: echosounder, Roxann, side-scan sonar, Aqua-Fact's SPI Camera and ROV.

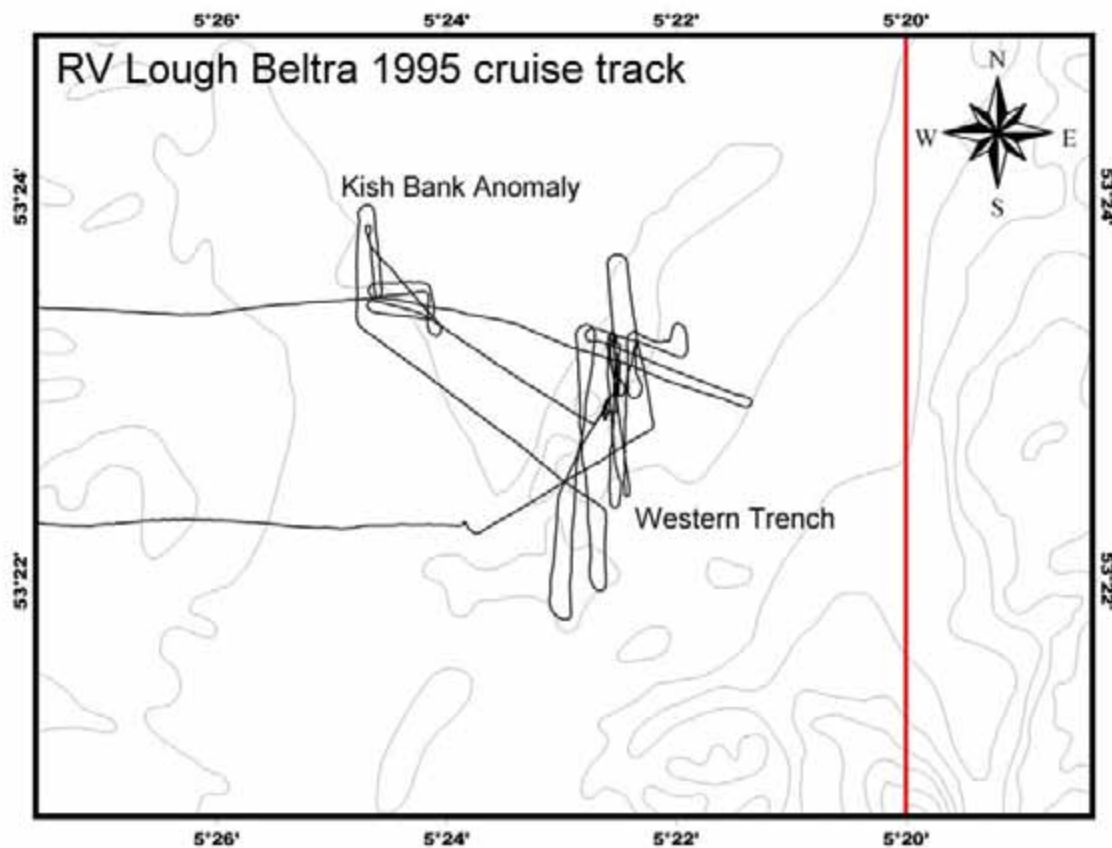


**Figure 2.4:** RV Lough Beltra 1995 cruise track with the key study sites named. The red line represents the boundary of the IRL-SEA6 sector. Bathymetric contours drawn at 10m intervals (courtesy of BGS).

The following data were collected during this cruise:

- Data recorded on the ship's Data Acquisition System (DAS) (including time, position and depth) was used to create detailed bathymetry of the Western Trench study area.
- Over 1 hour of video footage and a number of still photographs were recorded at three sites along the south-north transect in the Western Trench area.
- 10 clear images from 12 sites were recorded in the proximity of the western margin of the Western Trench with the SPI (sediment profile imagery) camera.
- 1hr 18m (at approx. 6 knots) of side-scan sonar imagery were recorded from the Western Trench area. Only the left-hand channel of the display was recorded due to an operational error. This provided some information on the seabed morphology.
- Part of the Western Trench was mapped with the Roxann system designed to analyse the numerical values for the reflection and absorption of acoustic signals at the seabed, thus allowing an automatic evaluation of the seabed sediment type.

### ***2.5.2 RV Lough Beltra cruise 1996***

The RV Lough Beltra 1996 cruise was undertaken between 23<sup>rd</sup> and 27<sup>th</sup> March 1996, during which additional data was collected from the following sites (Croker & Power, 1996a):

- 1) Kish Bank Anomaly (Lat 53°23'46"N Lon 5°24'38"W);
- 2) Western Trench (Lat 53°23'08"N Lon 5°22'20"W);
- 3) Central Trench (Lat 53°13'45"N Lon 5°24'15"W).

The cruise track is shown on Fig. 2.5. The equipment onboard the vessel during this survey included echosounder, Roxann, side-scan sonar and ROV.

The cruise succeeded in collecting the following datasets:

- Extensive ROV video footage over the Kish Bank Anomaly (KBA);
- ROV video footage over the Western Trench extending the RV Lough Beltra 1995 survey;

- Side-scan sonar imagery over a possible bedrock outcrop site in the Central Trench mapping approximately 4.2km<sup>2</sup> of seabed.

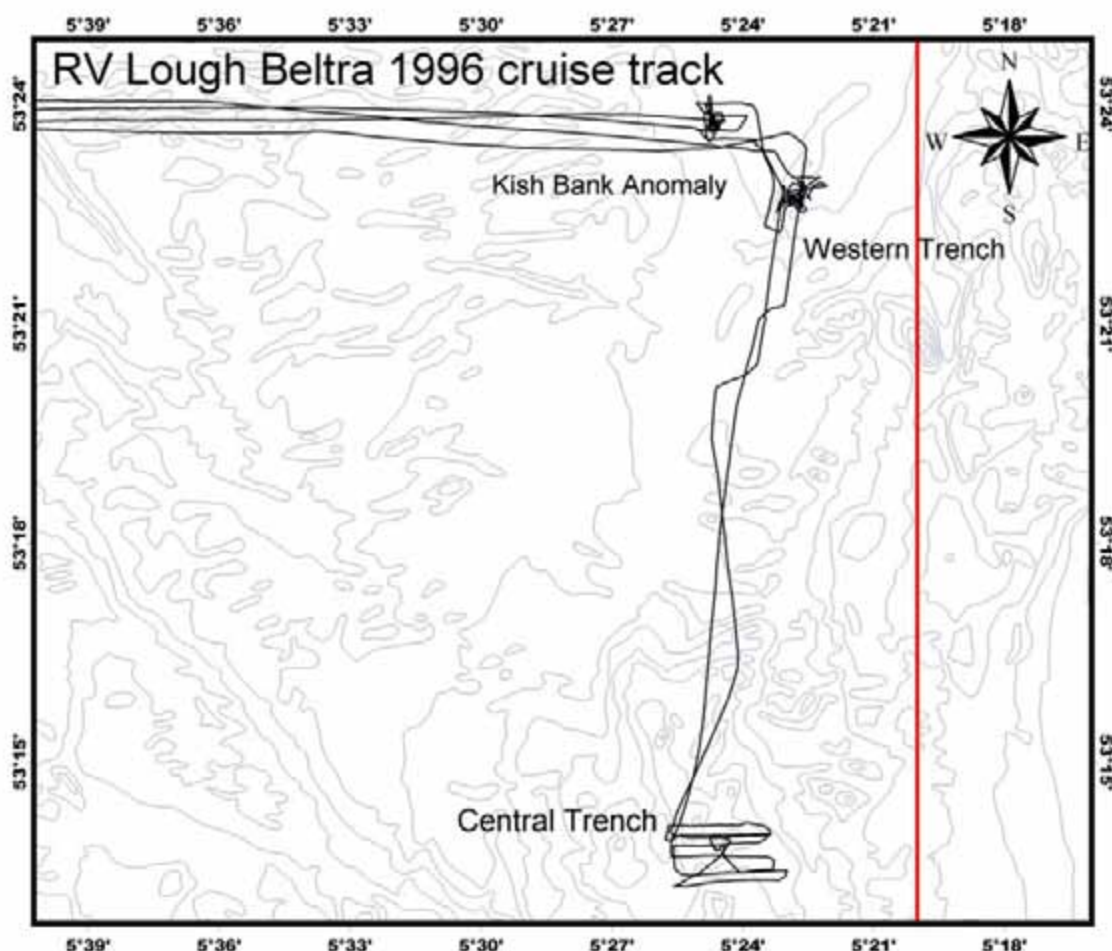


**Figure 2.5:** RV Lough Beltra 1996 cruise track with the key study sites named. Red line represents the boundary of the IRL-SEA6 sector. Bathymetric contours drawn at 10m intervals (courtesy of BGS).

### 2.5.3 RV Lough Beltra cruise 1997

This RV Lough Beltra cruise was undertaken from 14<sup>th</sup> to 16<sup>th</sup> April 1997, and was devoted to the investigation of the following study sites (Croker, 1997b):

- 1) The Codling Fault Branch mounds:
  - Target 1: Lat 53°19.754' N Lon 5°36.925' W (Line 11, SP 230)
  - Target 2: Lat 53°20.296' N Lon 5°37.750' W (Line 10, SP 295)
  - Target 3: Lat 53°20.839' N Lon 5°39.208' W (Line 9, SP 427)
- 2) The Liassic outcrop site (Lat 53°28.000' N Lon 5°45.000' W);
- 3) The Lambay Deep site (Lat 53°26.391' N Lon 5°48.143' W).

The onboard equipment during this cruise included the following: echosounder, side-scan sonar, ROV and gravity corer.

The RV Lough Beltra 1997 cruise track is shown on Figure 2.6, and the main datasets collected for each of the study sites are listed below:

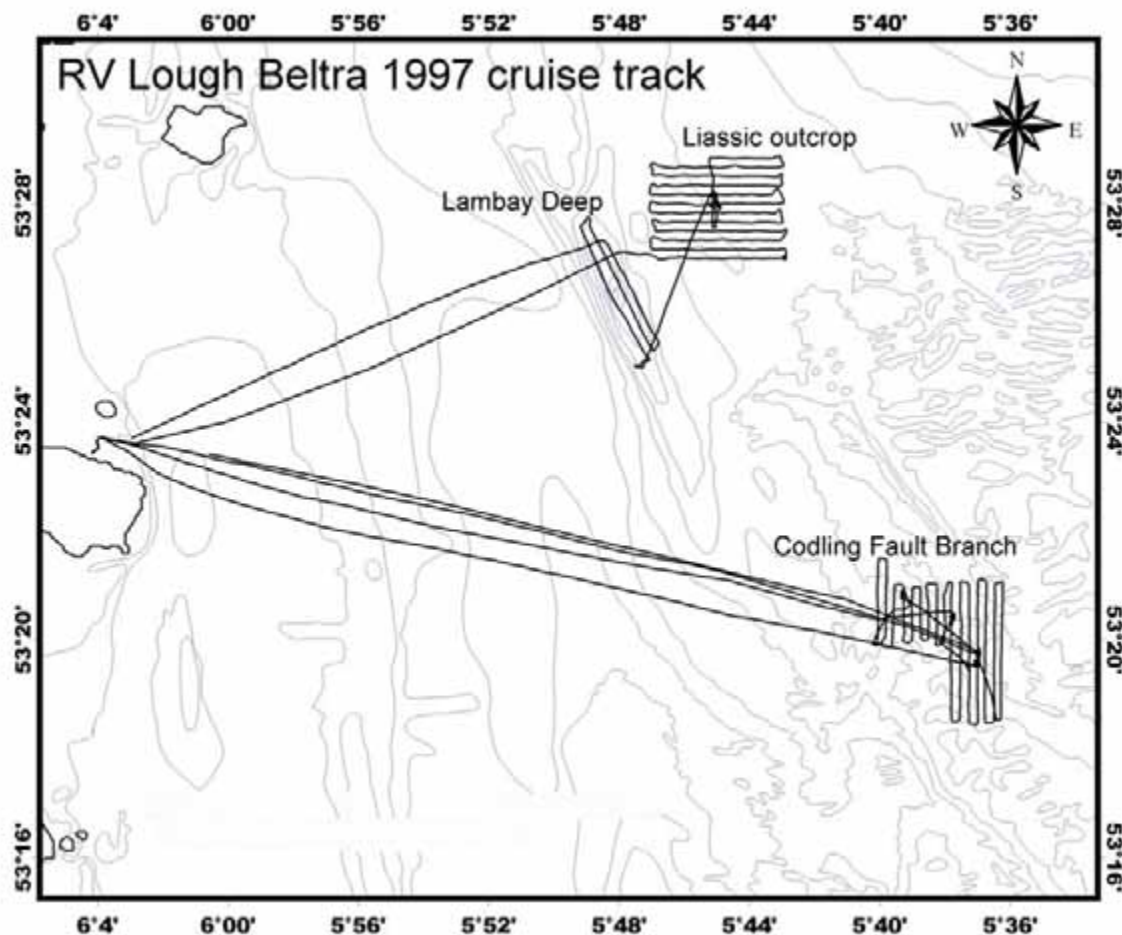


**Figure 2.6:** RV Lough Beltra 1997 cruise track with the key study sites named. Bathymetric contours drawn at 10m intervals (courtesy of BGS).

1) The Codling Fault Branch mounds:

- Echosounder imagery (16 lines);
- Side-scan sonar imagery (16 lines covering approximately 15km<sup>2</sup> of the seabed);
- ROV video footage of the mounds at targets 1, 2, 3 and 1A (located slightly to the north of target 1);
- 3 grab samples from target 2, and an anchor sample from target 3.

2) The Liassic outcrop site:

- Echosounder imagery (13 lines);
- Side-scan sonar imagery (13 lines covering approximately 18km<sup>2</sup> of the seabed);
- 1 gravity core that recovered approx. 30cm of sediment.

3) The Lambay Deep site:

- Echosounder imagery (3 lines);
- Side-scan sonar imagery (3 lines covering approximately 4.5km<sup>2</sup> of the seabed);

Both echosounder and side-scan sonar lines were recorded along the deepest part of the trough.

#### ***2.5.4 RV Celtic Voyager cruise 1998***

This cruise was undertaken from 23<sup>rd</sup> to 26<sup>th</sup> April 1998 with the aim of collecting data from the following areas (Croker & O'Loughlin, 1998):

- 1) Lambay Deep (Lat 53°26.391' N Lon 5°48.143' W);
- 2) Liassic outcrop (approx. Lat 53°28' N Lon 5°45' W);
- 3) Peel Basin 1 (PB1) (Lat 53°49.292' N Lon 5°25.471' W);
- 4) Peel Basin 2 (PB2) (Lat 53°50.109' N Lon 5°31.985' W);
- 5) Jones Trench (JT) (approx. Lat 53°55' N Lon 5°16' W).

Figure 2.7 shows the cruise track. The onboard equipment included the following: Data Acquisition System (DAS), Roxann, gravity corer, dredge, ROV (video, still camera), side-scan sonar, high-resolution seismic system (GeoChirp + SES4) and magnetometer.

The main data collected during this cruise were GeoChirp profiles that documented the seabed morphology of the study sites and in the key areas mapped the distribution of sub-surface shallow gas fronts and shallow reflectors. The Lambay Deep Mud Diapir was also discovered during this cruise.

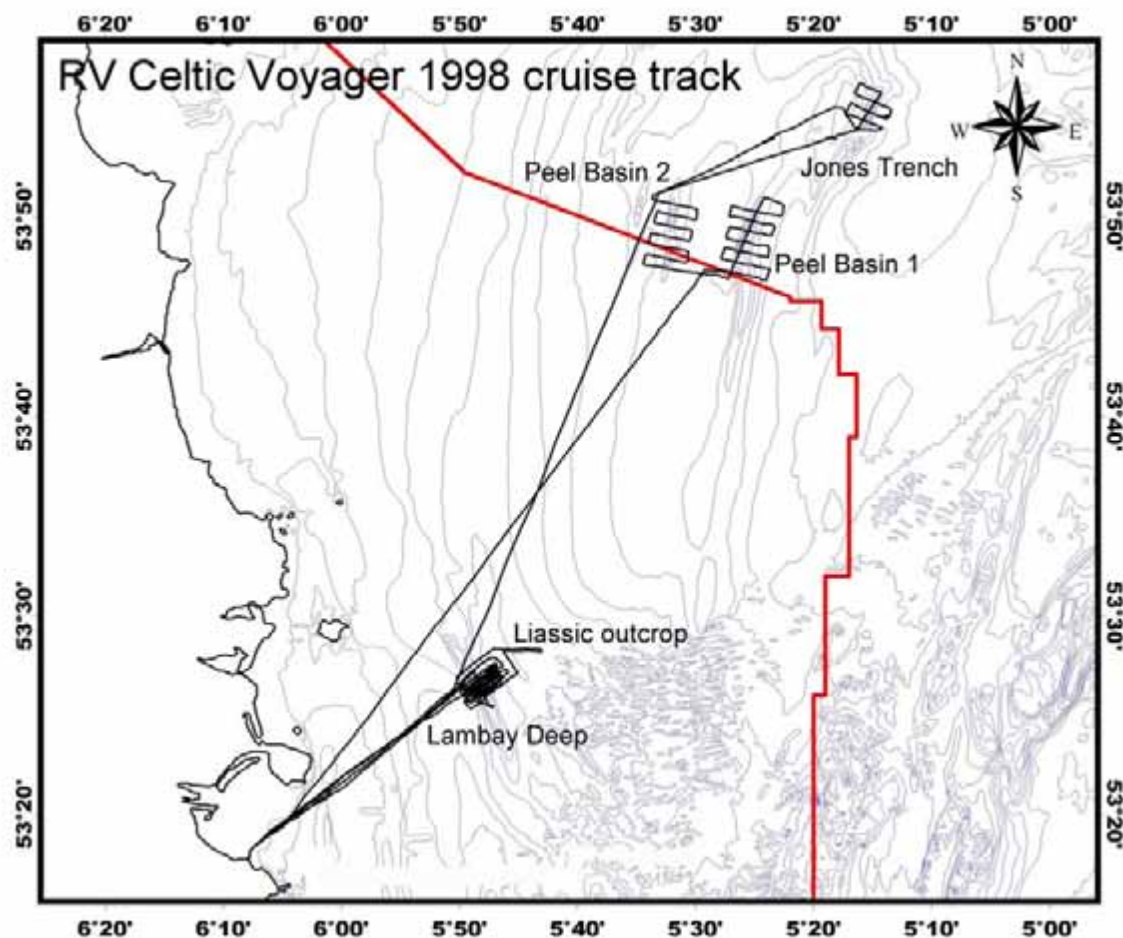


**Figure 2.7:** RV Celtic Voyager 1998 cruise track with the key study sites named. The red line represents the boundary of the IRL-SEA6 sector. Bathymetric contours drawn at 10m intervals (courtesy of BGS).

### 2.5.5 *RV Celtic Voyager* cruise 1999

This cruise was undertaken from 10<sup>th</sup> to 12<sup>th</sup> June 1999, during which data was collected from the following study sites (Croker & O'Loughlin, 1999a, 1999b):

- 1) Lambay Deep Mud Diapir (53°26.540' N, 05°47.680' W)
- 2) Liassic Outcrop (53°28.000' N, 05°45.000' W)
- 3) UCD/RPII sites (site 9: 53°52.000' N, 05°53.000' W; site 8: 53°53.000' N, 05°33.000' W; site 7: 53°52.000' N, 05°14.000' W)
- 4) Codling Fault site (53°13.350' N, 05°33.968' W)

The main instrument used onboard was the GeoChirp seismic profiler. The cruise track lines are shown on Figure 2.8, and collected data is listed below:

- 5 transverse and 4 longitudinal GeoChirp profiles were run over the Lambay Deep mud diapir discovered on the previous cruise in 1998.
- 6 GeoChirp profiles were run across the Codling Fault Zone, with Line 1 crossing the 33/22-1 exploration well location (see Table 2.1).
- 3 GeoChirp profiles across UCD/RPII sites 7, 8 and 9 that have been sampled on an annual basis since 1988 for radiological assessment purposes (Mitchell et al., 1999).

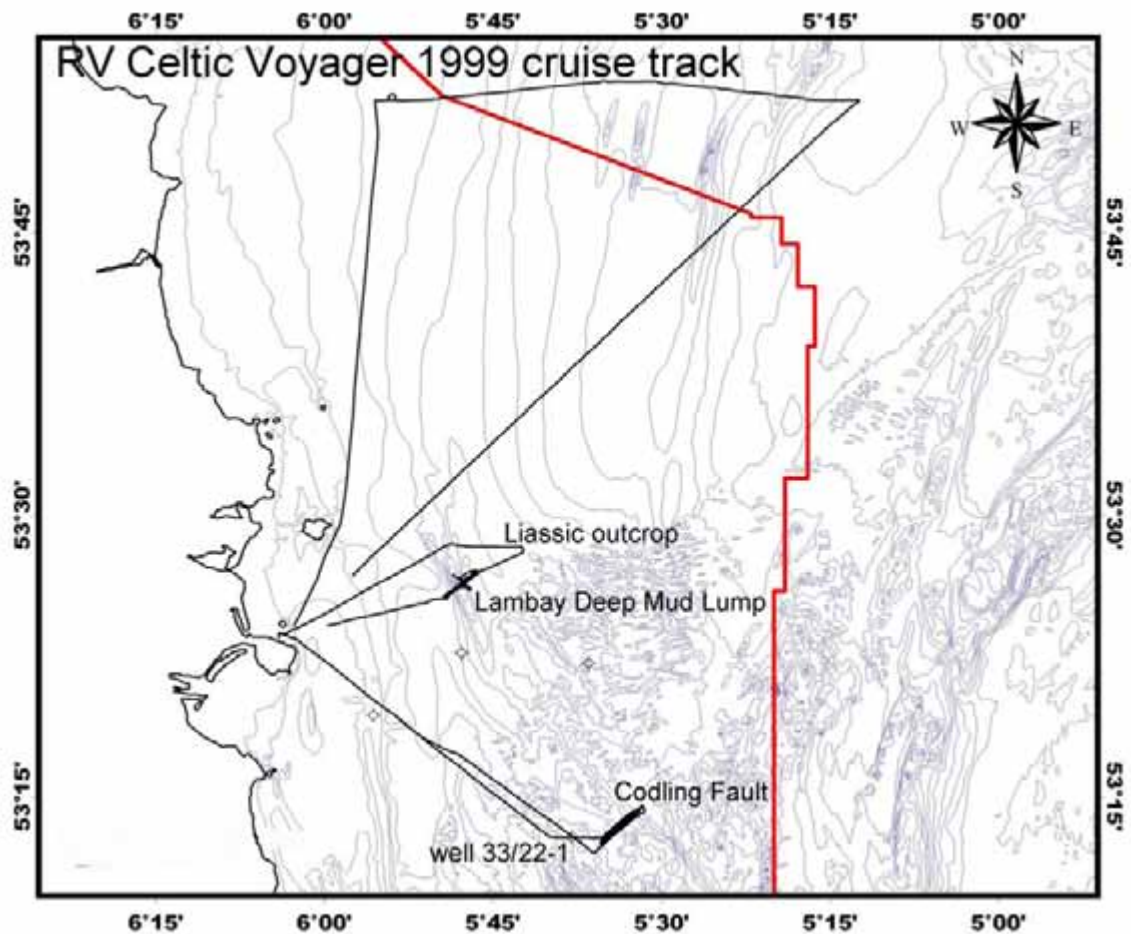


**Figure 2.8:** RV Celtic Voyager 1999 cruise track with the key study sites named. The red line represents the boundary of the IRL-SEA6 sector. Bathymetric contours drawn at 10m intervals (courtesy of BGS).

### 2.5.6 *RV Celtic Voyager cruise 2000*

This cruise was undertaken from 11<sup>th</sup> to 13<sup>th</sup> April 2000; however, due to poor weather conditions only one day of ship time could be used for data collection (Croker & O'Loughlin, 2000). The only equipment used was the Simrad EM1002 swath bathymetry system and only part of the Codling Fault site was surveyed (Fig. 2.9). A total of 10 lines were recorded using the side-scan sonar mode, with swath bathymetry recorded on lines 5-10 only. The line spacing was held at 400m thus providing full side-scan sonar and swath bathymetry coverage of c.30km<sup>2</sup> seabed. The recording and mosaicing of the side-scan sonar data was performed using the Hunter/Mapper software.

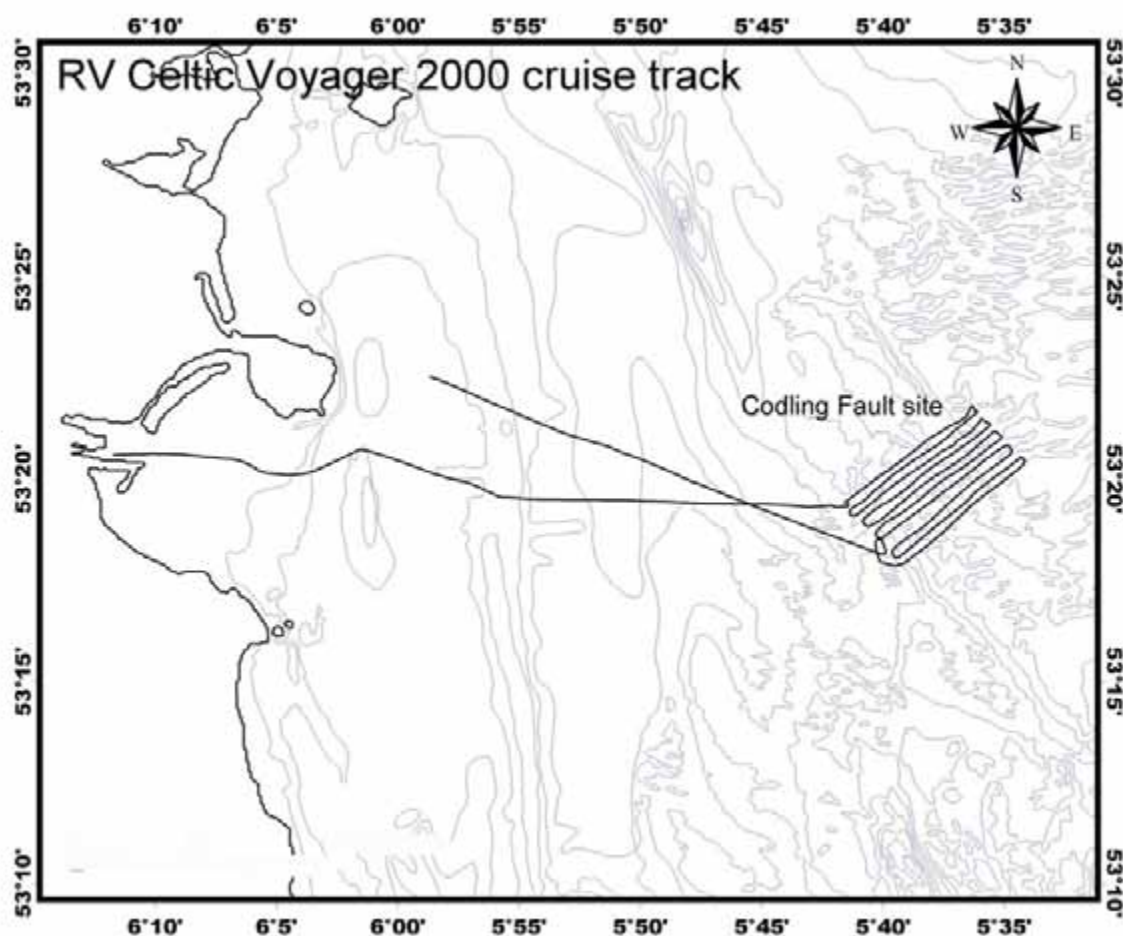


**Figure 2.9:** RV Celtic Voyager 2000 cruise track of the Codling Fault study site. Bathymetric contours drawn at 10m intervals (courtesy of BGS).

### 2.5.7 *RV Celtic Voyager cruise 2001*

The offshore investigations in 2001 were performed in two stages between 18-19<sup>th</sup> April and 4-6<sup>th</sup> May (Croker & O'Loughlin, 2001). This cruise was devoted to a multibeam

survey of the Lambay Deep and Codling Fault areas using the Simrad EM1002 swath bathymetry system (Fig. 2.10). This survey was continued in 2002 (see 2.5.8).

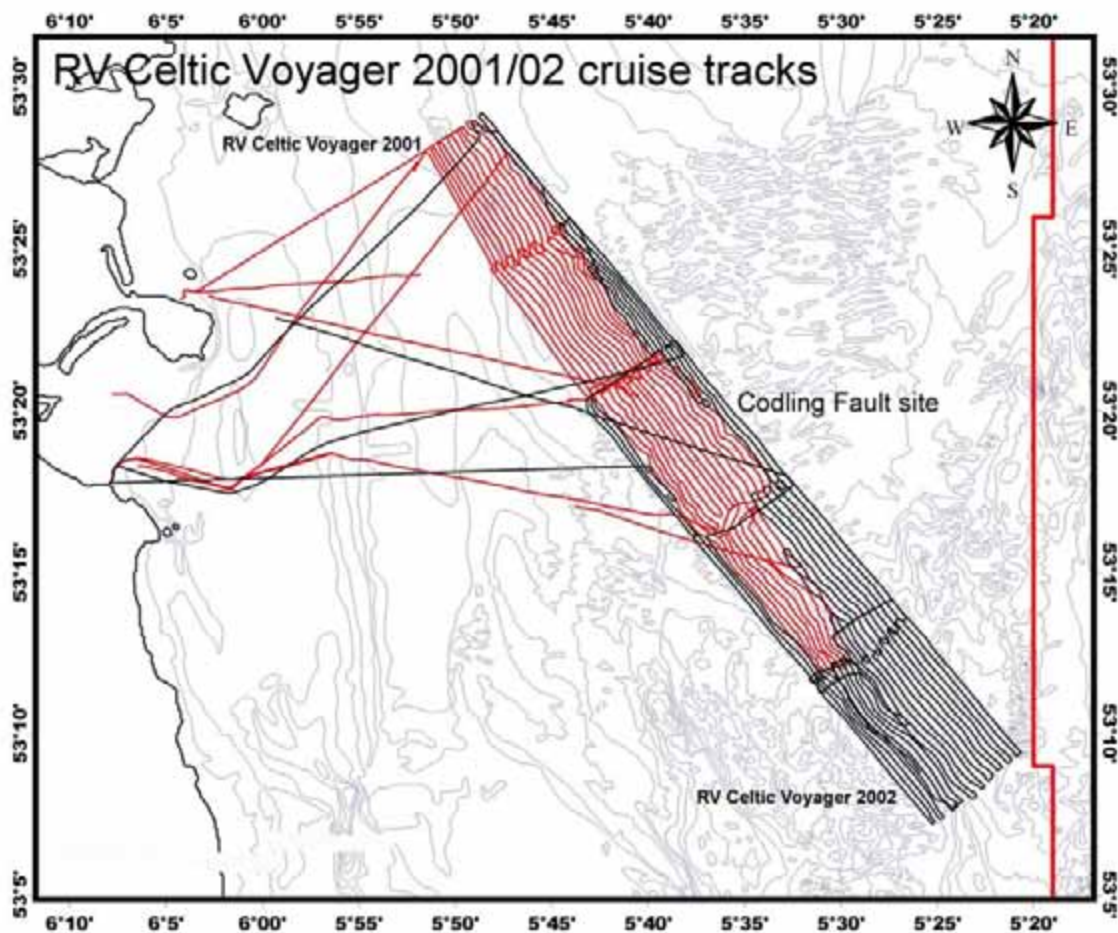


**Figure 2.10:** RV Celtic Voyager 2001/02 cruise tracks in the Codling Fault study area. The red line represents the boundary of the IRL-SEA6 sector. Bathymetric contours drawn at 10m intervals (courtesy of BGS).

### ***2.5.8 RV Celtic Voyager cruise 2002***

This cruise was undertaken between 11-12<sup>th</sup> May and 13-14<sup>th</sup> May 2002, with the aim to extend multibeam coverage of the Codling Fault and Lambay Deep study areas collected in 2001 using the Simrad EM1002 swath bathymetry system (Fig. 2.10). Collectively these two cruises mapped an area of c.310km<sup>2</sup> of seabed. This provided invaluable information on the seabed geomorphology and the seabed expression of deep structural features.

The raw multibeam data was processed using the CARIS software package by Xavier Monteys of the Geological Survey of Ireland (GSI).

## **2.6 GIS approach to data visualisation**

This project has collated, processed and analysed a considerable amount of remote sensing and ground-truthing data from IRL-SEA6. In order to assist the data analysis the study has used a Geographical Information System (GIS) approach for data integration and visualisation. Most of the GIS related work has been performed with the ArcView GIS 3.2a software package (<http://www.esri.com>). The integration of all obtained and derived datasets within the GIS environment makes possible the assessment of each particular dataset in the light of information given by other datasets and allows a comprehensive correlation between shallow gas accumulations, migration pathways and gas escape structures.

### **3. Distribution of Methane Sources**

This chapter provides an overview of the IRL-SEA6 in terms of potential sources of shallow gas. The chapter is divided into two sub-chapters describing separately the distribution of potential source rocks (Ch. 3.1) and the distribution of gas-bearing sediments (Ch. 3.2). The information presented is based on various datasets, including British Geological Survey (BGS) maps, exploration wells, seismic surveys and published data (see Ch. 2).

#### **3.1 Source rocks**

The solid geology of the Irish Sea has been previously published in the BGS 1:250,000 Solid Geology map series (Croker et al., 1982; Martindale et al., 1982; Ransome, 1982). More recently, the solid geology of part of the Irish Sea has been revised by Croker & Power (1996b) (Fig. 3.1). The details of this revision will be incorporated into the new edition of the solid geology map that is currently being prepared by the BGS with data contribution from PAD (Tappin & Croker, 1999). The general distribution of potential source rocks within IRL-SEA6 is described in section 3.1.1. Section 3.1.2 presents a concise overview of relevant information derived from exploration wells drilled in the area, while section 3.1.3 presents evidence derived from interpretation of seismic profiles.

##### ***3.1.1 General distribution of methane sources***

The majority of the Irish Sea is underlain with Carboniferous rocks that contain the main known sources of hydrocarbons. The principal source rocks are the Westphalian coal measures (gas) and the Namurian Holywell Shale (oil and possibly gas) (Croker, 1995). However, only the Westphalian source rocks have been encountered in wells within the IRL-SEA6 sector of the Irish Sea (see Ch. 3.1.2).

##### ***3.1.2 Exploration well data***

Metadata for all exploration wells that were drilled in IRL-SEA6 was summarised above (see Ch. 2.3). This section presents an overview of relevant information with regards to source rocks that could be derived from these wells (e.g. Croker, 1995; Maddox et al., 1995; Corcoran & Clayton, 1999; Floodpage et al., 2001).

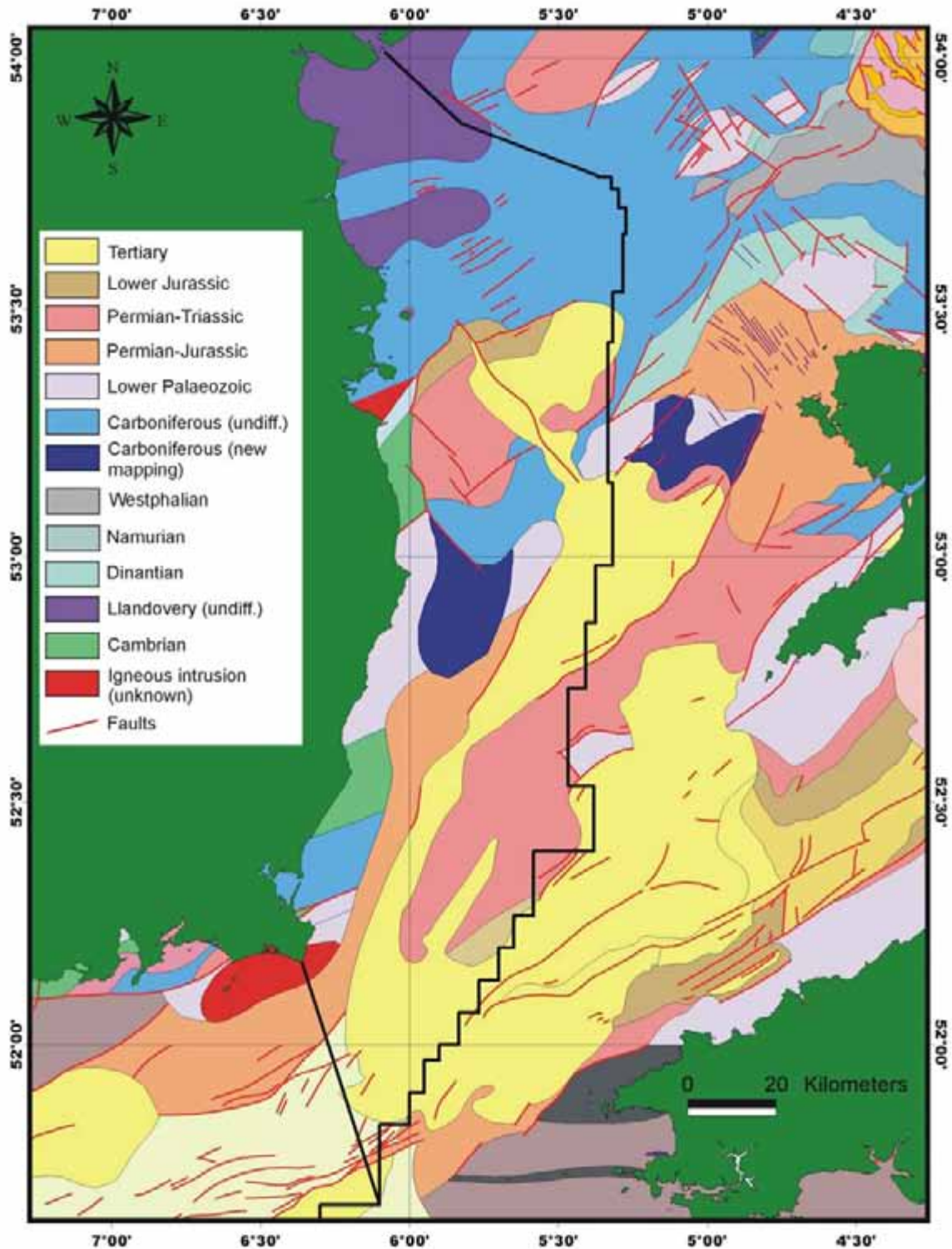


**Figure 3.1:** Solid geology of the western Irish Sea (IRL-SEA6) and adjacent areas (courtesy of BGS with new mapping after Croker & Power, 1996b). Carboniferous rocks represent the main known potential sources of methane in the area. The black line represents the boundary of the IRL-SEA6 sector.

### 3.1.2.1 Kish Bank Basin

Well 33/22-1 was drilled by Amoco in the Kish Bank Basin in 1977 (see Table 2.1 for additional information). Particulars of the source rock interval documented by this well have been previously reported by Croker (1995), and are summarised below. The hydrocarbon potential of the Kish Bank Basin has also been discussed by Dunford et al. (2001).

This well penetrated a 720m thick Upper Carboniferous Westphalian B-D succession resting unconformably on the Lower Palaeozoic Bray Group (Fig. 3.2). The fact that Westphalian A and older Carboniferous rocks are absent in well 33/22-1, together with seismic evidence, suggests the existence of a major unconformity with significant missing section (Croker, 1995).

Within the Carboniferous unit, this well (33/22-1) documents the presence of Westphalian coal (and claystone) source intervals, and fluvio-deltaic sandstones. The source rock interval contains a net 19m of coals that are also supplemented with coaly claystones, considered as good to rich gas-prone source rocks. The Westphalian is thermally mature and possesses vitrinite reflectance ( $R_m$ ) values ranging between 0.83 and 1.35% (Naylor et al., 1993), thus being at the early to peak stage of gas generation. The coal is of medium to high volatile bituminous type. During drilling gas peaks were identified across most of the seams. Sandstones within the Carboniferous interval possess a net thickness of 215m, with individual sandstone intervals being up to 22m thick. The porosity of the sandstones varies between 8-15%, averaging at about 10-13%. The highest porosity sandstones occur in the same interval as the thickest and most numerous coals. Several sandstones revealed residual oil staining and weak oil shows.

The three other wells drilled in the basin (33/17-1, 33/17-2A and 33/21-1) were not drilled deep enough to penetrate the Carboniferous, but seismic evidence suggests the presence of a Namurian section in the Kish Bank Basin (e.g. Corcoran & Clayton, 1999, Fig. 3a; Dunford et al., 2001, Fig. 11; Floodpage et al., 2001, Fig. 5a).

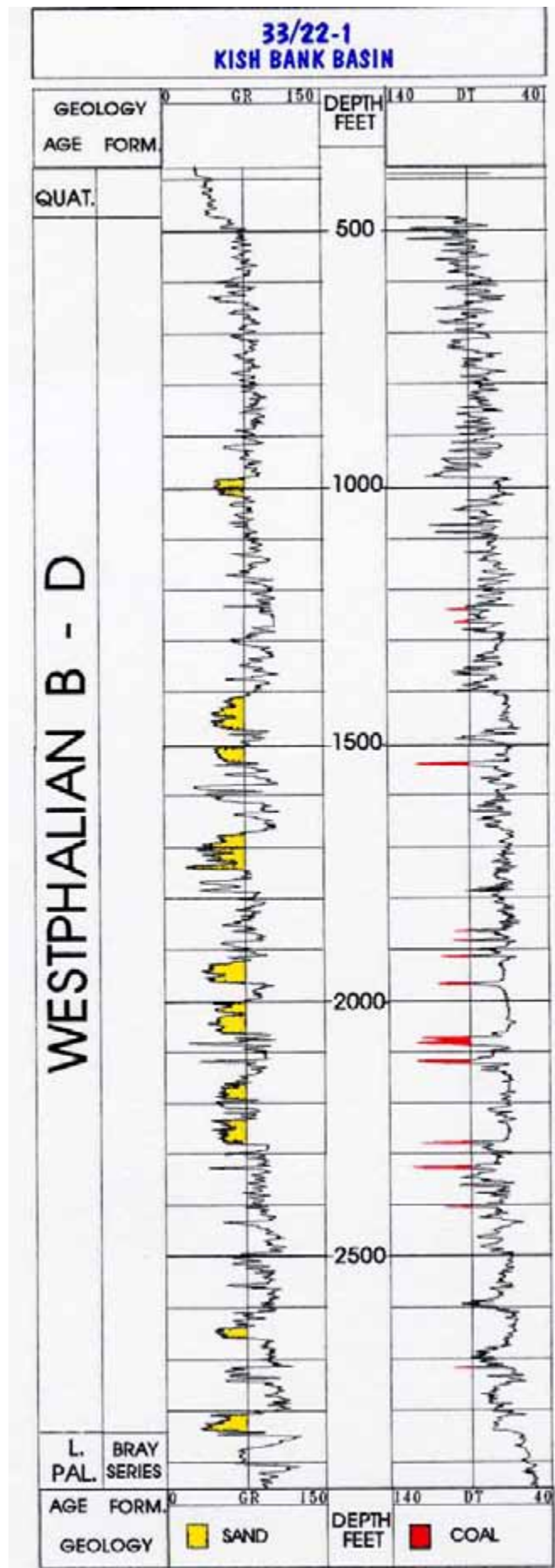


**Figure 3.2:** Carboniferous section in Well 33/22-1 showing gamma ray and sonic logs. The depth scale is in feet. See Figure 2.1 for location. (From Croker, 1995: Fig. 9.)

### 3.1.2.2 Central Irish Sea Basin

Wells drilled in the Central Irish Sea Basin (CISB) are as follows: 42/8-1, 42/12-1, 42/12-2, 42/16-1 and 42/17-1A (Fig. 2.1). Metadata information for these wells has been summarised above in Table 2.1. Assessments of the hydrocarbon prospectivity of the Central Irish Sea Basin with particular reference to the existing well data have been previously published by Maddox et al. (1995), Floodpage et al. (2001) and Green et al. (2001). The relevant information that can be derived from these wells with regards to source rocks is summarised below.

The existing wells did not document the presence of any Namurian deposits, although wells 42/12-1, 42/16-1 and 42/17-1A demonstrated the presence of the coal-prone Westphalian B-C succession, which is also present in the Kish Bank Basin (see Ch. 3.1.2.1). Wells drilled in the CISB also documented reddened Carboniferous rocks of probable Westphalian D to Stephanian age. These can be correlated with identical rocks identified in the KBB and onshore North Wales and the West Midlands (Naylor et al., 1993). In well 42/17-1A the Westphalian succession appears to rest unconformably on Lower Carboniferous Dinantian deposits due to the absence of Westphalian A and Namurian rocks.

The Westphalian B-C succession in the CISB is composed of shales and coals, which represent potential oil- and gas-prone source rocks as implied by hydrogen indices. These rocks possess total organic carbon (TOC) values between 2-74%, pyrolysis S<sub>2</sub> between 360-69,500ppm and hydrogen indices of 55 to 400 (Maddox et al., 1995).

Well 42/17-1A has documented gas shows within the lower part of the Upper Carboniferous (non-reddened) succession. Moreover, wells 42/16-1 and 42/17-1A have also detected gas shows within the Upper Carboniferous (reddened) sequence.

The vitrinite reflectance in the uppermost Carboniferous throughout the CISB indicates that at present the source rocks are at or near peak gas generation levels (Maddox et al., 1995: Fig. 10).

The Upper Carboniferous source rocks in the CISB are generally overlain by the Triassic Sherwood Sandstone Group (SSG) reservoir rocks, which in turn are sealed with evaporites and shales of the Triassic Mercia Mudstone Group (MMG).

Although just outside the IRL-SEA6 area, reference should also be made here to a gas discovery in UK block 103/1 (St. George's Channel) awarded in 1993 as part of the DTI's 14<sup>th</sup> Licensing Round. The first well (103/1-1) in this block was drilled by Marathon in 1994 and tested gas and oil from Middle Jurassic reservoirs. This discovery was named the Dragon Field and is located approximately 3km from the Ireland/UK median line. The second appraisal well in this block will be drilled by Marathon in 2005 (Marathon Oil U.K. Ltd., 2004). The preliminary site surveys did not document any direct evidence of shallow gas in the immediate vicinity of the well site (<200m). Given the nature of the tested hydrocarbons, it is assumed that the source rocks are Lower Jurassic in age, as is the case further SW in the Celtic Sea.

#### 3.1.2.3 Conclusions

Well data from IRL-SEA6 documents the existence of reservoir, seal (cap) and source rocks. The source rocks are represented by Carboniferous shales and coals and reservoir rocks are mainly represented by the Lower Triassic Sherwood Sandstone Group. The reservoir rocks are sealed with the Triassic Mercia Mudstone Group consisting of evaporites and shales. However, the distribution of Triassic reservoir and cap rocks is not uniform throughout the IRL-SEA6, and they are largely absent in the northern part of the IRL-SEA6. This tends to support a model for a thermogenic origin for the shallow gas, which shows an extensive presence in the form of gas fronts and plumes in the northern part of IRL-SEA6 (see Ch. 5).

#### ***3.1.3 Evidence from seismic data***

IRL-SEA6 has been extensively surveyed with oil industry 2D seismic surveys (see Ch. 2.2 & Fig. 2.1). This seismic data complements exploration well data and provides valuable information for the assessment of the distribution and proximity to the seabed of potential source rocks. Presented below are some selected examples of seismic profiles from different parts of IRL-SEA6 (see Fig. 3.3 for location).

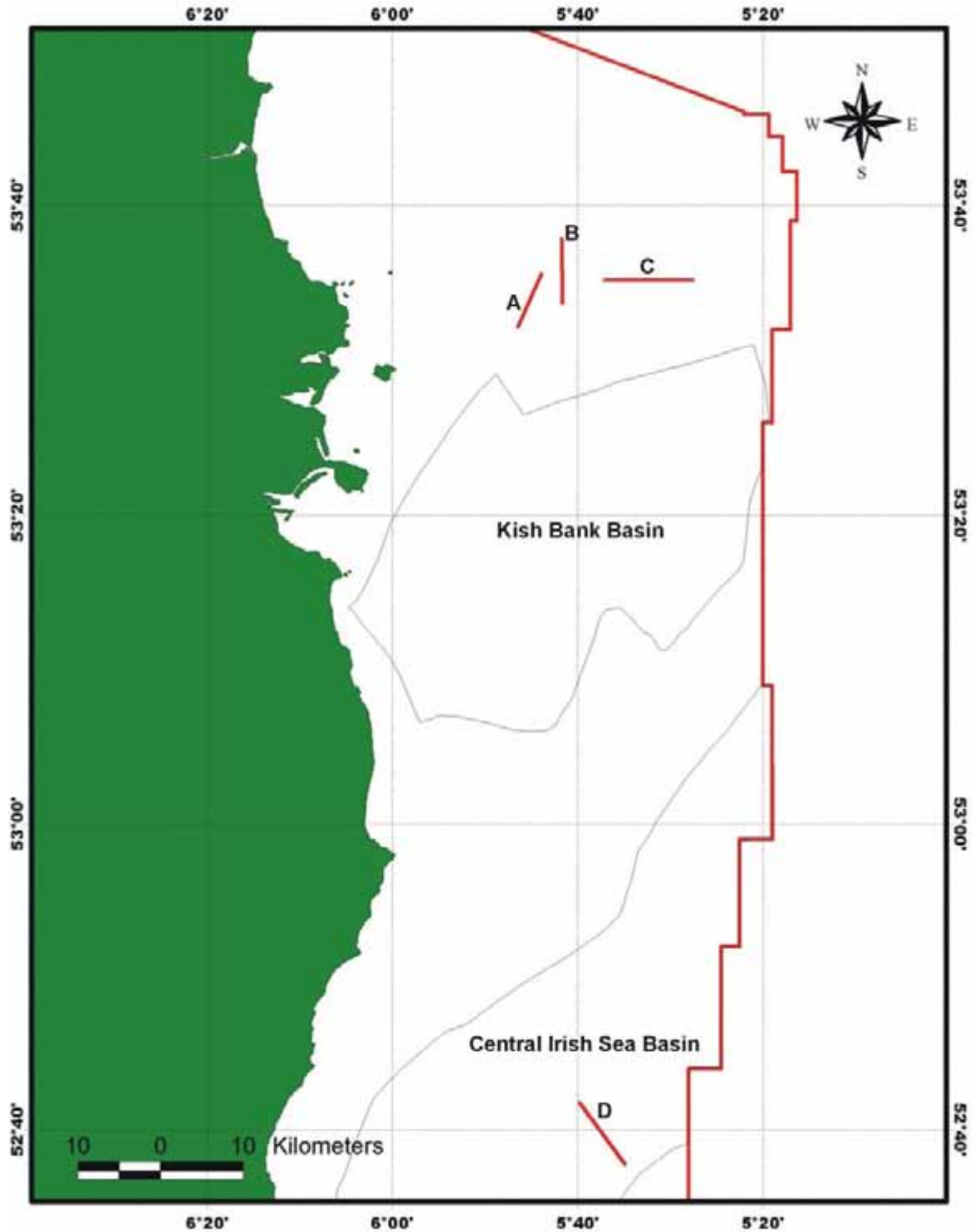


**Figure 3.3:** Map showing the location of selected seismic profiles presented on Figures 3.4-3.7, and also showing the outline of Mesozoic sedimentary basins. The red line represents the boundary of the IRL-SEA6 sector.

Figures 3.4 to 3.6 show parts of three conventional seismic lines from the northern part of IRL-SEA6 located north of the Kish Bank Basin (from Croker, 1995). Seismic line A

(Fig. 3.4) reveals a thick reflective Carboniferous sequence gently dipping to the north-east. The interpretation suggests that the thickness of the Upper Carboniferous on this line is approximately 1s 2XTT (c.2km). No Triassic reservoir or cap rocks are present in this area.

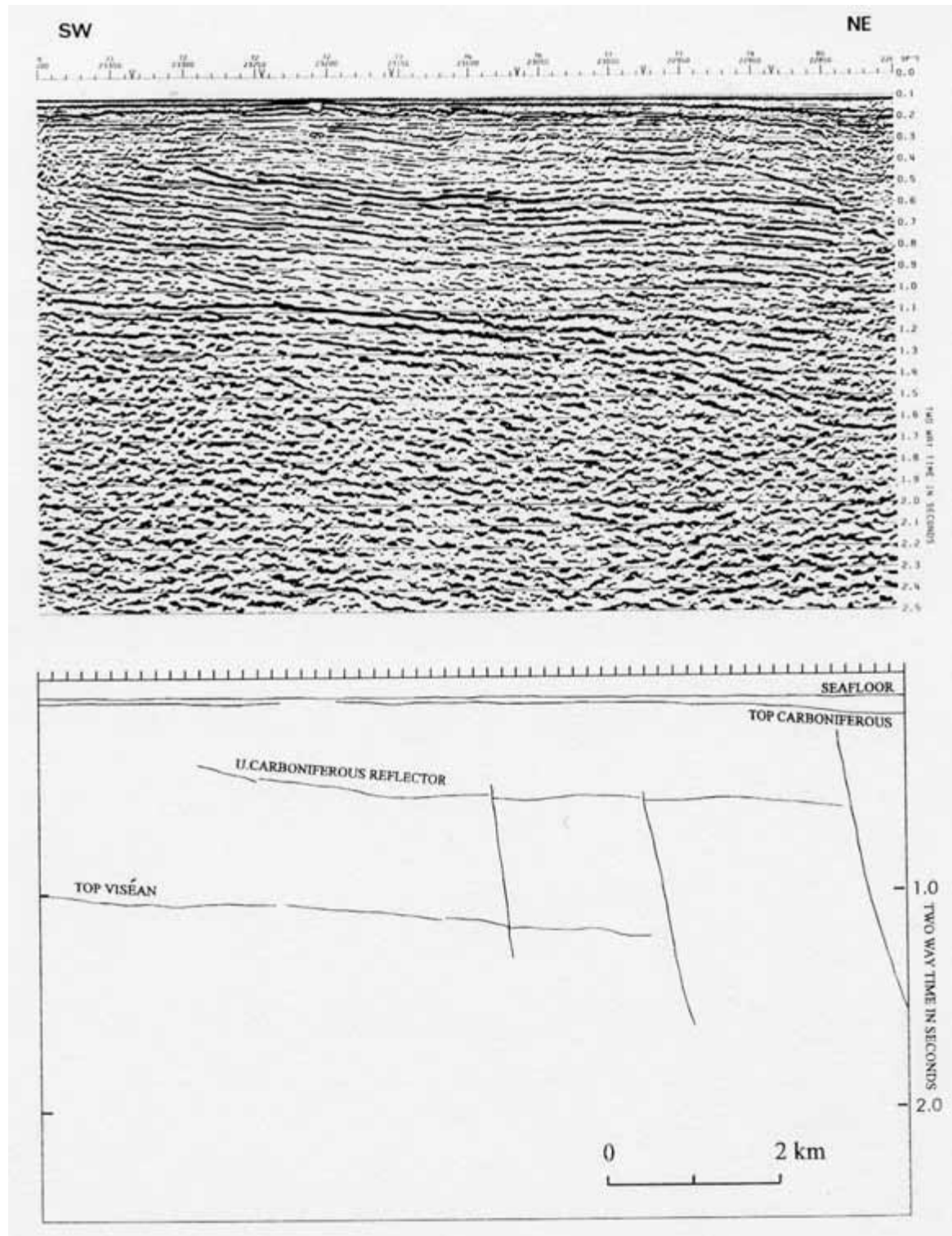


**Figure 3.4:** Seismic line A with interpretation. See Figure 3.3 for location. (From Croker, 1995: Fig. 11.)

Seismic line B (Fig. 3.5) shows a well-defined top Carboniferous (base Quaternary) reflector. The Quaternary-Recent sediment cover is approximately 100-140ms 2XTT (c.90-125m) thick. An apparent seafloor anomaly is imaged on the southern part of the profile near SP1000 and a shallow amplitude anomaly can be seen at SP610-660. Both anomalies occur in close proximity to sub-cropping reflections and near faults.

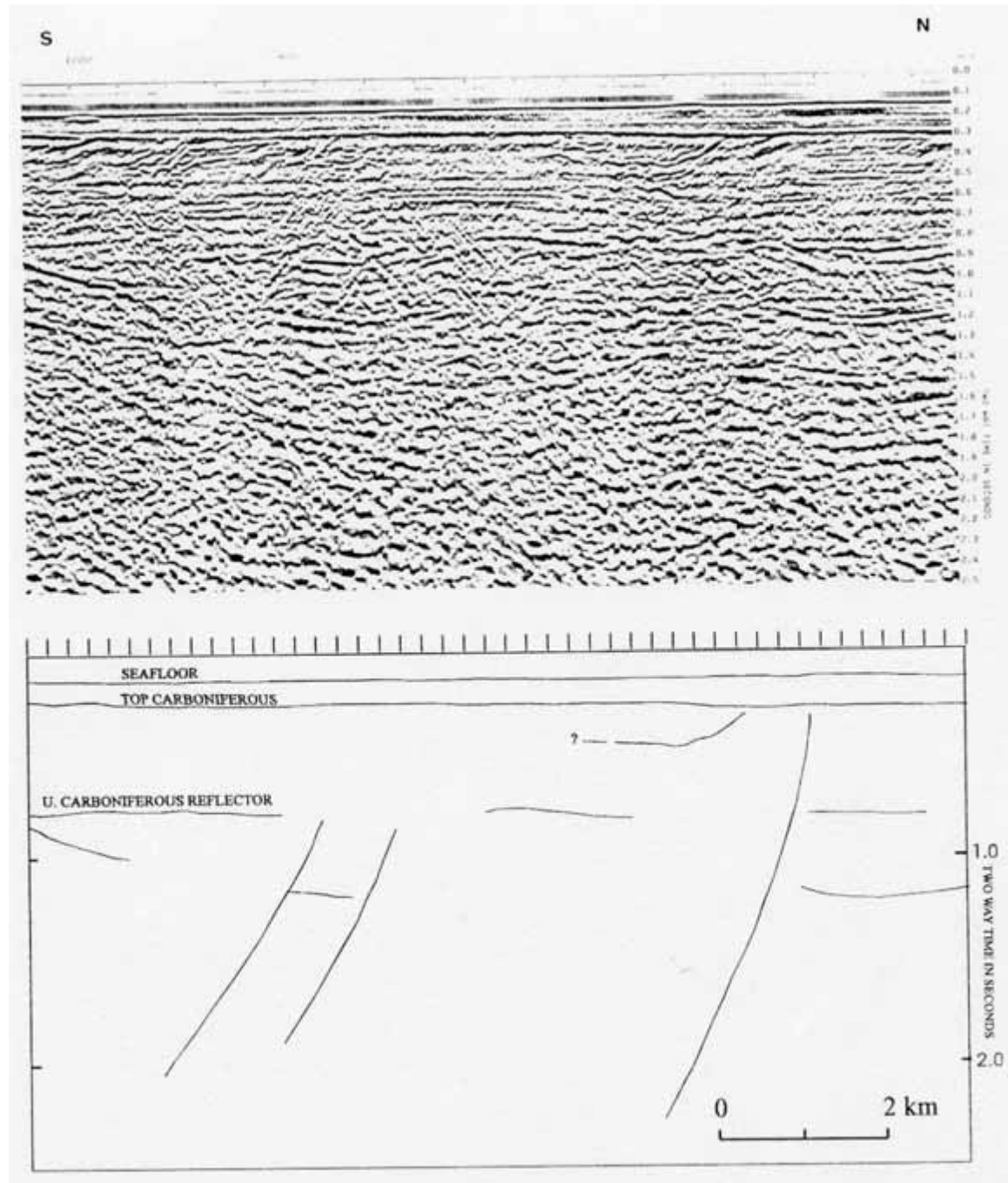


**Figure 3.5:** Seismic line B with interpretation. See Figure 3.3 for location. (From Croker, 1995: Fig. 13.)

Seismic line C (Fig. 3.6) images apparent seafloor anomalies related to obvious faults in the proximity of SP400 and SP720. The Carboniferous section appears to be at least 1.5s 2XTT (c.3km) thick on this line and there is extensive evidence of faulting. Boomer and sparker surveys of the same area indicated extensive gas fronts and plumes occurring approximately 15m beneath the seafloor (see Ch. 5).

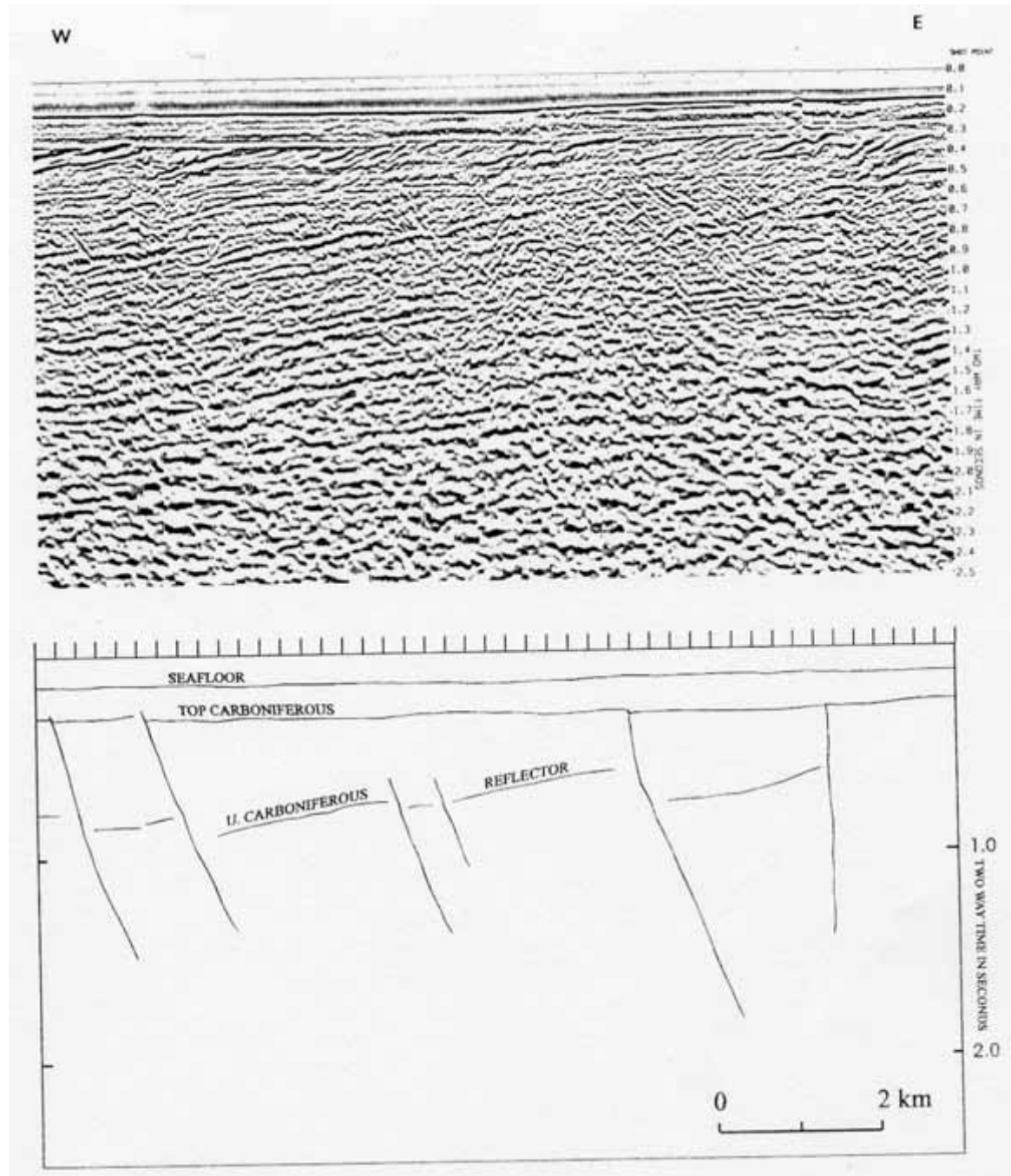


**Figure 3.6:** Seismic line C with interpretation. See Figure 3.3 for location. (From Croker, 1995: Fig. 14.)

Figure 3.7 shows a seismic line from the southern part of the IRL-SEA6 area which runs through the location of well 42/12-2 drilled in the Central Irish Sea Basin. This profile images well-defined Carboniferous reflectors, suggesting that the Upper Carboniferous sequence in this area is about 0.6s 2XTT (c. 1200m) thick. This is overlain by the Triassic Sherwood Sandstone Group and Triassic Mercia Mudstone Group, and unconformably covered with Quaternary-Recent sediments. This seismic line also shows evidence of faults within the Carboniferous unit, some of which reach to seabed.

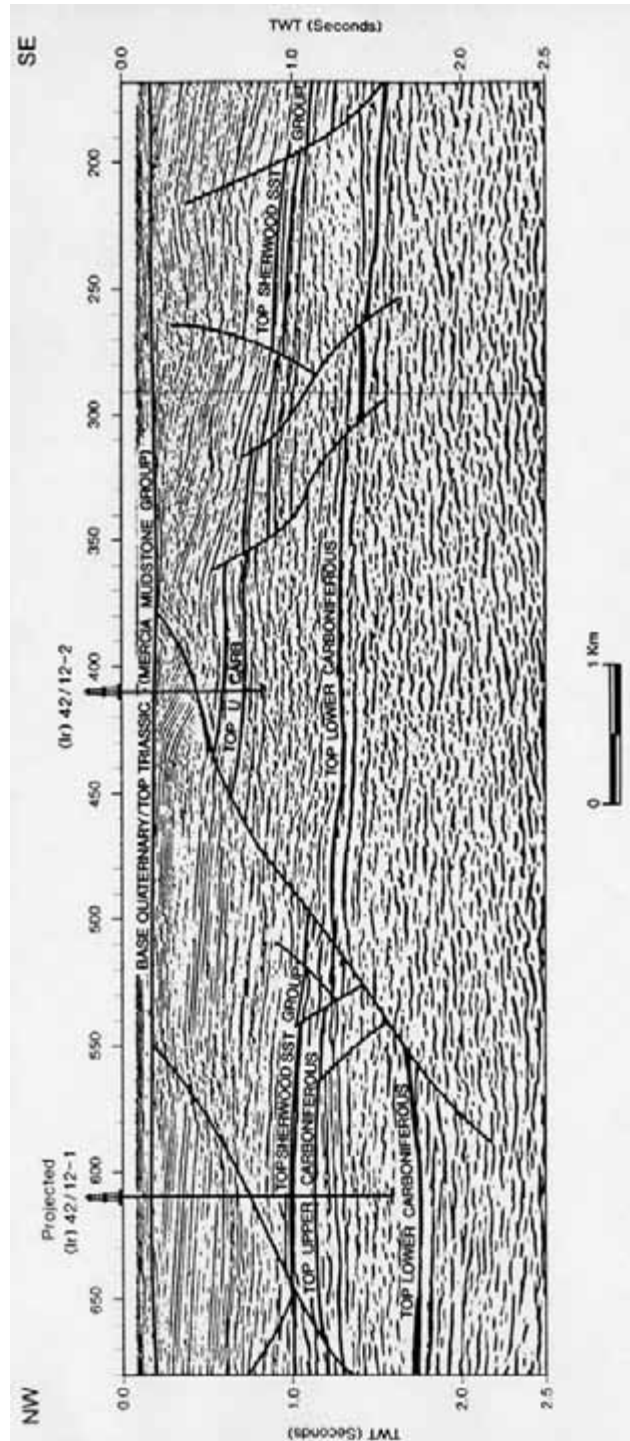


**Figure 3.7:** Seismic line D (HIL-86-15) with interpretation. See Figure 3.3 for location. (From Maddox et al., 1995: Fig. 5.)

### **3.2 Gas-bearing sediments**

The general distribution of the seabed sediment types in the Irish Sea has been previously published in the BGS 1:250,000 Seabed Sediments map series (James, 1988; James, 1990). The deeper sedimentary structure of the Irish Sea has been presented on the BGS Quaternary Geology map series (Wingfield et al., 1990a; Wingfield et al., 1990b). The information derived from these maps, complimented by remotely sensed and ground-truthing surveys, contributes towards our understanding of the distribution and types of gas escape structures documented by this study.

The thickness of Quaternary sediments in the western Irish Sea varies between 50-150m. However, areas characterised by thinner Quaternary cover or by its total absence (rock outcrops) are also present. GIS integration of the sediment distribution and thickness along with documented evidence of sub-surface shallow gas accumulation and migration does not reveal any obvious link between the presence of shallow gas and any particular sediment types. Figure 3.8 illustrates that sub-surface gas accumulations can be found in both muddy and sandy areas. However, the sediment type has a significant impact on the types of gas-related seabed structures found in the area.

Pockmarks have only been documented in the northern part of IRL-SEA6 where the seabed consists mainly of muddy sediments and hence is suitable for pockmark formation. Furthermore, in cases of active sub-surface gas migration the muddy area may accommodate mud diapirs (see Ch. 4.3 & Ch. 6). To the south of the muddy area, the seabed is covered with sandy sediments thus making it unsuitable for pockmark formation. However, gas seepage is able to facilitate the creation of carbonate mounds composed of sand cemented with methane-derived authigenic carbonate (MDAC) precipitate (see Ch.4 & Ch. 6). Further south again, due to enhanced tidal currents the seabed is mainly covered with coarse sediments with patchy areas of high-energy bedforms. Therefore, the chance of gas escape structures not being removed by seabed erosion or buried by active sediment transport is quite low. Nevertheless, some of the high-energy bedforms (abnormal sand waves) have been tentatively associated with gas seepage (Croker, 1994) (see Ch. 6).

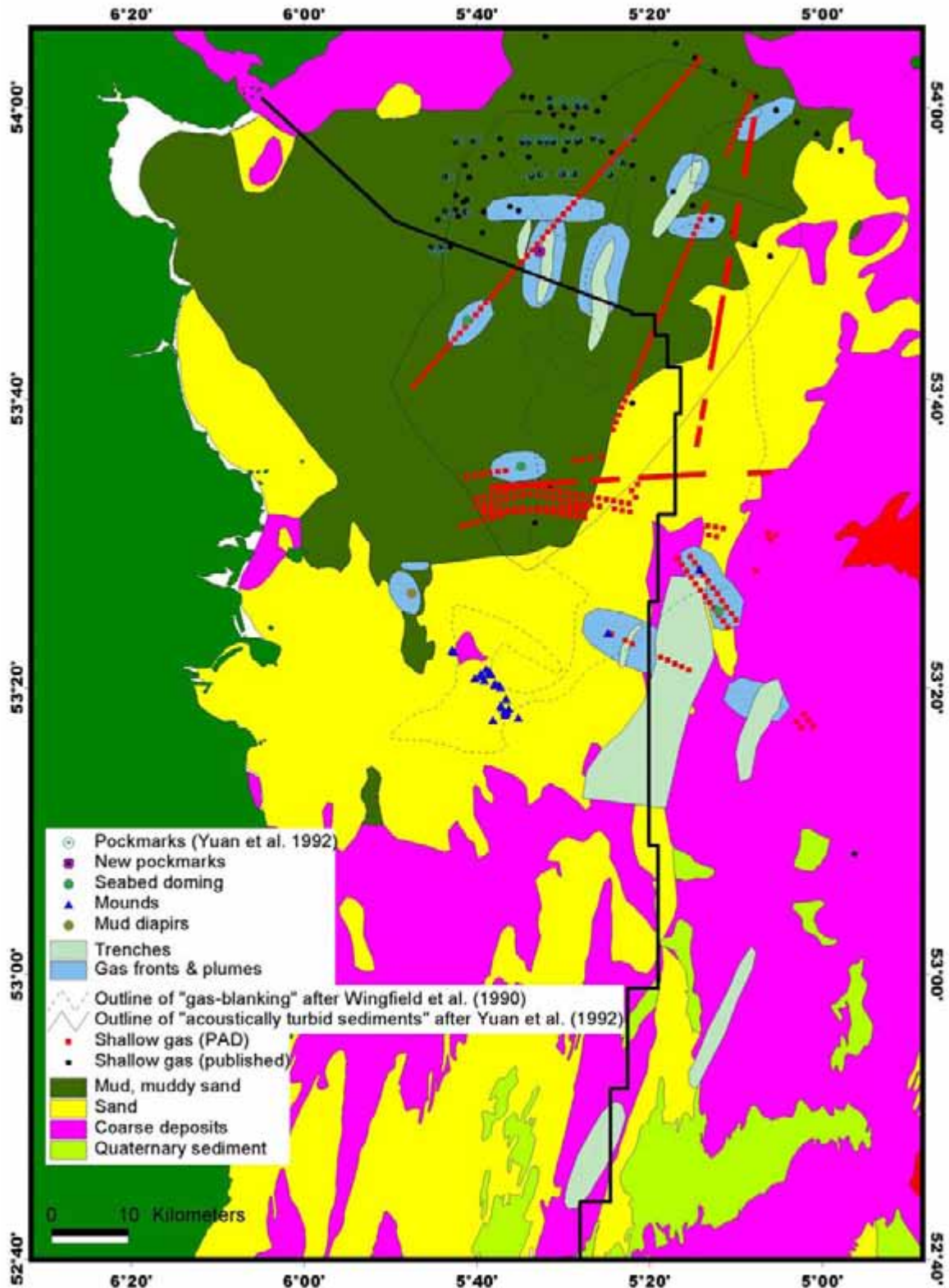


**Figure 3.8:** Map showing the distribution of sediment types, gas accumulations and gas escape structures in the northern part of the IRL-SEA6 area.

## **4. Gas Migration Pathways**

Gas generated in source rocks generally migrates upward via permeable carrier beds and faults. In the case of thermogenic methane, it can be supplied to the upper sediment layer and seafloor via migration along major regional faults and less apparent faults of localised significance. Gas migration can also occur where unconsolidated sediments are underlain with subcrops of methane-generating source rocks. Other migration pathways may be represented by gas chimneys, and faulting or disruption of sediments due to salt and mud diapirism. However, mud diapirism itself may be triggered by gas escape. Diapiric structures, created by excessive fluid pressure, are likely to generate a fracture pattern in surrounding sediments thus providing pathways for gas migration. The existing data suggests that most of the above-mentioned types of gas migration pathways are present in IRL-SEA6. Salt diapirism is known to occur in the Cardigan Bay/St. George's Channel area but is not covered by this report.

### **4.1 Major faults**

Major faults of regional significance can be observed on the Bouguer gravity map of Ireland and surrounding waters presented by Readman et al. (1995). Particularly well-pronounced are the Codling, Lambay, Dalkey and other faults that bound the Kish Bank and the Central Irish Sea basins.

Faults within the IRL-SEA6 sector have also been shown on the BGS solid geology maps (Croker et al., 1982; Martindale et al., 1982; Ransome, 1982), which are shown on Figure 4.1.

The Codling Fault Zone was surveyed in detail using multibeam and other methods, and is described separately in Ch. 4.3.

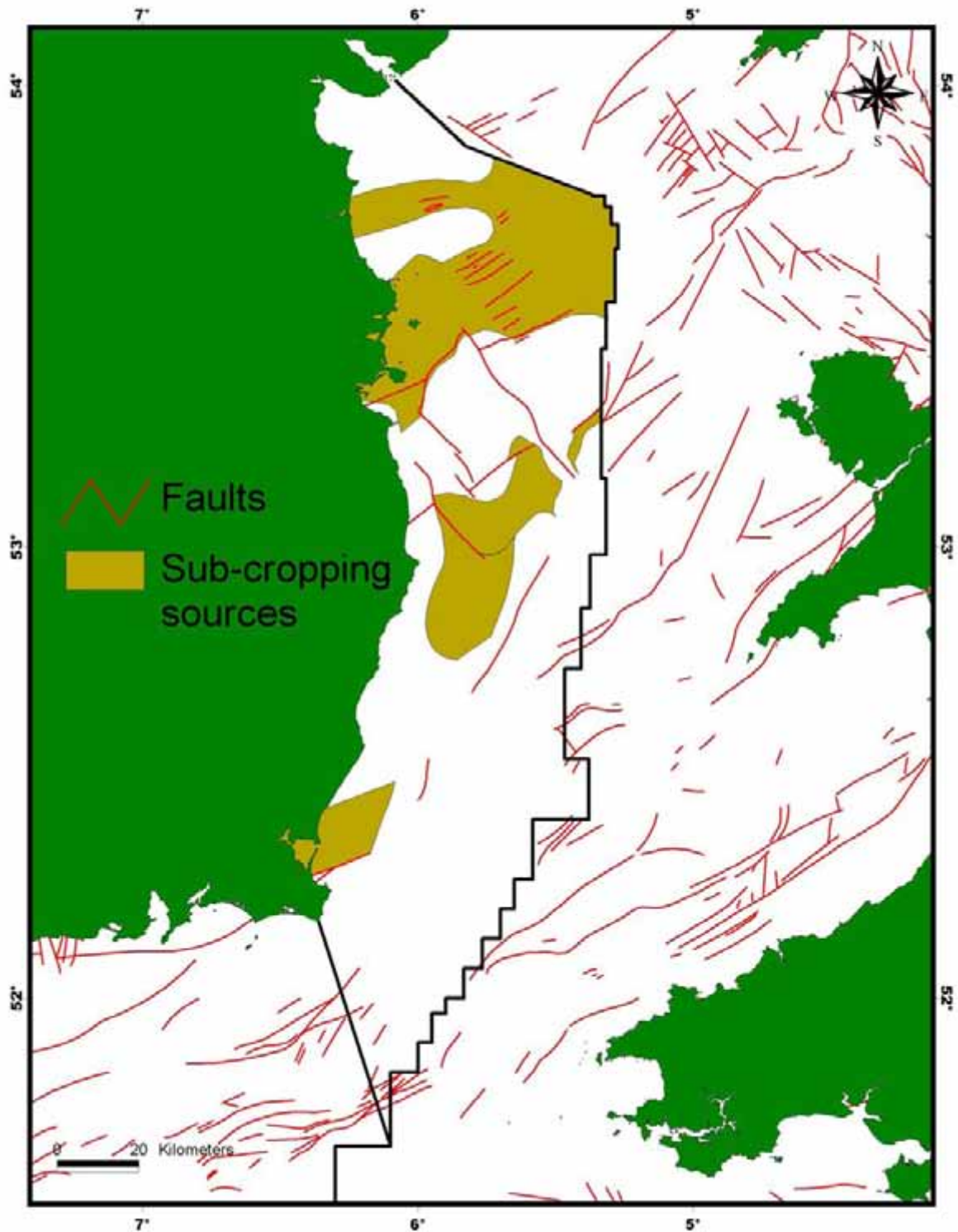


**Figure 4.1:** Map showing distribution of potential migration pathways (faults) and subcropping Carboniferous source rocks in the western Irish Sea (courtesy of BGS with new mapping after Croker & Power, 1996b). The black line represents the boundary of the IRL-SEA6 sector.

#### **4.2 Faults observed on conventional seismic data**

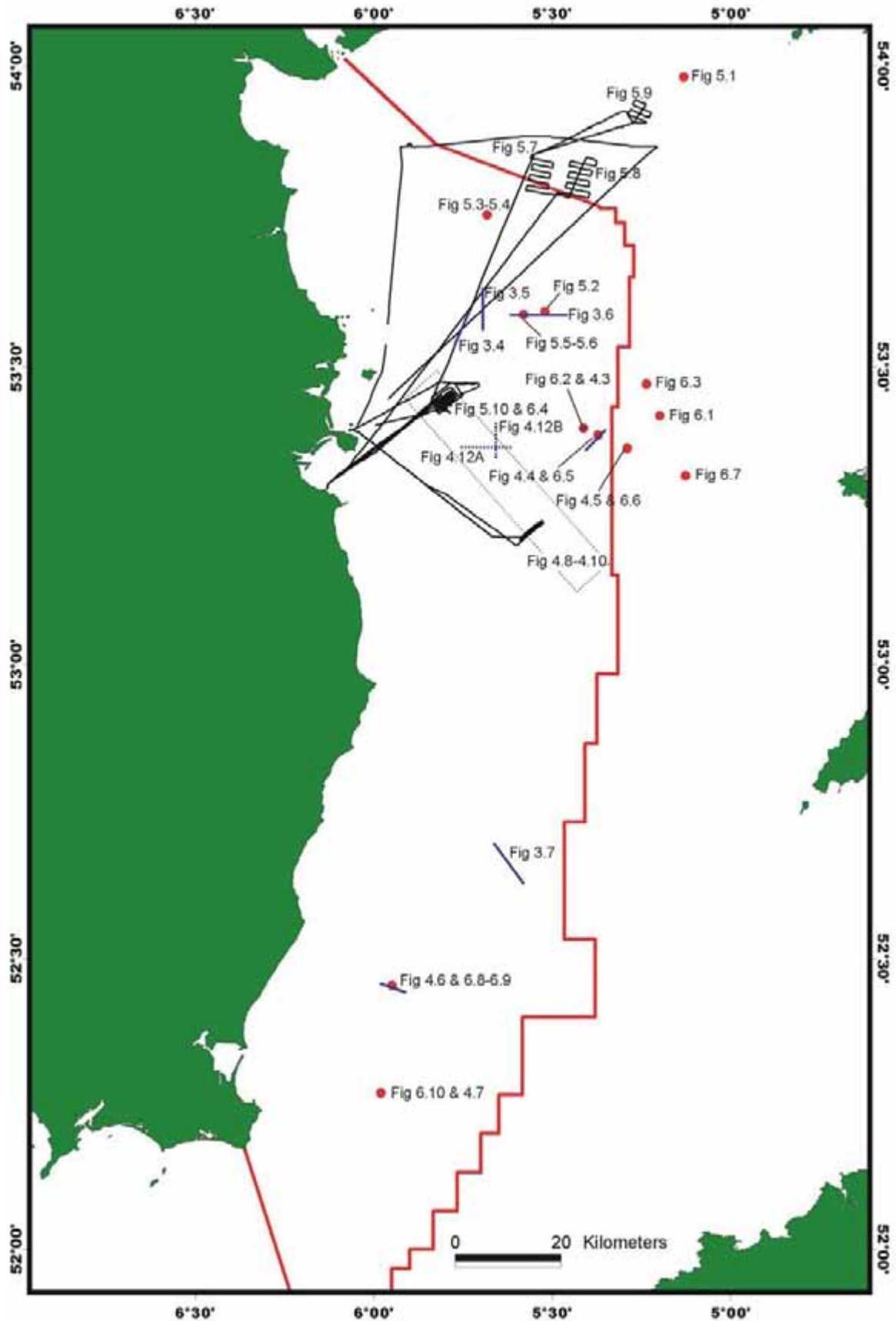
Visual analysis of conventional seismic profiles (Fig. 2.1) provides extensive evidence of numerous faults fracturing Carboniferous and Jurassic successions with some reaching the seafloor. Moreover, the spatial distribution of many of these faults coincides with gas-related phenomena mapped by shallow penetration seismic methods. Presented below are some selected examples of seismic lines that demonstrate such faults. The locations of the seismic sections described below are indicated on Figure 4.2.

Figure 4.3 presents part of conventional seismic line JSMANX-160C imaging an area in the vicinity of what is thought to be a seep mound, the KBA (see Ch. 6). This line, although of poor quality, shows a fault reaching seafloor just underneath the location of the seep mound. One of the reflectors was also interpreted to represent the shallow gas front based on the high-resolution data across this feature (Fig. 6.2).

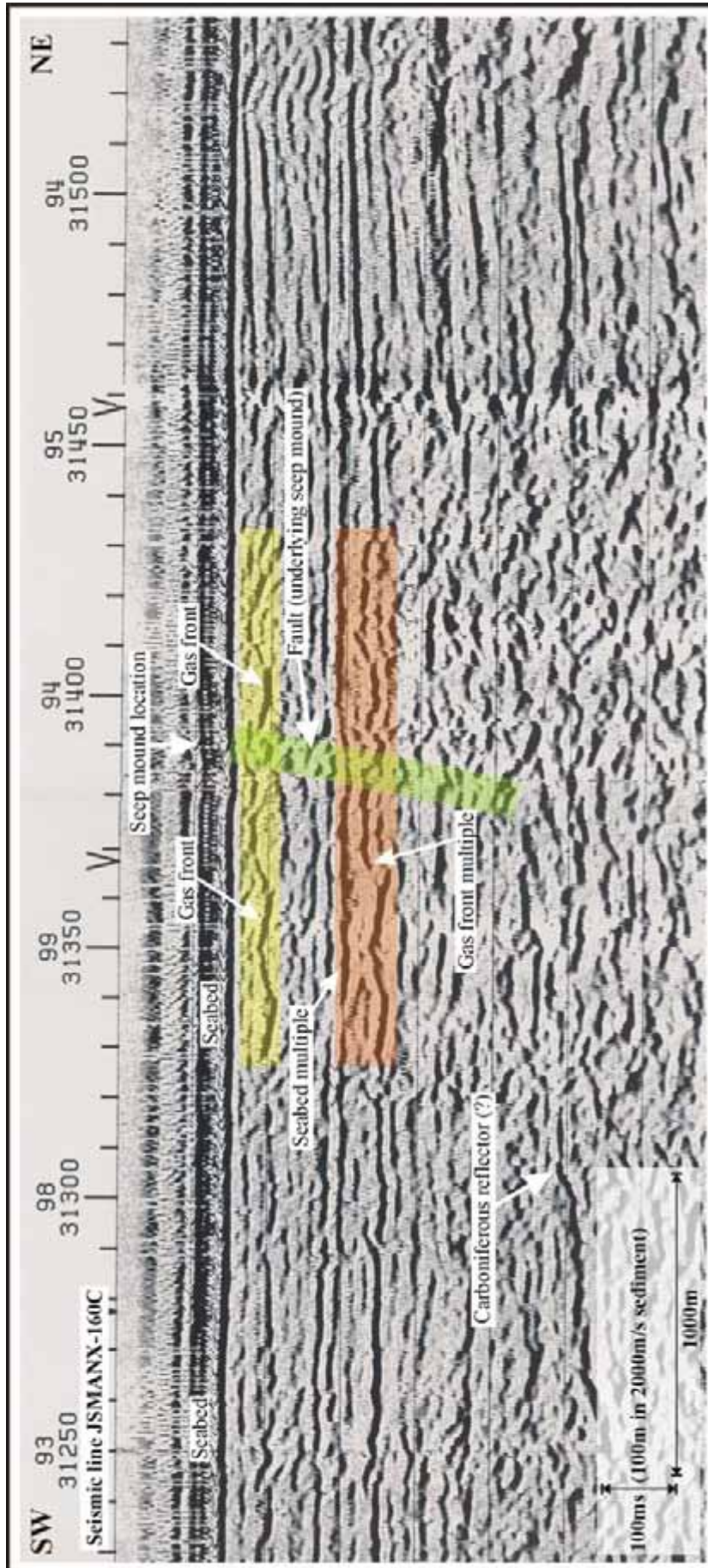
Figure 4.4 presents part of conventional seismic line JSMANX-146 illustrating the irregular seabed morphology of the Western Trench. An apparent Upper (?) Carboniferous reflector can be seen in the left part of the image. Some faulting can also be interpreted below the trench thus providing migration pathways from Carboniferous source rocks to the seabed.

Figure 4.5 presents part of conventional seismic line CB92-5 illustrating the irregular seabed morphology of the Central Trench. Some faulting of sub-surface reflectors is apparent below the trench. The Central Trench appears to coincide with the subcrop of the dipping Carboniferous reflectors.

Figure 4.6 shows part of conventional seismic line C42/85-10. This line images a tentatively identified Jurassic reflector and illustrates faults extending to seabed from the Jurassic interval. The location of the right-hand fault coincides with the occurrence of an abnormal sand wave (see Fig. 6.8, 6.9).



**Figure 4.2:** Map showing location of figures referred to in Chapters 3, 4, 5 and 6. The red line represents the boundary of the IRL-SEA6 sector.



**Figure 4.3:** Part of conventional seismic line JSMANX-160C adjacent to the Kish Bank Seep Mound also shown on Fig. 6.2. The position of the gas front, fault underlying seep mound and possible Carboniferous reflector are labelled. (From Croker, 1994 (Fig. 13) with additional interpretation.)

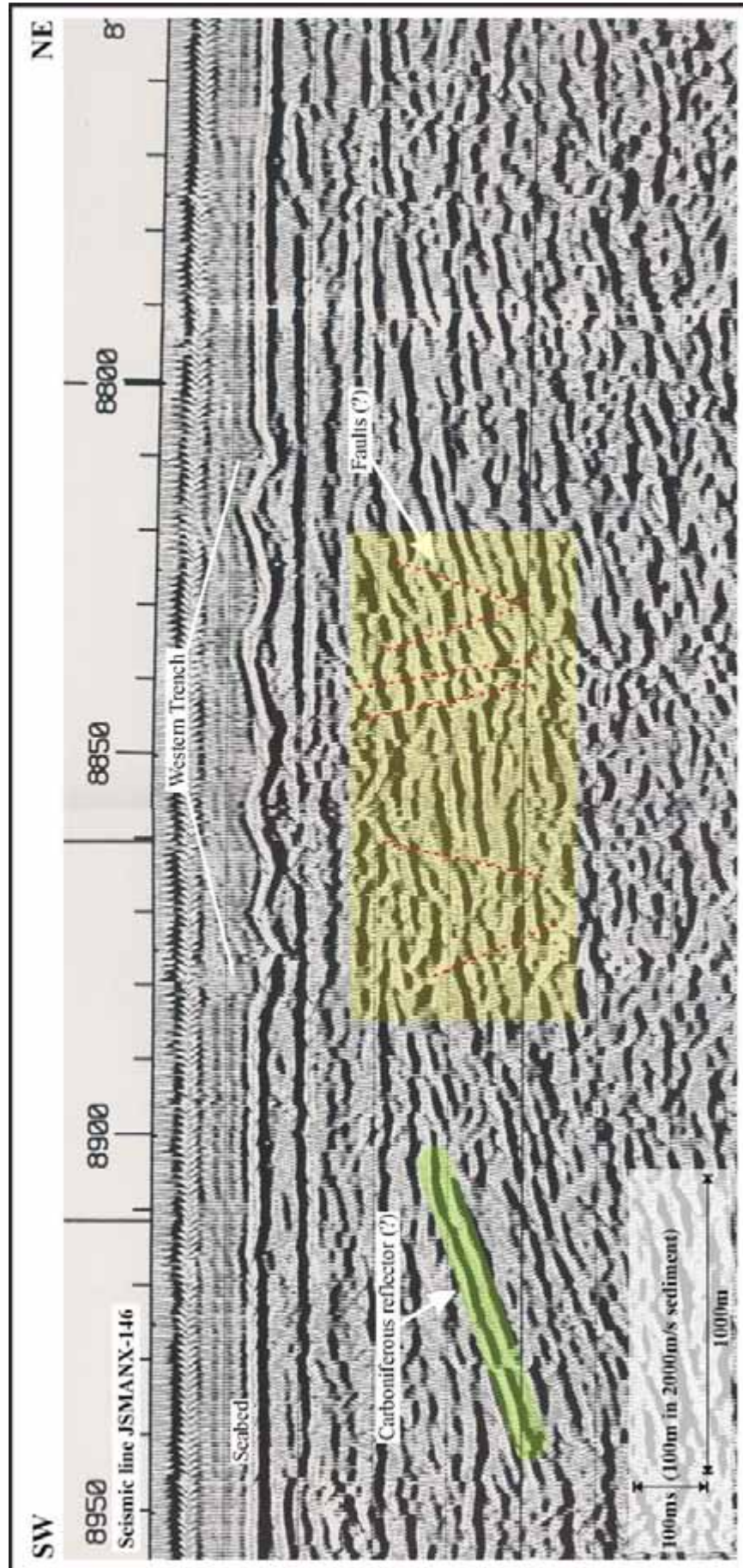


**Figure 4.4:** Part of conventional seismic line JSMANX-146 illustrating irregular seabed morphology of the Western Trench. The apparent Carboniferous reflector can be seen in the left part of the image. (From Croker, 1994 (Fig. 15) with additional interpretation.)

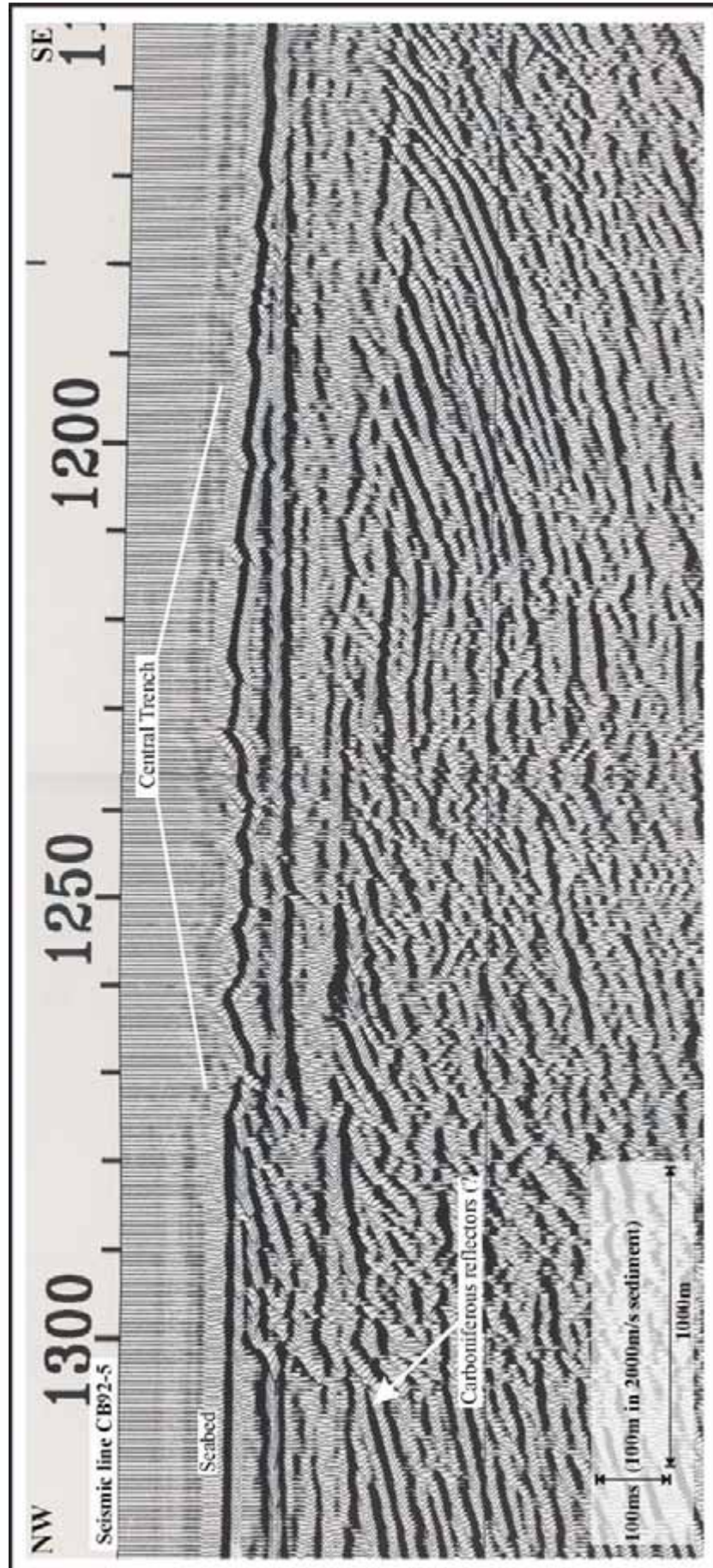


**Figure 4.5:** Part of conventional seismic line CB92-5 illustrating the irregular seabed morphology of the Central Trench, which appears to coincide with the subcrop of the dipping Carboniferous reflectors. (From Croker, 1994 (Fig. 17) with additional interpretation.)

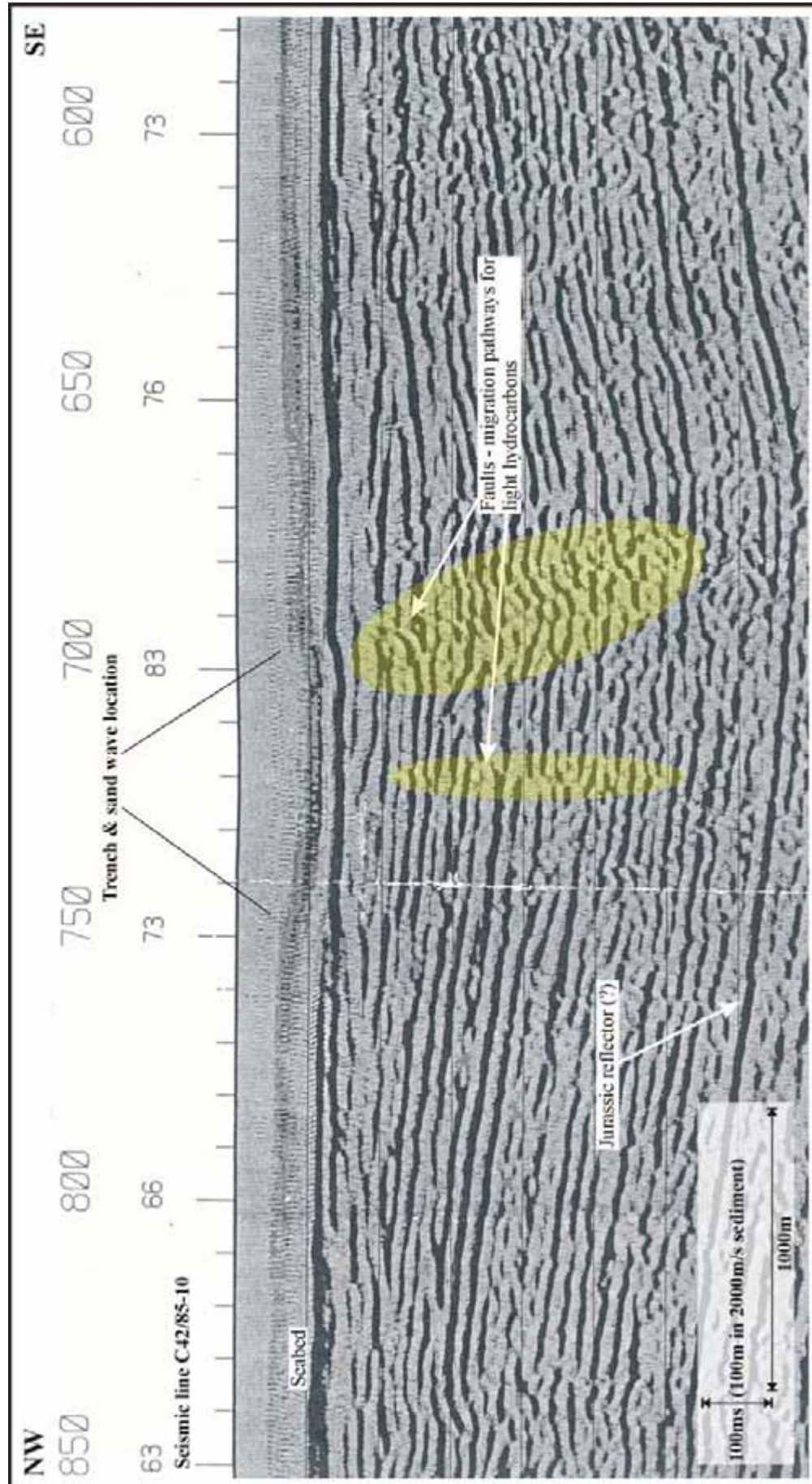


**Figure 4.6:** Part of conventional seismic line C42/85-10 showing faults extending to surface from the Jurassic interval. It is speculated that these might represent migration pathways for light hydrocarbons. The sand wave and trench occur within the indicated interval between SP 700-750. (From Croker, 1994 (Fig. 24) with additional interpretation.)

Figure 4.7 shows part of a high-resolution seismic line GH85-41-01. This line shows the nature of the bedrock subcrop and confirms the presence of a fault below the large sand wave (at SP 270). The dipping reflectors are of Middle to Lower Jurassic age. See also Fig. 6.10 for further details.

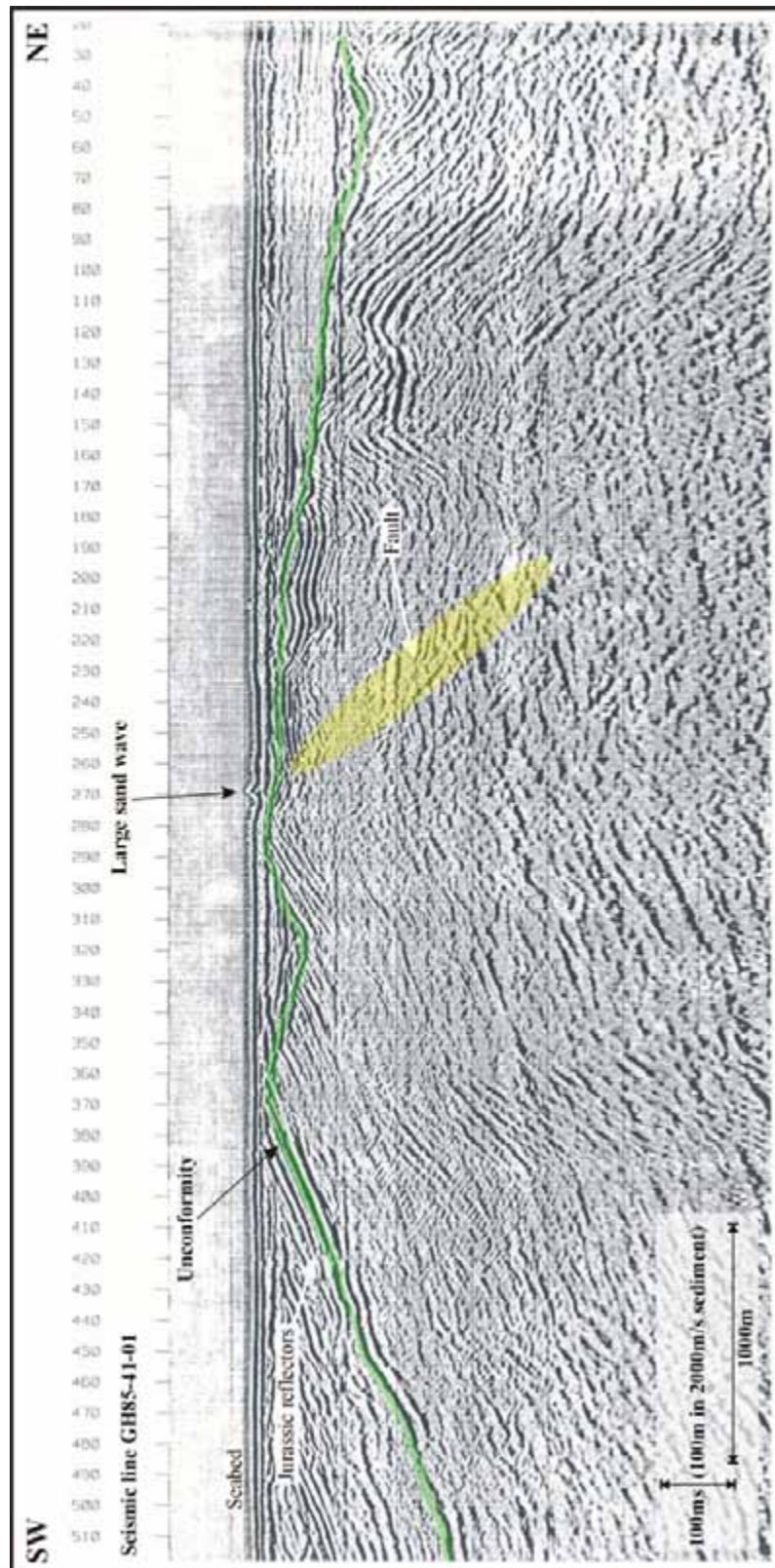


**Figure 4.7:** Part of high resolution seismic line GH85-41-01 showing the nature of the bedrock subcrop and confirming the presence of a fault below the large sand wave (at SP 270). The dipping reflectors are of Middle to Lower Jurassic age. (From Croker, 1994 (Fig. 26) with additional interpretation.)

Additional information with regards to the distribution of faults identified on seismic surveys within IRL-SEA6 can be found in Corcoran & Clayton, 1999; Maingarm et al., 1999; Dunford et al., 2001; Floodpage et al., 2001 and Izatt et al., 2001.

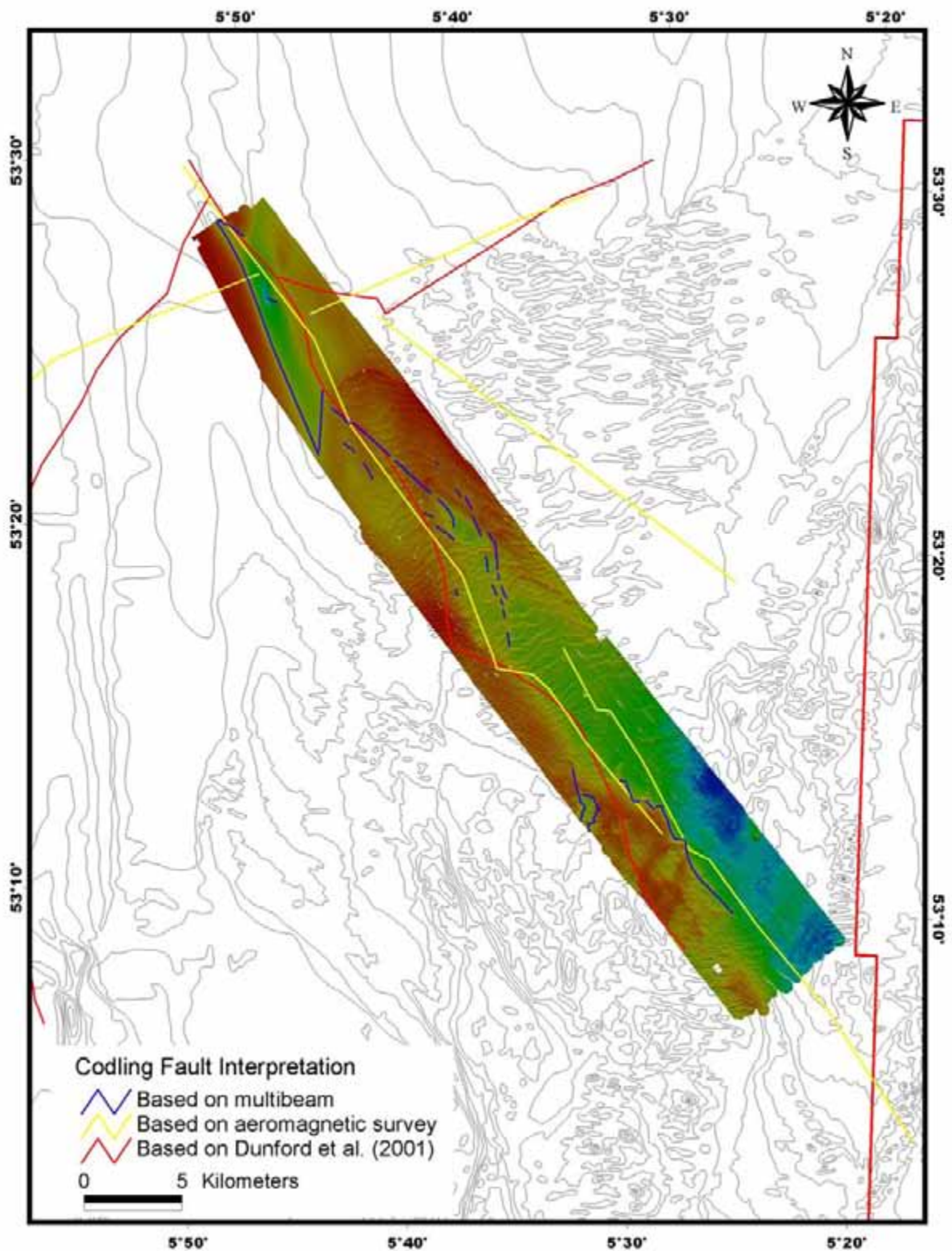
### **4.3 Multidisciplinary mapping of the Codling Fault**

The Codling Fault area was the focus of several PAD research cruises and has been surveyed using multibeam, sidescan sonar, video truthing and seabed sampling (see Ch. 2). In addition, GeoChirp sub-bottom profiler data have been obtained from the Lambay Deep located on the northern trace of the Codling Fault. The datasets collected from the Codling Fault area, together with the conventional seismic data, provided evidence of gas migration and gas escape structures coincident with the fault.

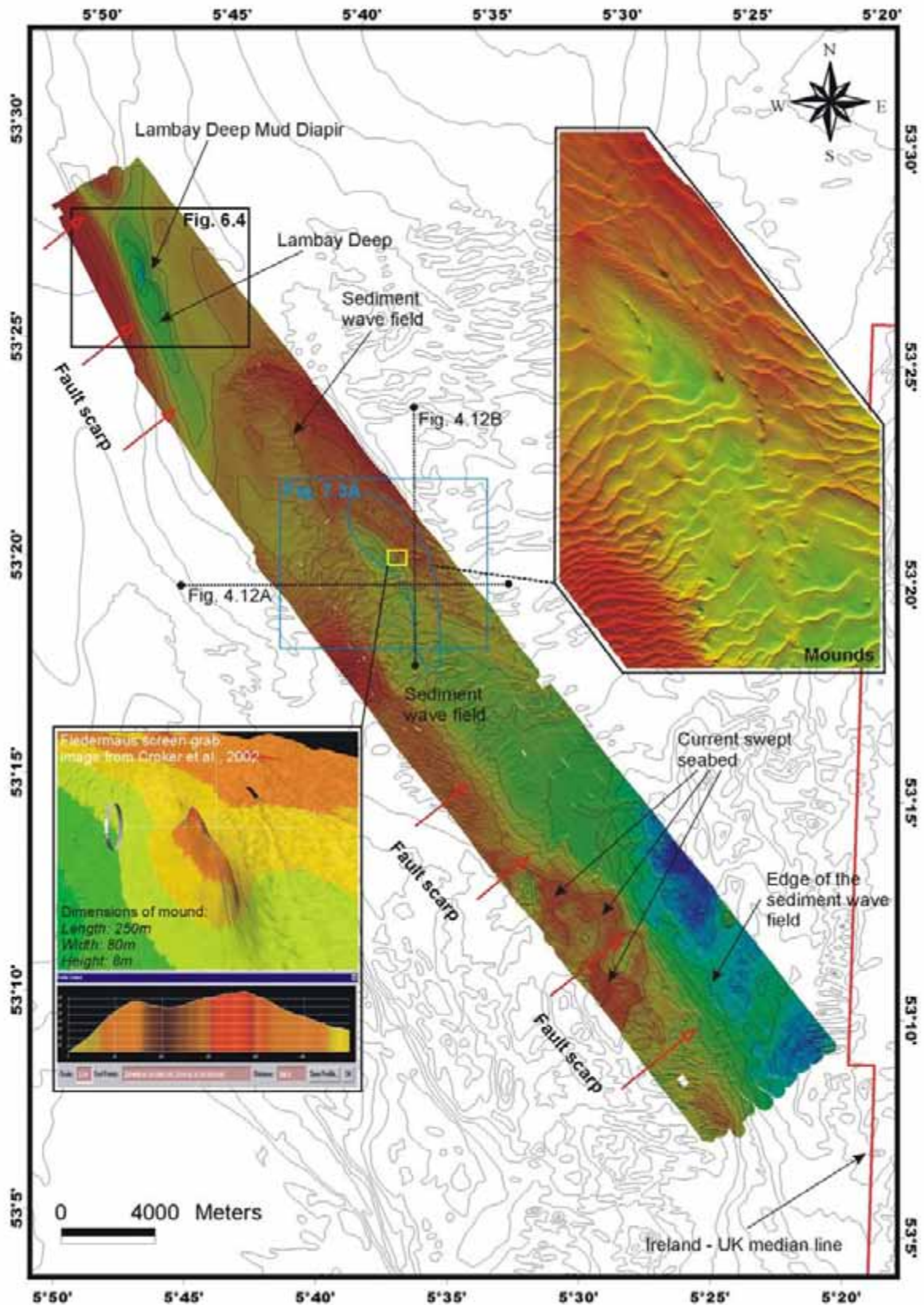
#### ***4.3.1 General setting***

The Codling Fault represents a major NW-SE trending strike-slip fault. On the basis of seismic investigations, it has been recently suggested that approximately 9km of strike-slip displacement has occurred during the Cenozoic (Dunford et al., 2001). The Codling Fault extends from the Kish Bank Basin across the Central Irish Sea Basin into Cardigan Bay. In doing so it divides the Kish Bank basin into two sub-basins. At present, the Codling Fault displays a c.4-5km dextral offset, which can be observed in the offset between the Dalkey and Lambay faults. The Cenozoic tectonic deformation along the Codling Fault has been recently discussed by Cunningham et al. (2004).

The water depth in the Codling Fault area varies between 50-60m to the west of the fault and between 80-120m to the east. The fault creates a well-defined east-facing scarp on the multibeam imagery (Fig. 4.8).



**Figures 4.8:** Multibeam image of the Codling Fault with fault interpretations. Bathymetric contours at 10m intervals (courtesy of BGS). The red line represents the boundary of the IRL-SEA6 sector.



**Figures 4.9:** Multibeam coverage imaging the seabed morphology of the Codling Fault area. Highlight images illustrate the zone of mounds development and a terrain model of one of the mounds. Bathymetric contours at 10m intervals (courtesy of BGS). The red line represents the boundary of the IRL-SEA6 sector.

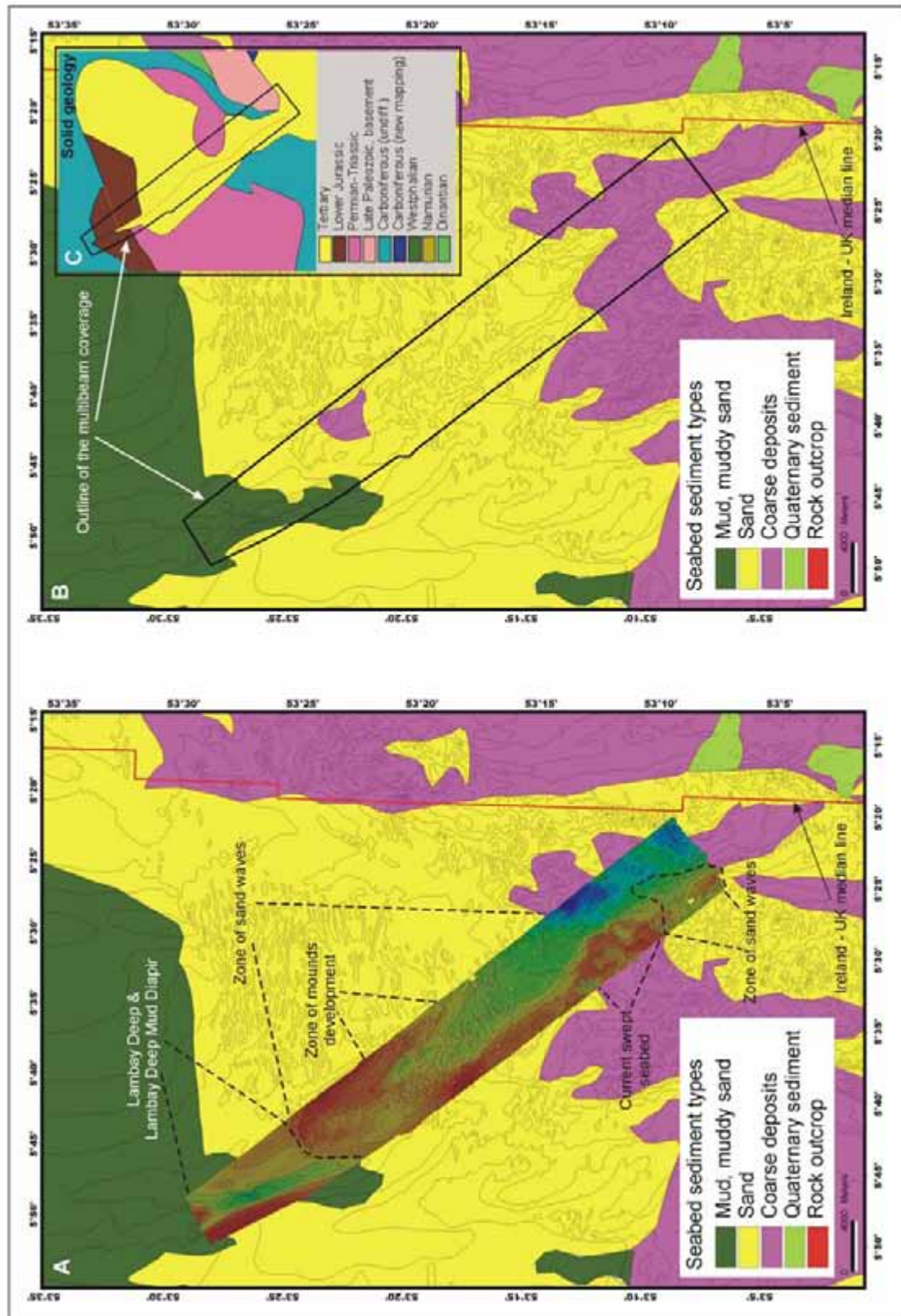


**Figure 4.10:** Maps of the Codling Fault area showing: (A) multibeam coverage and seabed sediment types; (B) outline of the multibeam coverage and seabed sediment types; (C) outline of the multibeam coverage and solid geology. Bathymetric contours at 10m intervals (courtesy of BGS). The red line represents the boundary of the IRL-SEA6 sector.

#### ***4.3.2 Multibeam mapping***

Multibeam mapping provided details on the seabed morphology of the Codling Fault Zone (Fig. 4.9). Figure 4.10 demonstrates that there is a strong link between the seabed morphology and the distribution of the seabed sediment types. The mapped area can be subdivided into three zones: (1) the northern muddy zone containing the Lambay Deep and its mud diapir; (2) the central sandy zone largely covered with sand waves; (3) the southern zone, which in places demonstrates a current-swept seabed corresponding to patches of coarse sediments (Fig. 4.10). Figure 4.10C shows the outline of the mapped area in relation to the solid geology map.

Earlier digitised fault traces of the Codling Fault are shown on Figure 4.11A. This figure also indicates the epicentres of two minor earthquakes recorded in 1982, thus suggesting that some parts of the fault are still active.

The multibeam survey revealed a number of mound-like structures in the central part of the mapped area (Fig. 4.9). The mounds appear to be aligned along curvilinear fault trends (Fig. 4.9 inset, Fig. 4.11B). In total, 23 mounds have been identified in the Codling Fault area. Figure 4.9 includes a terrain model of one of these mounds, illustrating that the mounds possess measurable relief (c.5-10m). ROV video surveys and seabed sampling proved that these mounds are composed of carbonate-cemented sandstones. SEM analysis of the seabed samples suggested that the carbonate-cemented slabs on top of the mounds are formed by MDAC (see Ch. 7: Fig. 7.6). Moreover, contemporary gas seepage has been documented from some of the mounds on echosounder records (see Ch. 7: Fig. 7.3, Fig. 7.4). The distribution of the Codling Fault mounds in the western Irish Sea regional context is shown on Figures 6.11 and 6.12.

Vertical gas migration via faulting under some of the mounds has been confirmed by high-resolution seismic data (Fig. 4.12). Figure 4.12A shows part of seismic line E96IE15D-5 crossing one of the mounds in the west-east direction, and reveals the fault underlying the mound (this line is also shown in Dunford et al., 2001, Fig. 10). Figure 4.12B shows part of the seismic line E96IE15D-20 crossing the same mound, but in the north-south direction. This same mound is seen on conventional seismic line E95IE18-11/B, SP 230, which also clearly shows the fault at depth (Fig. 4.13). Another good

example of a mound located above a fault on conventional seismic data is presented in Dunford et al., 2001, Fig. 12. The seabed mound can be seen at SP 420 on line E95IE18-09A, above a branch of the Codling Fault (Fig. 4.14).

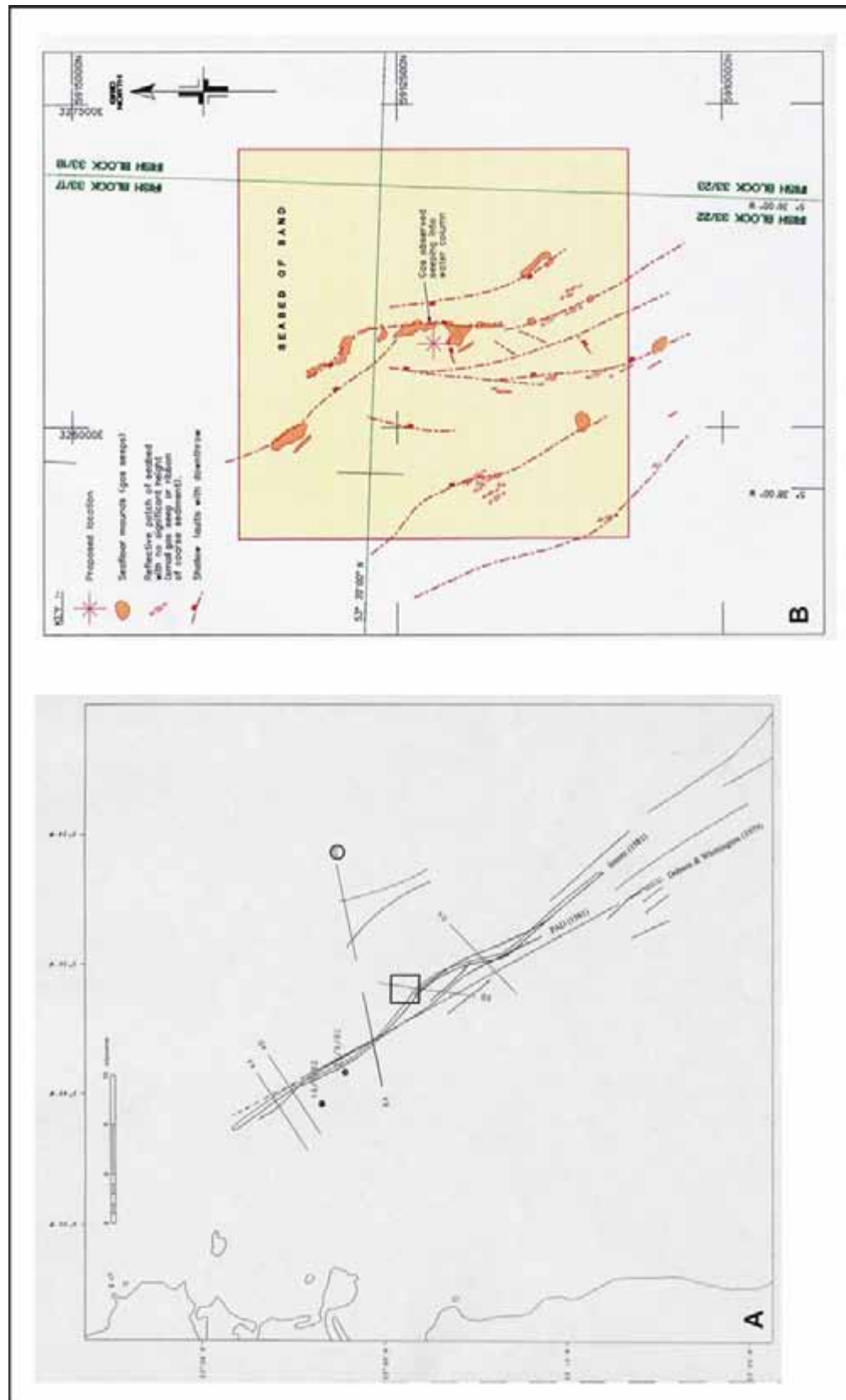


**Figure 4.11:** (A): Digitised fault traces based on Dobson & Whittington (1979), Jenner (1981), PAD (1981) and aeromagnetic interpretation. The black dots indicate the epicentres of two minor earthquakes recorded in 1982 (from Jacob, 1993). (From Croker, 1997a: Fig. 18.) (B): Britsurvey (1996) map showing relationship between seafloor mounds and shallow faults in the Codling Fault study area. (From Croker, 1997a: Fig. 8.)

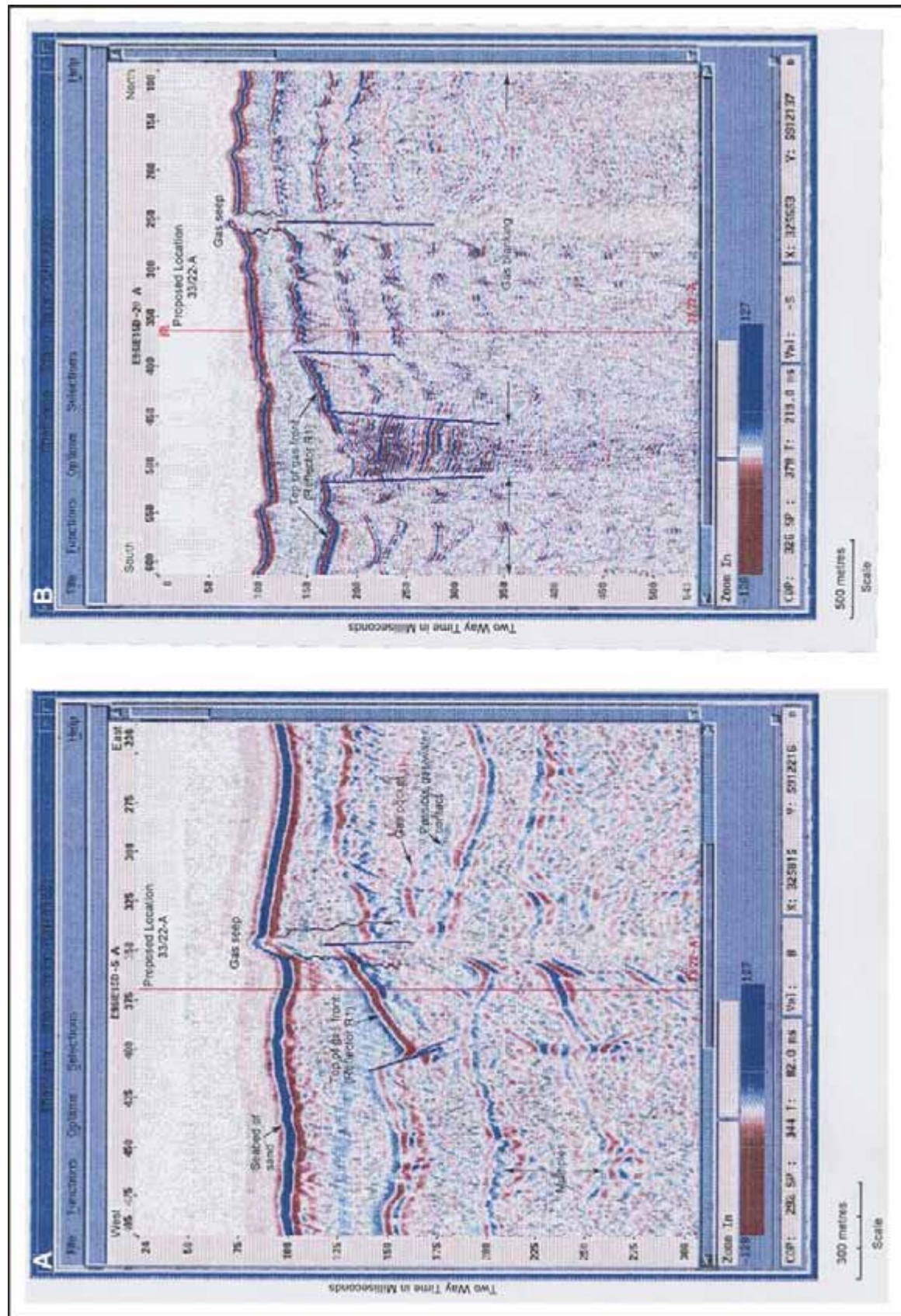


**Figure 4.12:** Parts of the high-resolution seismic lines: (A) E96IE15D-5; (B) E96IE15D-20. See Figures 4.2 & 4.9 for location. (From Croker, 1997a: Fig. 9 & Fig. 10.)

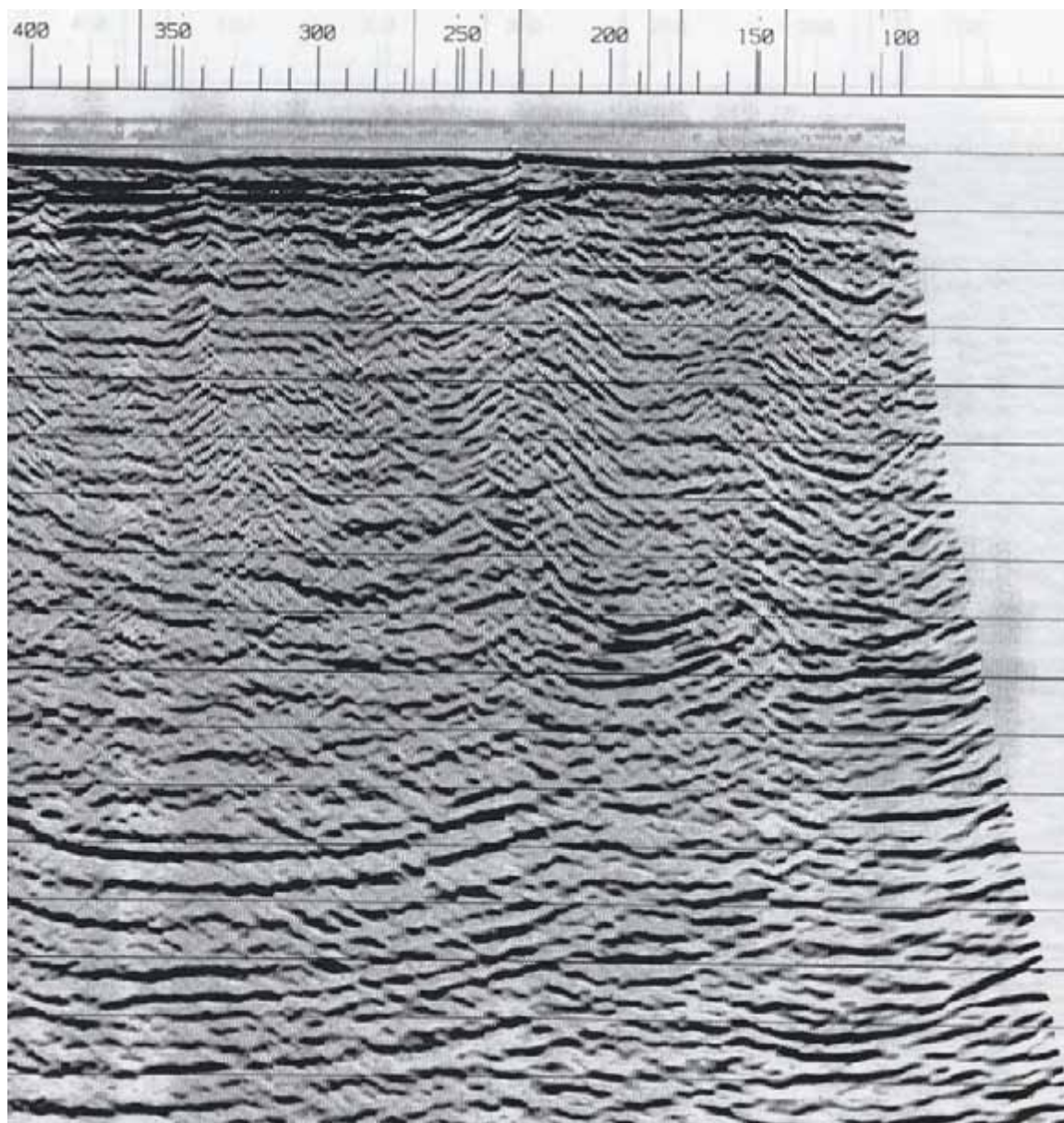


**Figure 4.13:** Part of conventional seismic line E95IE18-11/B showing seabed mound at SP 230 and underlying near-vertical fault. (From Croker, 1997a: Fig. 13.)

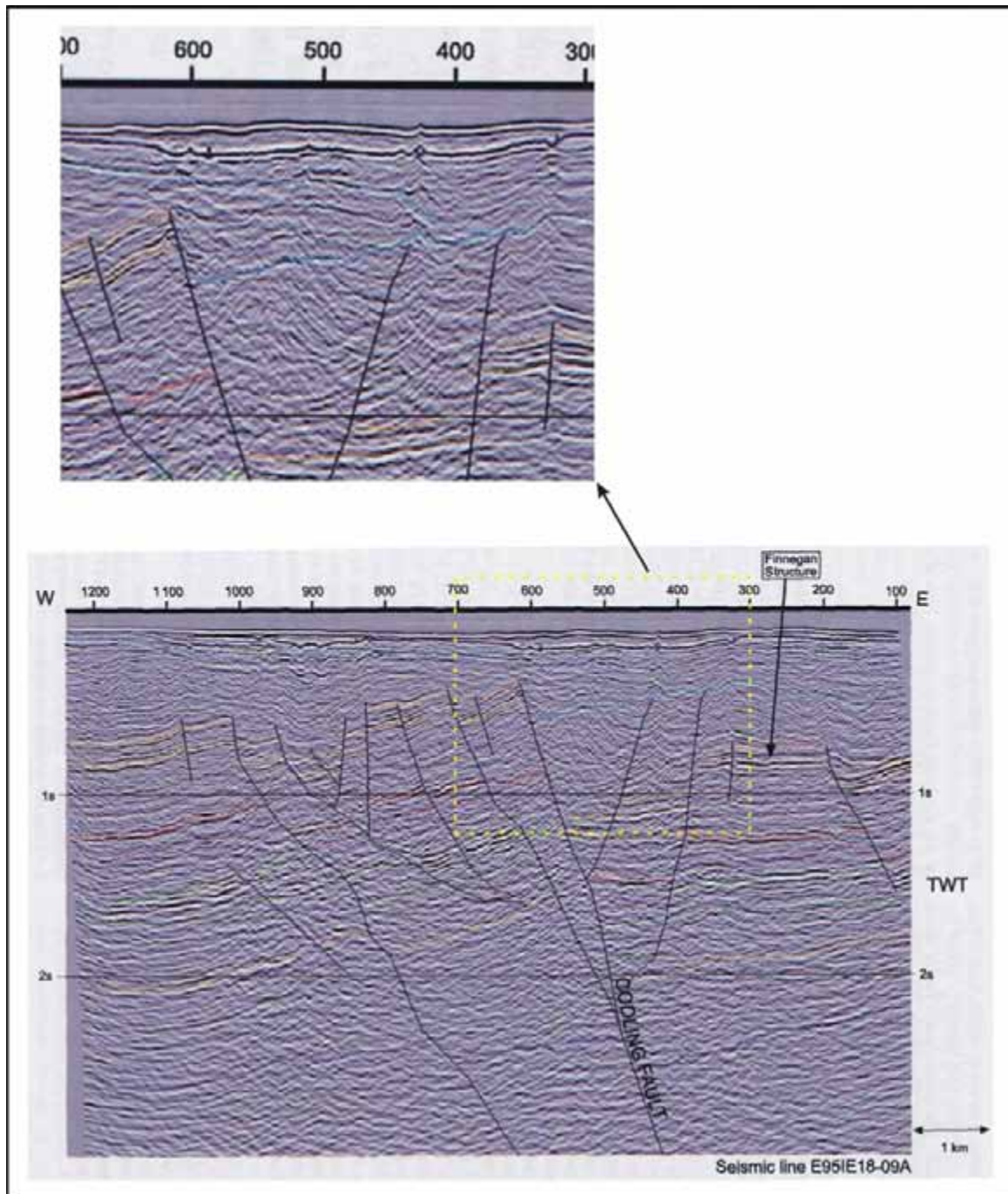


**Figure 4.14:** Part of conventional seismic line E95IE18-09/A showing seabed mound at SP 420 above a branch of the Codling Fault. (From Dunford et al., 2001: Fig. 12.)

A combined interpretation of all available datasets suggests a strong genetic link between the mounds and gas migration along faults. Dunford et al., 2001 (Fig. 9), present additional evidence from an airborne seep detection survey for leakage of hydrocarbons along the Codling Fault Zone. A geochemical sampling survey was also carried out in this area on behalf of Enterprise Oil in 1997 (Hatton, 1997).

The Lambay Deep mud diapir (LDMD) was discovered during the 1998 Celtic Voyager cruise in the middle of the Lambay Deep (Fig. 4.9). The Lambay Deep is a linear trench-like feature located on the trace of the Codling Fault. It is topographically 50-60m lower than the surrounding seabed with maximum depths reaching 110m. The morphology and internal structure of the LDMD was imaged on both multibeam bathymetry and GeoChirp profiles (Fig. 6.4). The detailed GeoChirp mapping of the Lambay Deep provided evidence that this area is largely affected by sub-surface gas fronts (Fig. 5.10). Thus it is possible to assume a genetic connection between the Lambay Deep mud diapir formation and gas migration processes.

It would appear from the evidence presented above that the Codling Fault Zone is perhaps the most active site of gas migration and seepage in the entire IRL-SEA6 area.

## **5. Shallow Gas Accumulations**

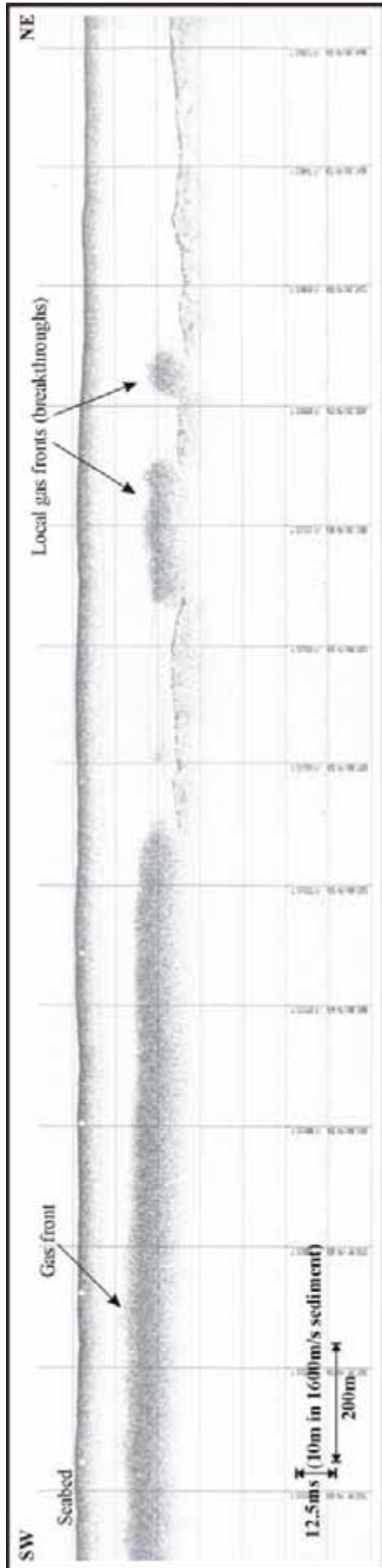
Accumulations of shallow gas in IRL-SEA6 are mainly represented by gas fronts and plumes. These features have been defined in Chapter 1.2.2.

Where gas is sealed by impermeable seabed sediments, gas accumulations may not be associated with any characteristic seabed morphology (e.g. seabed doming). However, seismic data may still provide strong evidence of subsurface gas fronts and plumes. Subsurface gas accumulations start to form a seabed expression in the event of excessive gas pressure or favourable seabed sediment types.

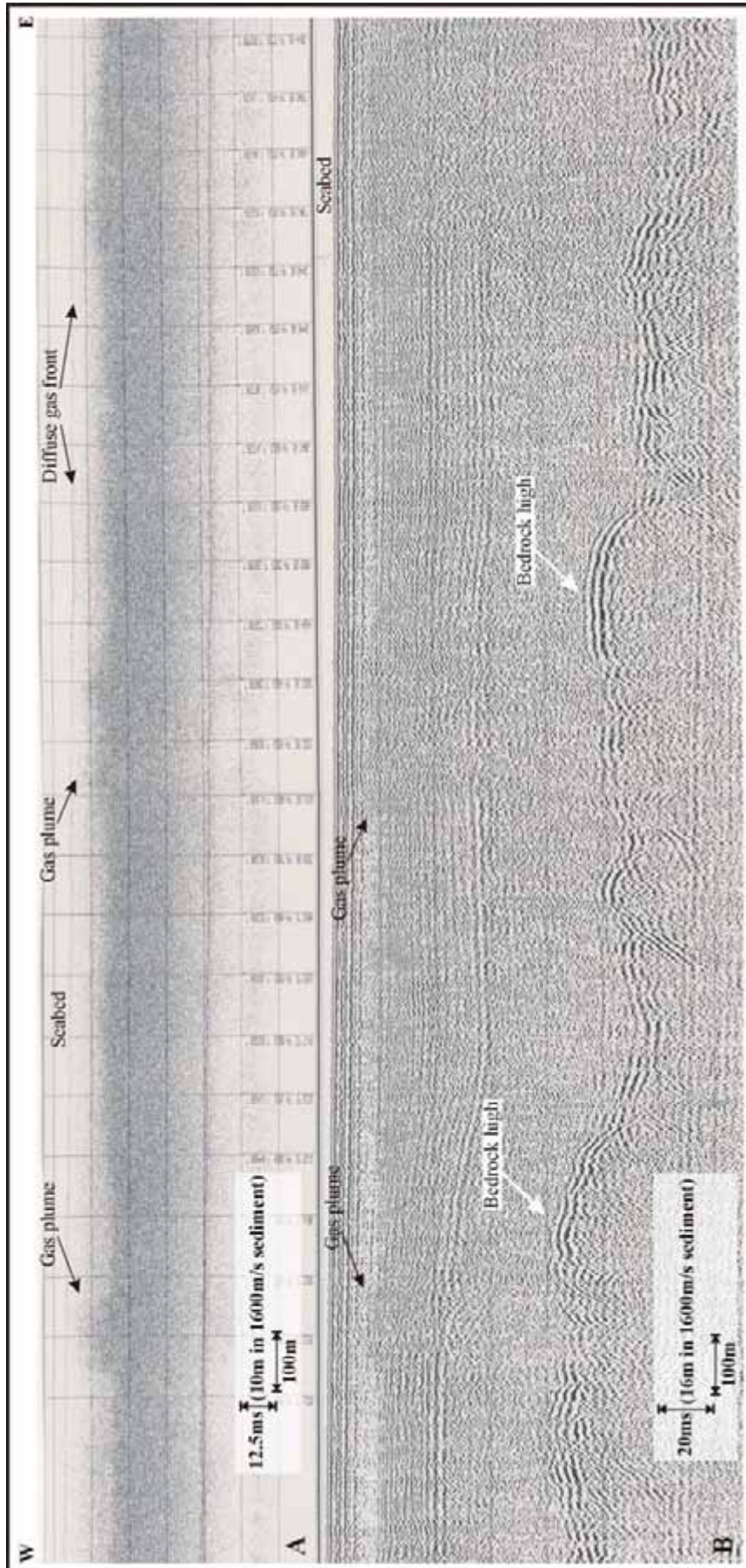
Described below are some selected examples of various data illustrating the type and nature of gas accumulations in the northern part of the IRL-SEA6 area.

Figure 5.1 shows part of Pinger–Seapro SBP 5.5kHz profile (route survey data) recorded in the muddy area of the western Irish Sea. This profile images a subsurface gas front and breakthroughs (local gas fronts). The gas front is sealed with muddy sediments at approximately 15m below seafloor.

Figure 5.2 presents part of dual Boomer (A) and 0.8kHz Sparker (B) profiles illustrating a good example of a diffuse gas front and gas plumes. The Sparker (Fig. 5.2B) record shows that the gas plumes are underlain by bedrock highs thus suggesting a thermogenic origin for the gas. The seafloor on both records appears to be smooth and unaffected by the shallow gas. Note that the gas front here appears at about 6m below seafloor. Gas plumes are about 100m across, possess a dome-like shape and appear to almost reach the seafloor.



**Figure 5.1:** Pinger Seapro SBP 5.5kHz profile showing subsurface gas front and breakthroughs within the muddy area. See Figure 4.2 for location. (From Croker, 1994 (Fig. 4) with additional interpretation.)



**Figure 5.2:** Boomer (A) and 0.8kHz Sparker (B) records illustrating a diffuse gas front and gas plumes. The Sparker (B) record shows that gas plumes are underlain with bedrock highs thus suggesting a thermogenic origin for the gas. The seafloor on both records appears to be smooth and unaffected by the shallow gas. See Figure 4.2 for location. (From Croker, 1994 (Fig. 5) with added interpretation.)

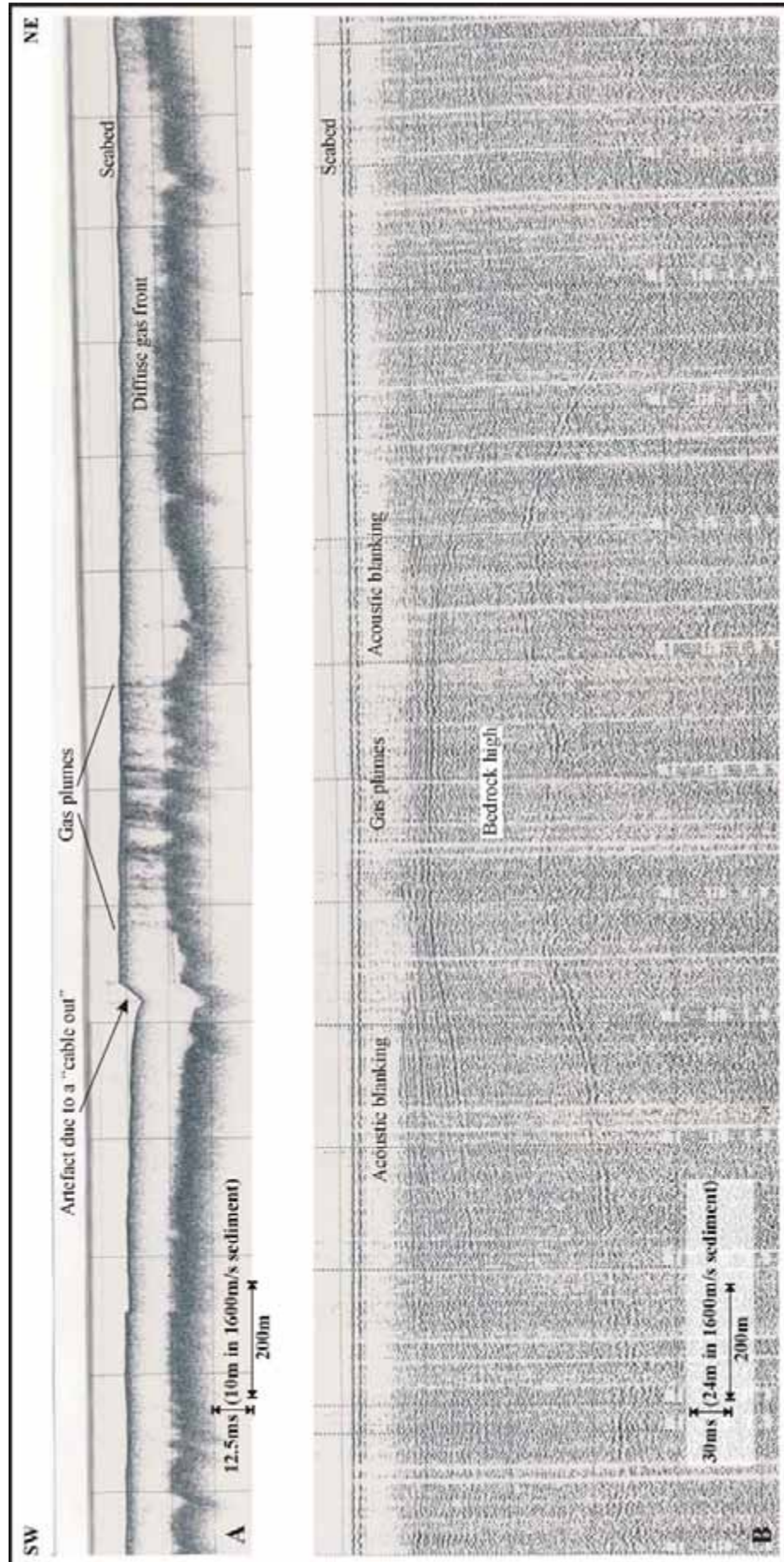
Another example of a diffuse gas front and gas plumes is presented on Figure 5.3. The gas front lies at about 10m below seafloor. The middle part of both profiles shows several closely spaced gas plumes that appear to reach the seabed (Fig. 5.3A). The Sparker profile (Fig. 5.3B) demonstrates that the gas plumes are associated with a bedrock high. The seafloor on both records appears to be relatively smooth and unaffected by the shallow gas.

Figure 5.4 shows part of conventional seismic line IS-2, which crosses the same area as the gas front and plumes described above. This line shows the same bedrock high (SP 1275) as in Figure 5.3, but from a slightly different perspective. Data quality does not allow an interpretation of the deeper structure. Two seabed anomalies associated with other bedrock highs can be observed at SP1330 and SP1400, which are also probably the result of shallow gas.

Figure 5.5 illustrates that, in places, gas plumes may be associated with seabed doming. Figure 5.6 suggests again that gas plumes are associated here with local bedrock highs, similar to the situation seen in Figure 5.2 and 5.3.

Figures 5.7-5.10 present GeoChirp lines from the Peel Basin sites, Jones Trench and from the Lambay Deep (recorded during the 1998 Celtic Voyager cruise) demonstrating that the surveyed areas are dominated by shallow gas fronts with occasional gas plumes and pockmarks.

More examples of shallow gas accumulations and their relationship with gas escape structures are presented in Chapter 6.



**Figure 5.3:** (A): The 5.5kHz Pinger–Seapro SPB record shows a diffuse gas front with gas plumes reaching to the seafloor in the central part of the section. The step in the seafloor topography is an artefact due to a “cable out”. (B): 1000J Sparker record indicating that the gas plumes observed on “A” are related to a bedrock high. The seafloor on both records appears to be relatively smooth and unaffected by the shallow gas. See Figure 4.2 for location. (From Croker, 1994 (Fig. 6) with additional interpretation.)

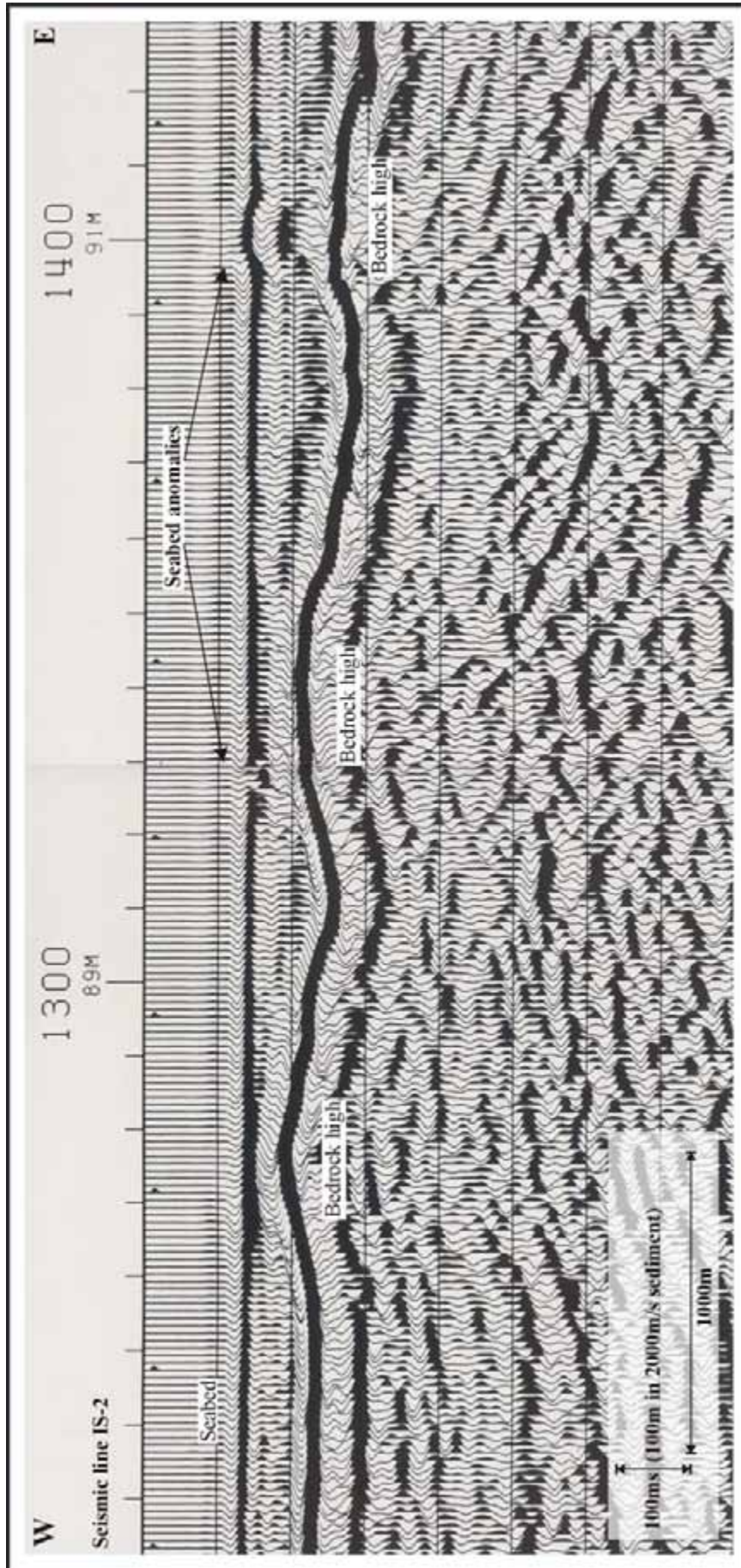


**Figure 5.4:** Part of conventional seismic line IS-2 showing the same bedrock high (SP 1275) as in Figure 5.3, but from a slightly different perspective. Data quality does not allow an interpretation of the deeper structure. Two seabed anomalies associated with bedrock highs can be observed at SP 1330 and 1400. See Figure 4.2 for location. (From Croker, 1994 (Fig. 7) with additional interpretation.)

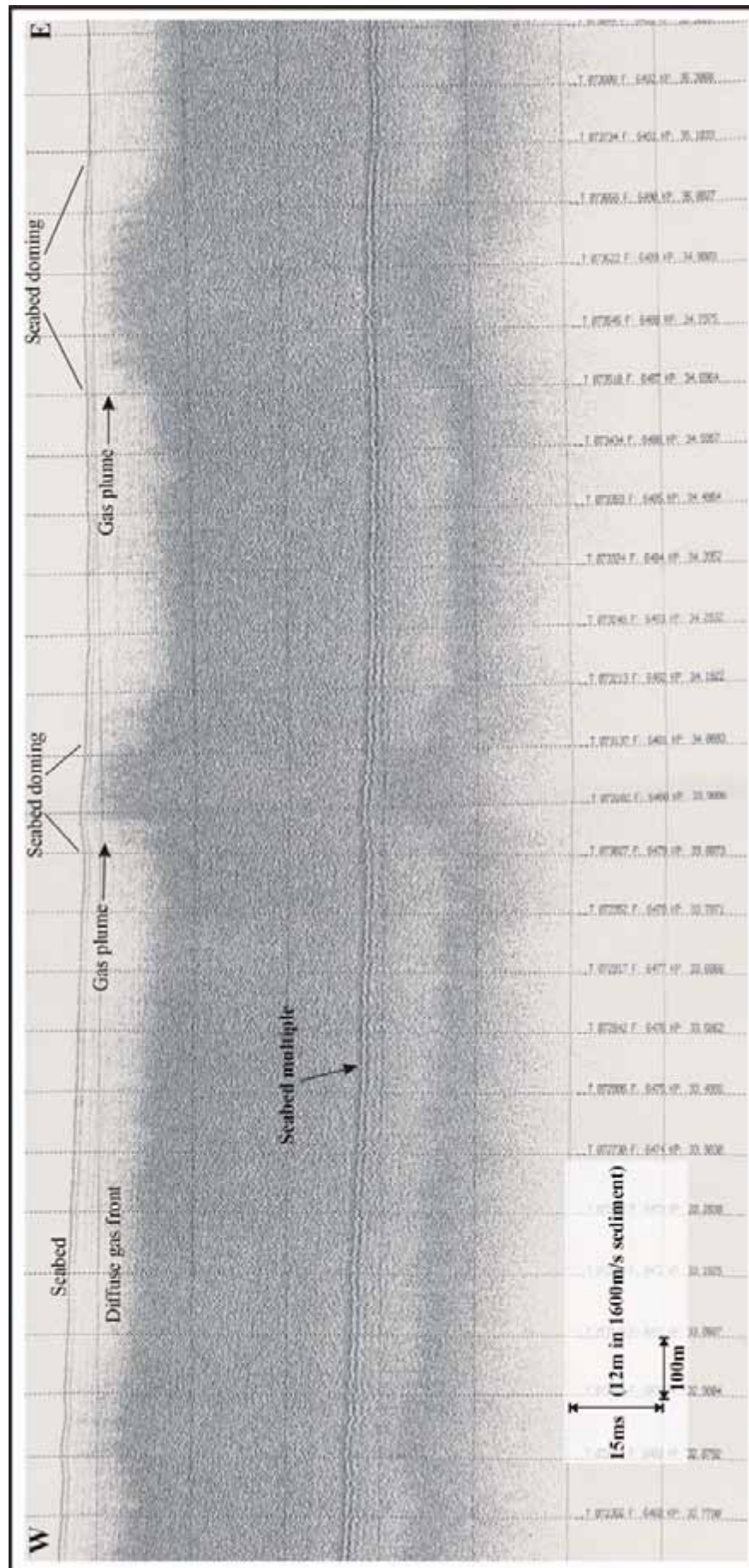


**Figure 5.5:** Boomer record illustrating gas plumes and corresponding gentle doming of the seabed. See Figure 4.2 for location. (From Croker, 1994 (Fig. 8) with additional interpretation.)

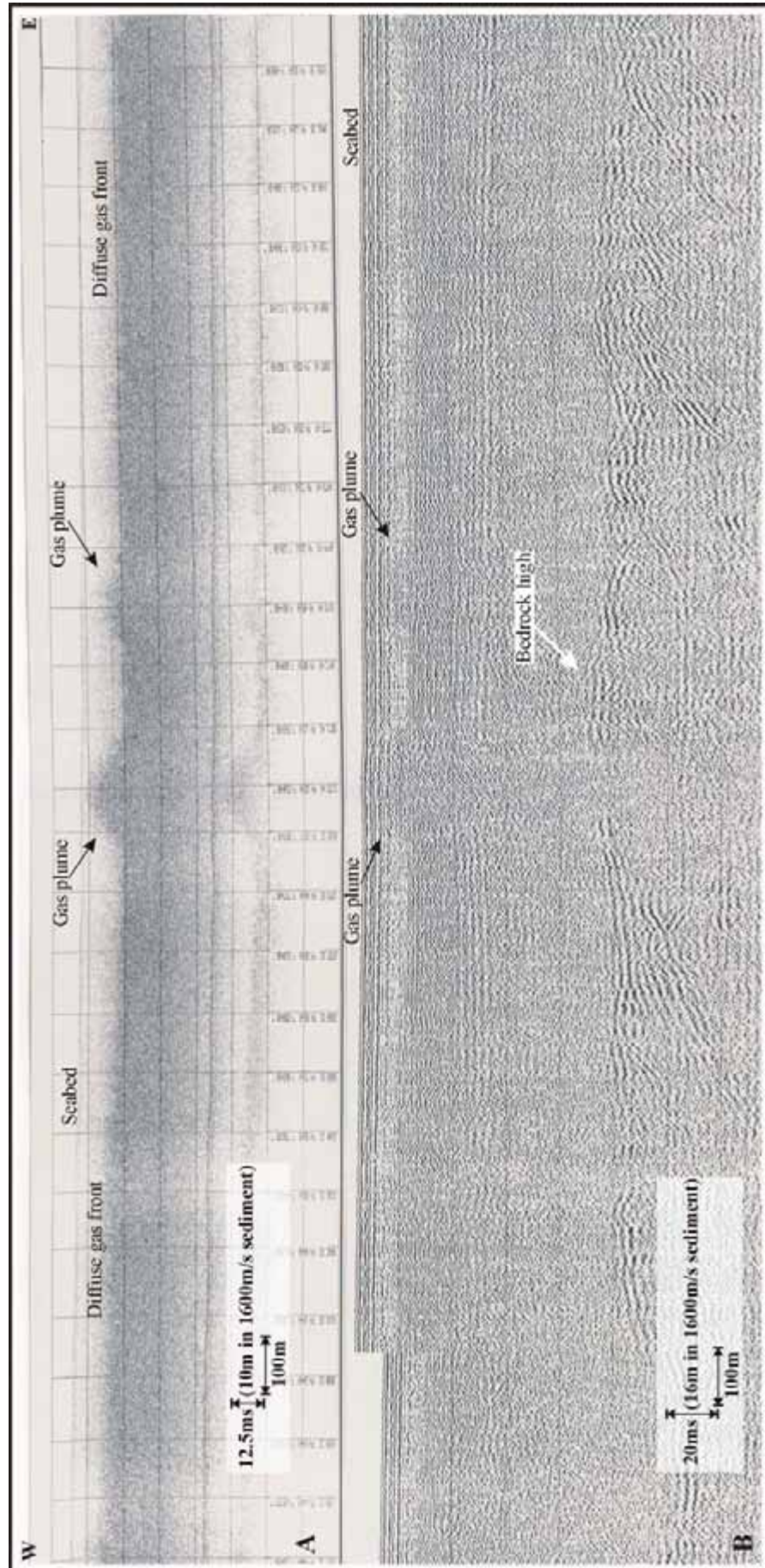


**Figure 5.6:** (A): Boomer record and (B): Sparker record imaging two distinctive gas plumes and suggesting that the main gas plume might be associated with a local bedrock culmination. See Figure 4.2 for location. (From Croker, 1994 (Fig. 8) with additional interpretation.)

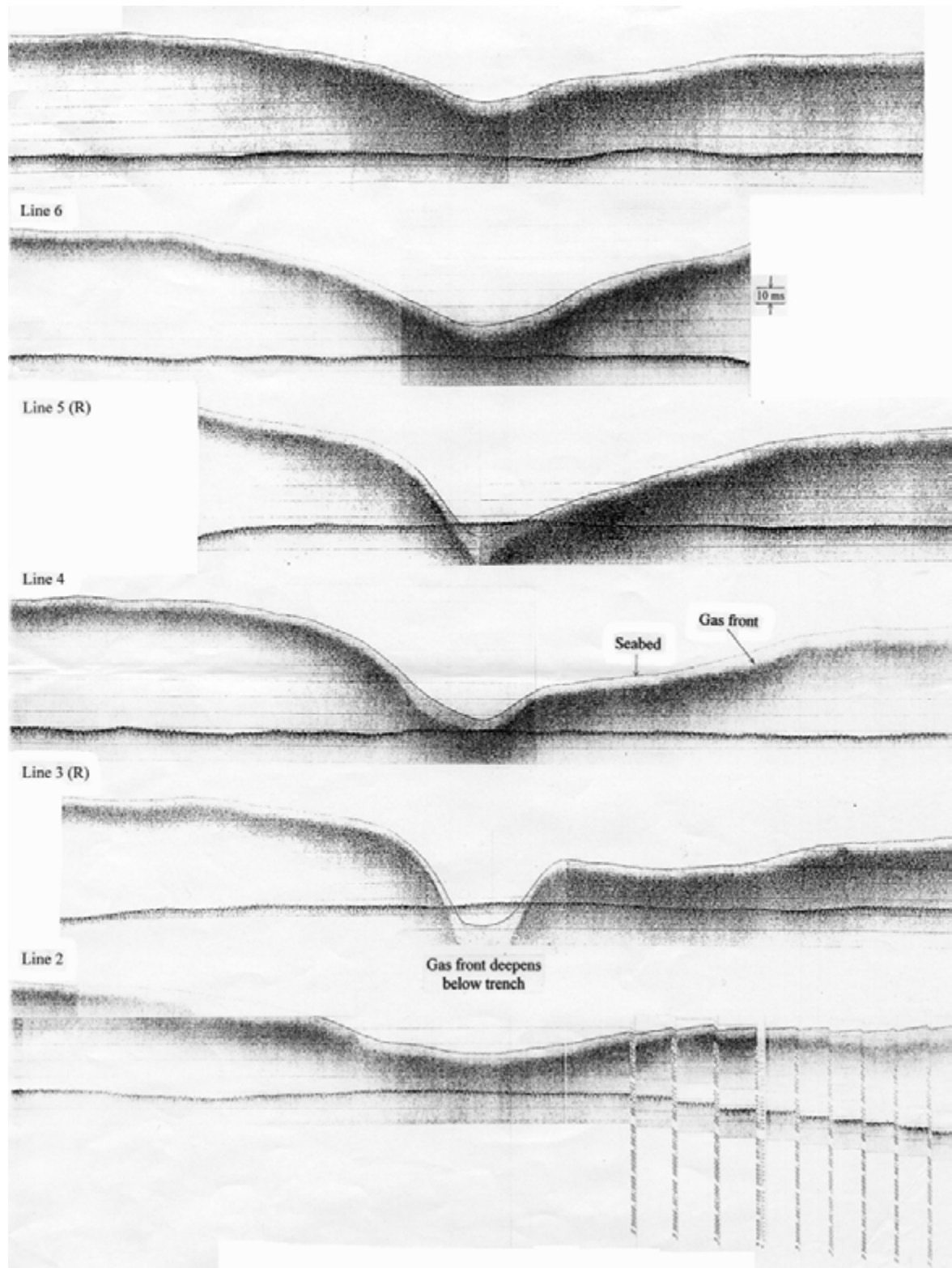


**Figure 5.7:** GeoChirp lines 2-7 over the Peel Basin 1 site, illustrating the presence of a shallow gas front. Profiles collected during RV Celtic Voyager 1998 cruise. See Figure 4.2 for location. (From Croker & O'Loughlin, 1998.)

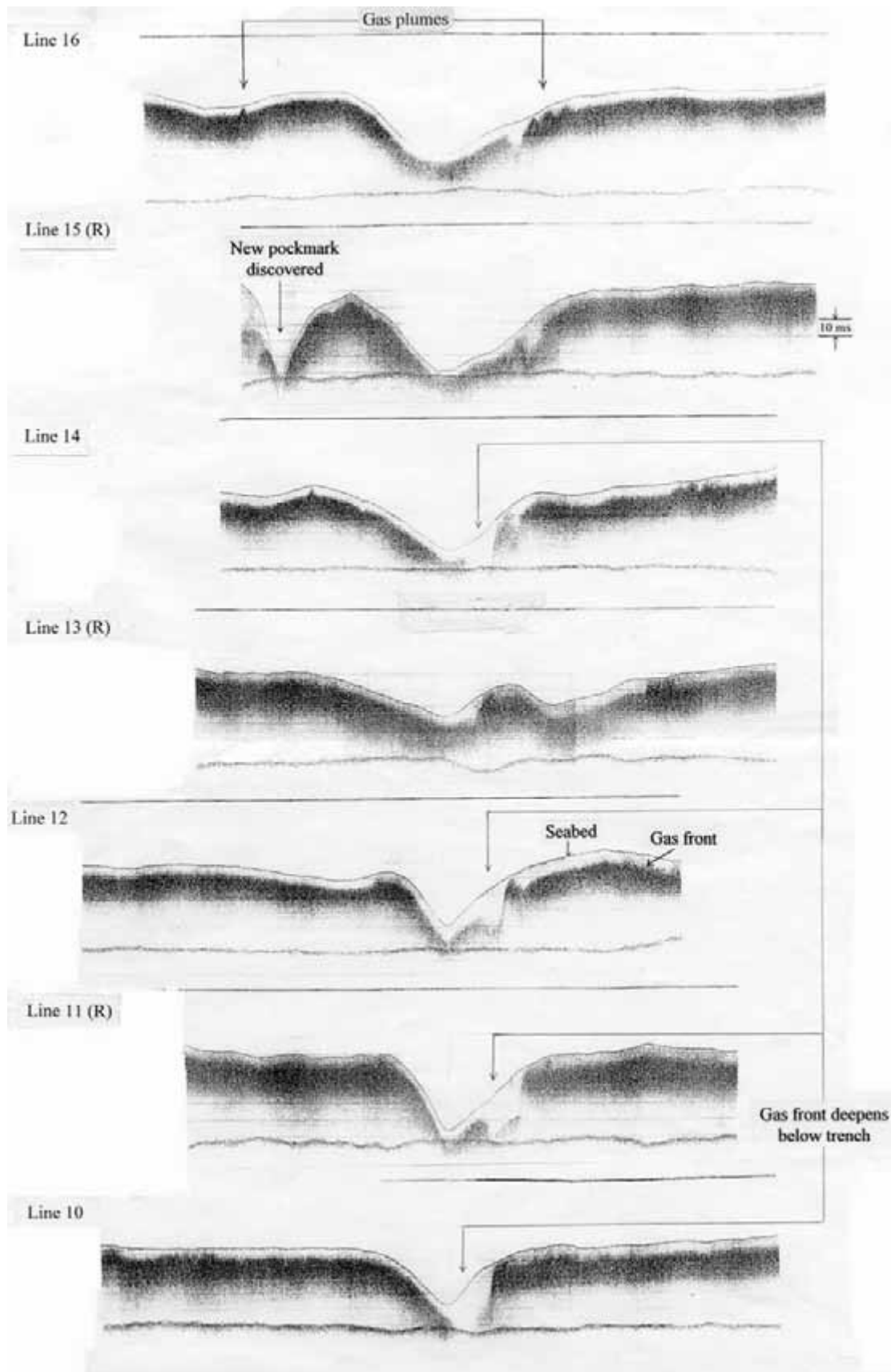


**Figure 5.8:** GeoChirp lines 10-16 over the Peel Basin 2 site, illustrating the presence of a shallow gas front and pockmark. Profiles collected during RV Celtic Voyager 1998 cruise. See Figure 4.2 for location. (From Croker & O'Loughlin, 1998.)

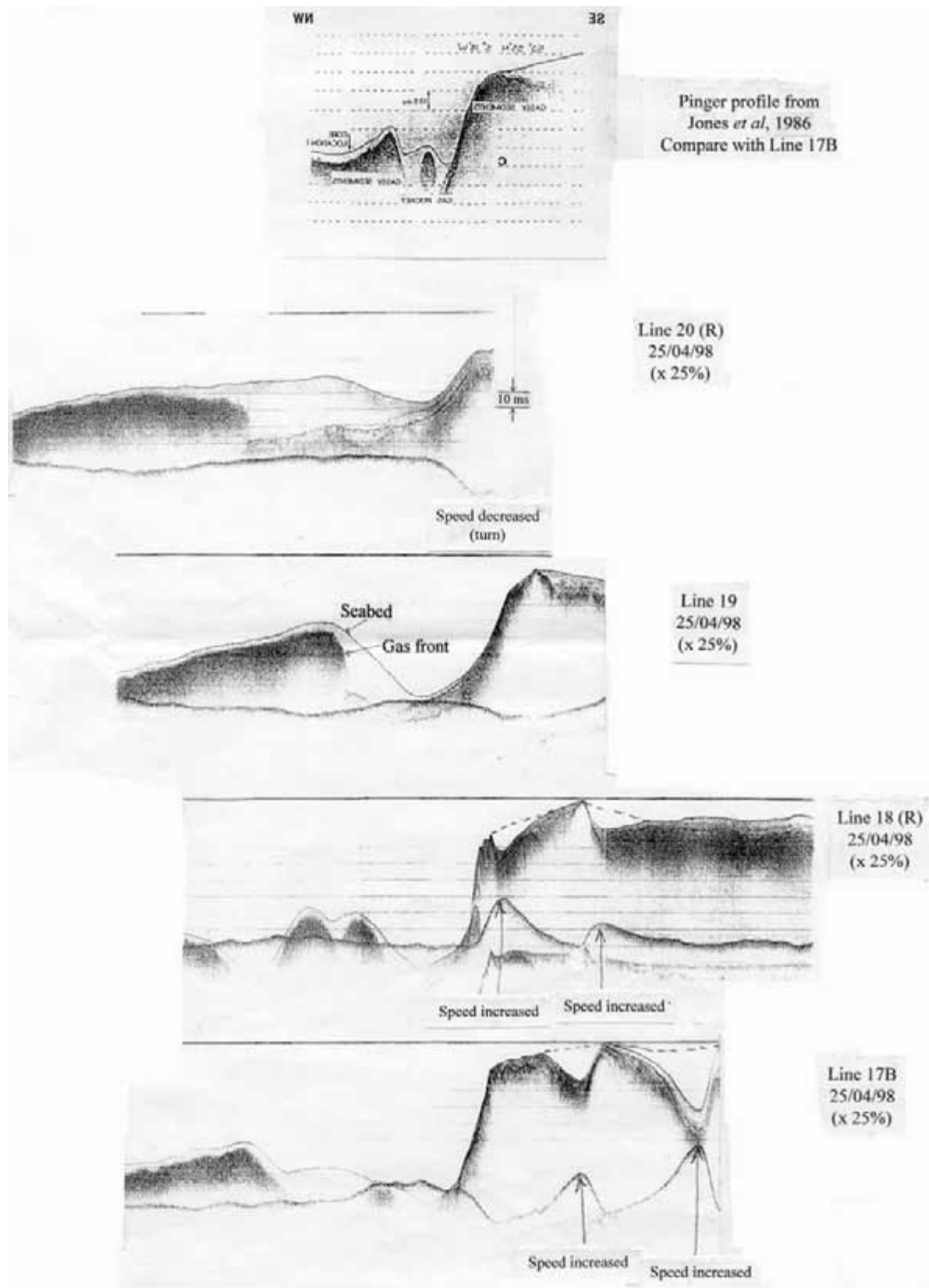


**Figure 5.9:** GeoChirp lines 17B-20 over the Jones Trench site, illustrating the presence of a shallow gas front. Profiles collected during RV Celtic Voyager 1998 cruise. See Figure 4.2 for location. (From Croker & O'Loughlin, 1998.)

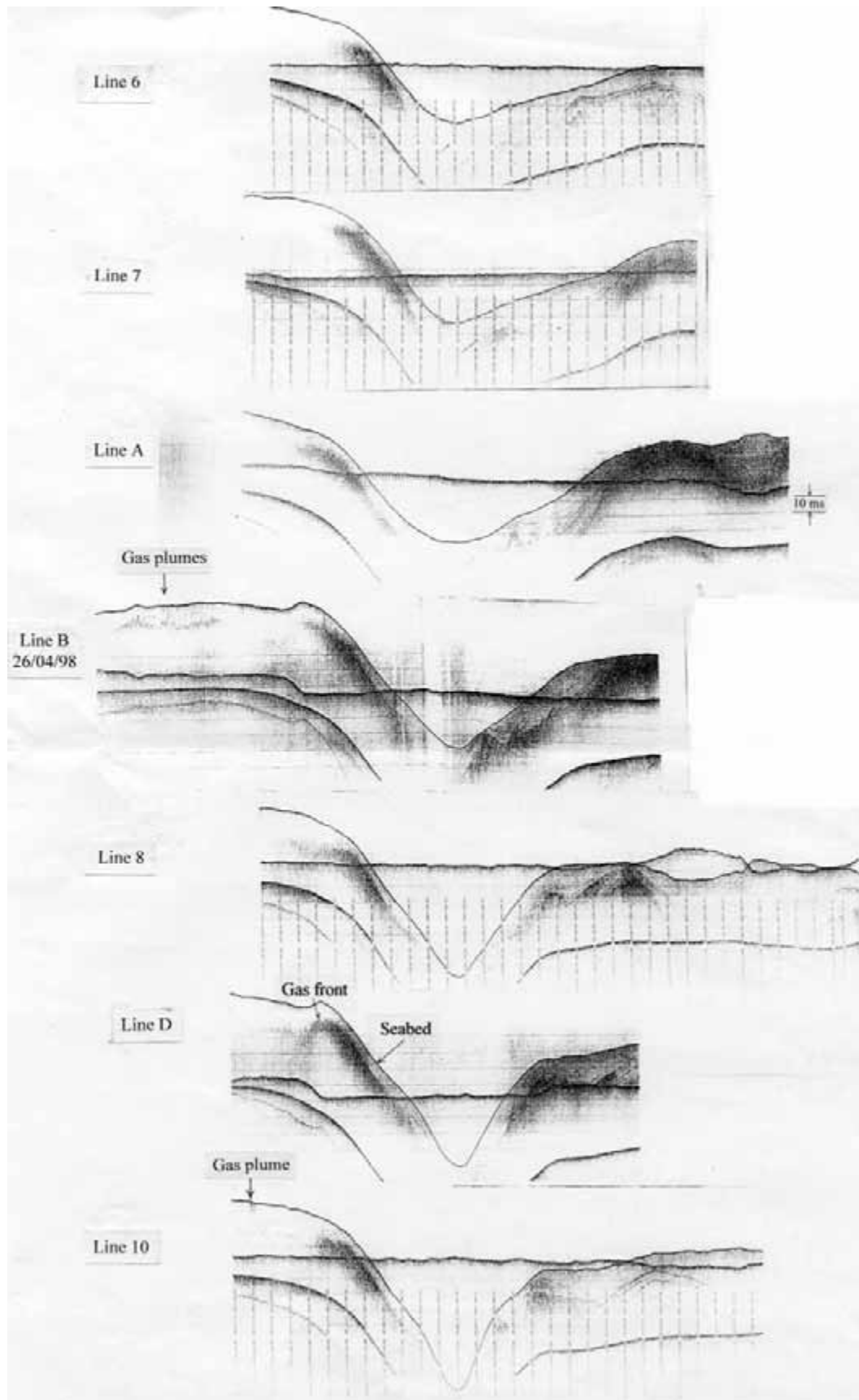


**Figure 5.10:** GeoChirp lines over the Lambay Deep site, illustrating the presence of a shallow gas front and occasional plumes. Profiles collected during RV Celtic Voyager 1998 cruise. See Figure 4.2 for location. (From Croker & O'Loughlin, 1998.)

## **6. Gas Escape Structures and their Distribution**

The existing data from the western Irish Sea demonstrates the following gas escape structures:

### **6.1 Pockmarks**

The occurrence of pockmarks is limited to the northern part of the IRL-SEA6 sector where muddy sediments are dominant. A newly discovered pockmark is presented on Figure 5.8 as imaged on the GeoChirp line from the Peel Basin site 2. The location of this pockmark is shown on Figures 6.11 and 6.12, which also show previously published occurrences.

### **6.2 Seabed doming**

Seabed doming occurs where gas accumulations create sufficient pressure to cause some deformation to the overlaying sediment layers. These features normally represent the initial phase of development of gas escape structures. Depending on the sub-surface gas pressure and sediment type seabed doming can evolve into pockmarks (fine sediments) or irregular topography or seep mounds (coarse sediments).

Examples of gentle seabed doming have been presented above on Figure 5.5. Figure 6.1 shows the development of an irregular seabed topography. This image is from an area dominated by coarse-grained material. Both profiles shown in Figure 6.1 confirm that these features are associated with the vertical migration of shallow gas. Below this area the gas front lies at about 16-20m below seafloor.

### **6.3 Mounds**

Mounds, formed due to the migration and escape of shallow gas, have been imaged on seismic and multibeam data (see Ch. 4.3). Moreover, echosounder records also provided evidence that some of the mounds are actively seeping fluid at present (Fig. 7.4).

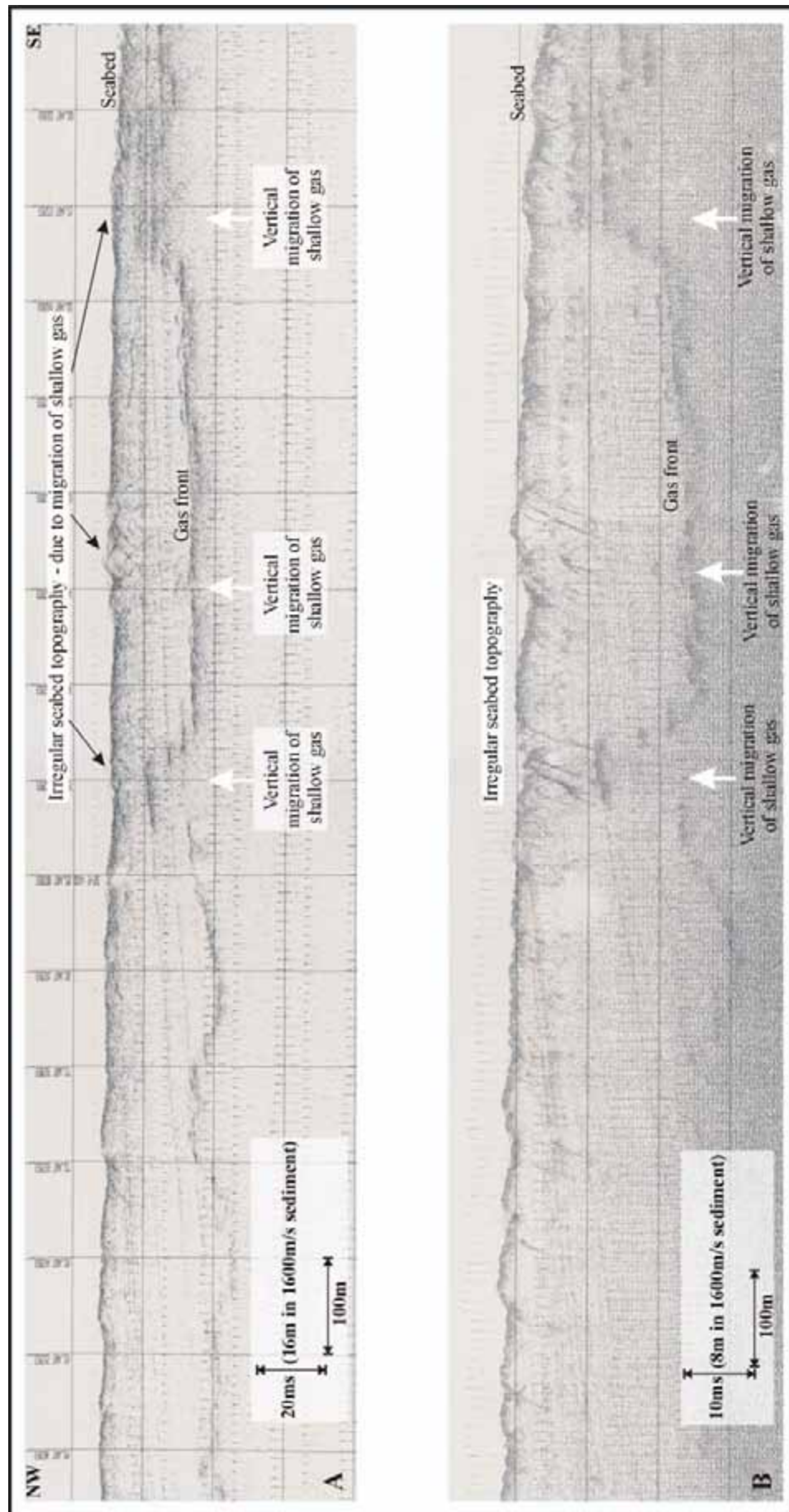


**Figure 6.1:** (A): 200J Boomer profile. (B): 5KW Pinger profile. Both profiles demonstrate the extensive gas front at about 20ms below the seabed. At the centre and far right of the image the gas-enhanced amplitudes of the gently dipping reflector can be observed. See Figure 4.2 for location. (From Croker, 1994 (Fig. 10) with additional interpretation.)

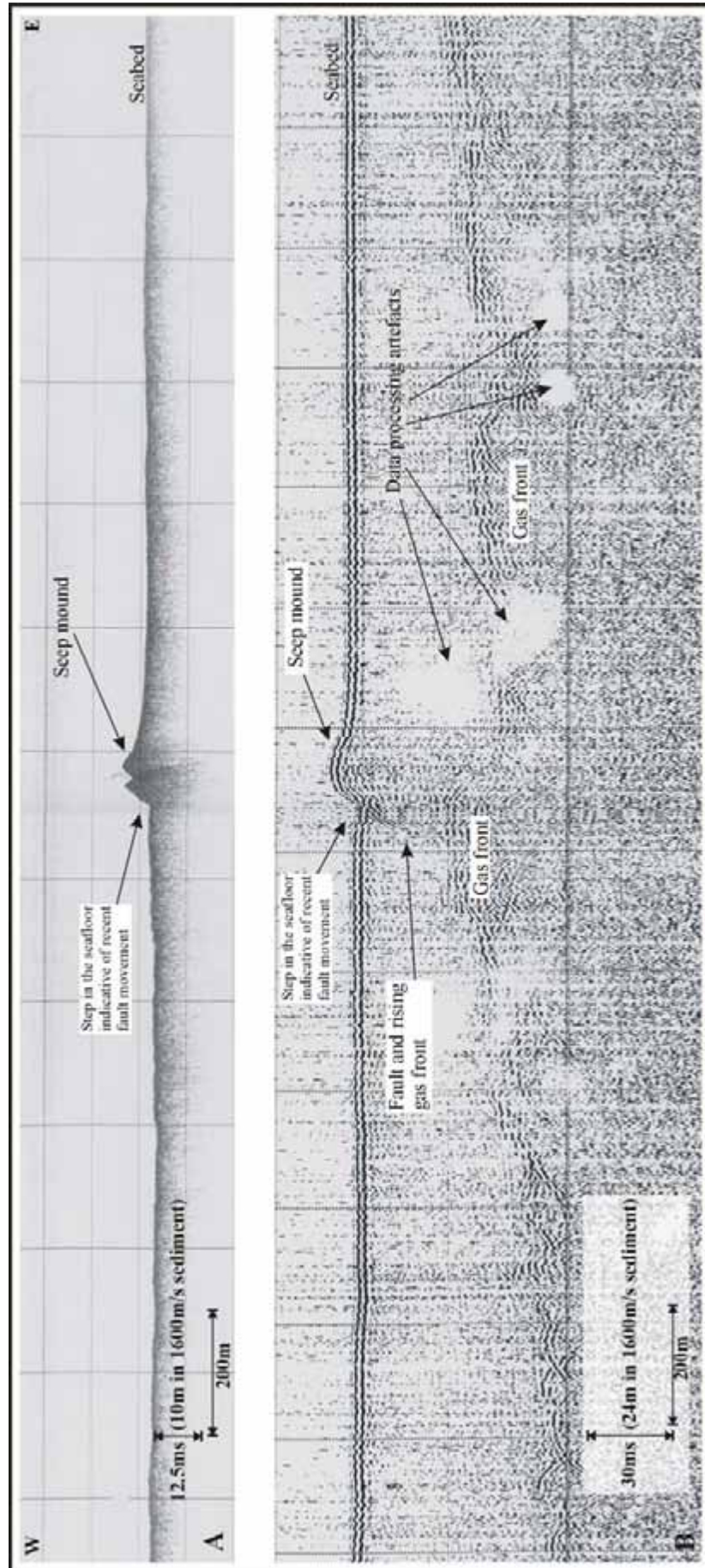


**Figure 6.2:** (A): Pinger–Seapro SBP 5.5kHz profile. (B): 1000J Sparker profile. Both profiles illustrate an example of an apparent seep mound from an area of sandy sediments in the Kish Bank Basin. Both profiles illustrate a step in the seafloor, which most likely indicates recent fault movement. The mound occurs above the site where this fault intersects the gas front. The lower profile (B) demonstrates that the gas front is rising from west to east. (From Croker, 1994 (Fig. 12) with additional interpretation.)

On Figure 6.2 both profiles illustrate an example of a seep mound (KBA) from an area of sandy sediments in the Kish Bank Basin and indicate a step in the seafloor that suggests recent fault movement. The lower profile (Fig. 6.2B) demonstrates a gas front rising from west to east. The seep mound occurs above the site where this fault intersects the gas front. The existence of a fault underneath the mound has been also confirmed with conventional seismic data (Fig. 4.3).

Figure 6.3 is located to the north-east of the mound presented on Figure 6.2. Initially these features were interpreted as seep mounds underlain with apparent gas chimneys. However, a 2004 multibeam survey showed them to be sand waves with very sharp crests (Alan Judd, pers. comm.). This therefore provides a good example of possible misinterpretation that might occur if it is based on limited datasets.

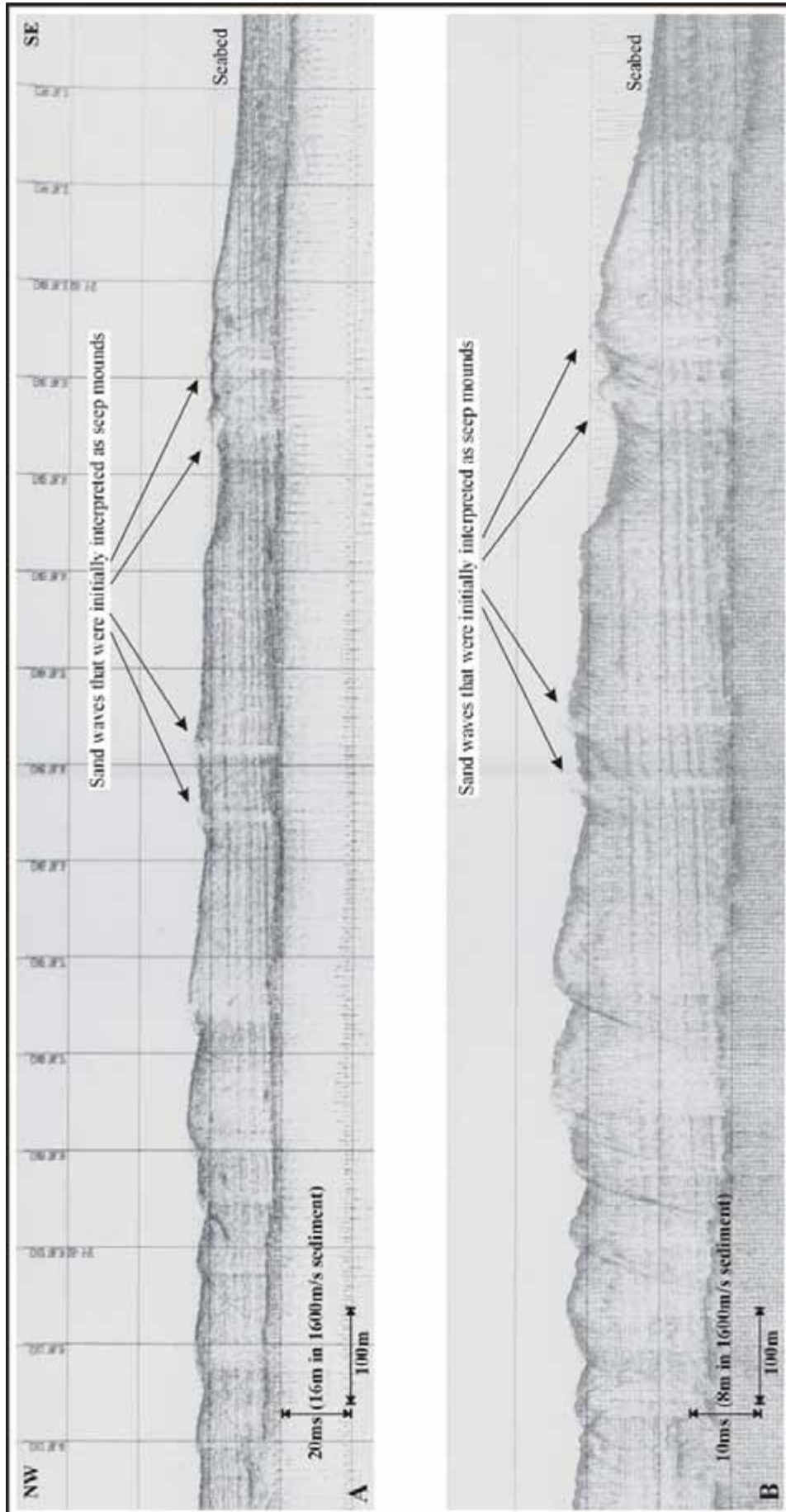
Mounds imaged on multibeam data have been illustrated and described in Chapter 4.3 and Chapter 7 (see Fig. 4.9, 4.10, 7.2 & 7.3).

#### **6.4 Mud diapirs**

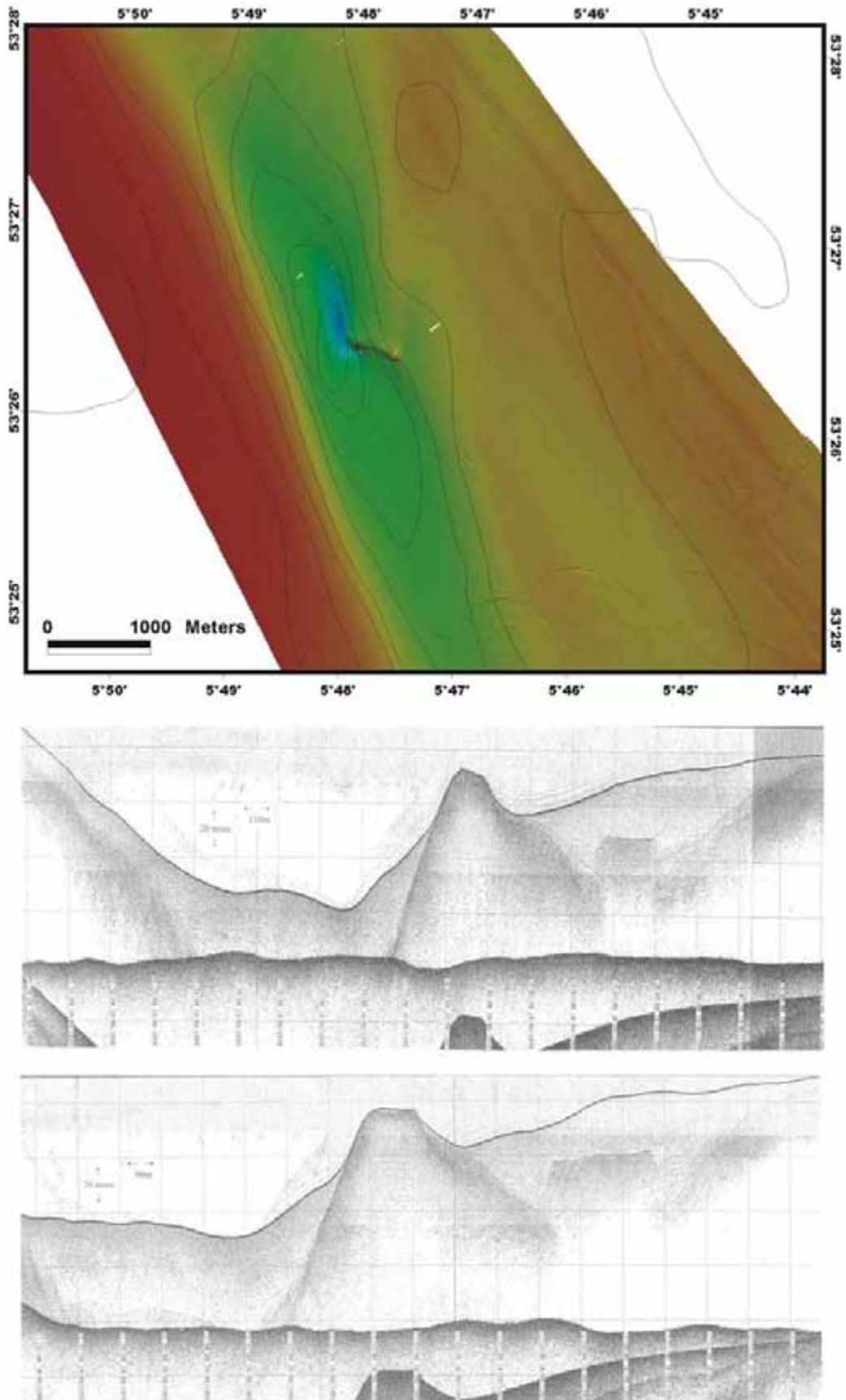
The Lambay Deep mud diapir represents the only documented example located within the IRL-SEA6 sector to date. The RV Celtic Voyager 1998 GeoChirp survey has shown that it occurs in an area dominated by shallow gas fronts (see Ch. 5). It is assumed that this mud diapir was formed due to a combination of gas-pressured sediments and dilation along the Codling (strike-slip) Fault. Figure 6.4 shows the surface and internal structure of the Lambay Deep mud diapir as imaged on multibeam and GeoChirp data. Note that the crest line of the feature strikes at an angle to the main Codling Fault trend (see also Figure 4.8).

#### **6.5 Trenches**

It is apparent that gas escape processes may also facilitate the creation of regional scale structures represented by submarine trenches. The distribution and bathymetric expression of the trench-like structures is shown on Figure 1.3.



**Figure 6.3:** (A): 300J Boomer profile. (B): 5KW Pinger profile. Both records show faint mounded features, which proved to be sand waves with very sharp crests (Alan Judd, pers. comm.). Initially these features were interpreted as seep mounds underlain with apparent gas chimneys. See Figure 4.2 for location. (From Croker, 1994 (Fig. 11) with additional interpretation.)



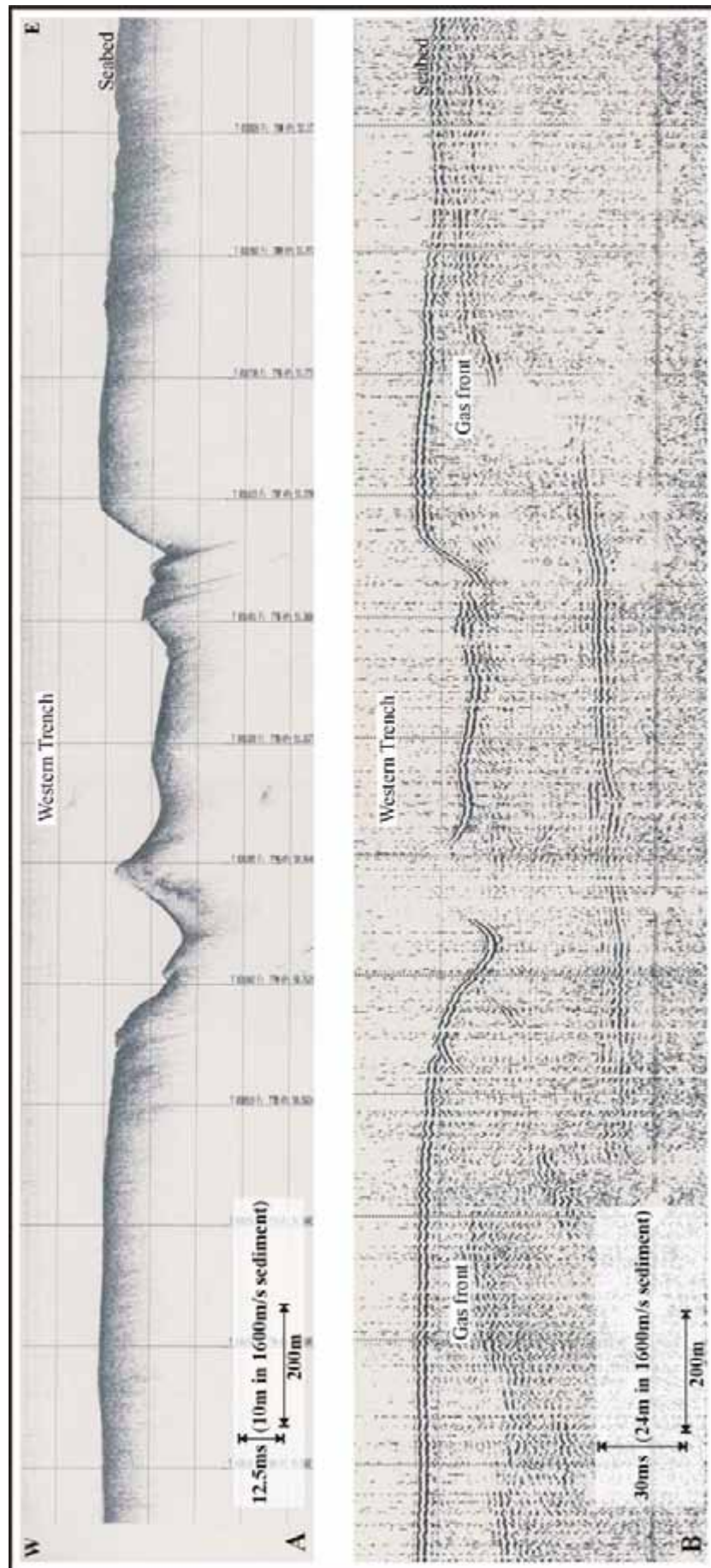
**Figure 6.4:** The Lambay Deep mud diapir as imaged on multibeam and GeoChirp data. See Figure 4.2 for location.

Figure 6.5 shows a west-east cross section of the Western Trench, which represents a narrow depression. The Western Trench possesses steep sides and irregular seabed morphology (Fig. 6.5A). The Sparker profile (Fig. 6.5B) illustrates that the trench occurs where the gas front reaches the surface; however, no gas is evident beneath the trench. Conventional seismic data shows that this trench is associated with underlying Carboniferous reflectors and apparent faulting (Fig. 4.4). Ground-truthing video surveys have revealed possibly unusual concentrations of benthic biology on the bottom of the trench (see Ch. 7.2.2).

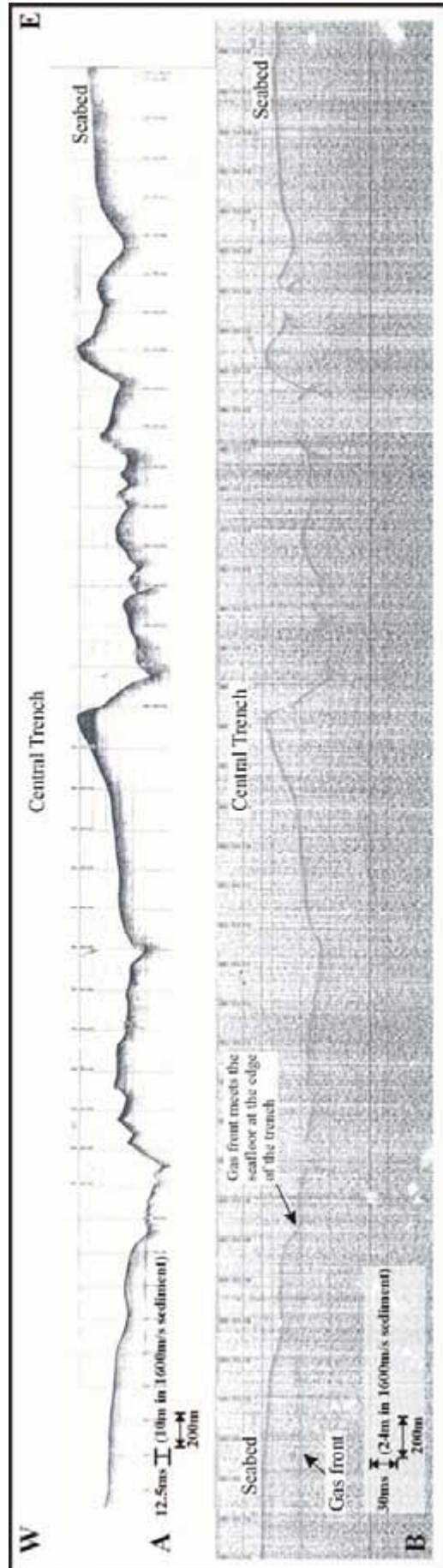
Figure 6.6 shows the Central Trench located to the east of the Western Trench. The upper profile (Fig. 6.6A) shows the irregular seabed topography and suggests that major peaks have been created by erosion of the flanking areas. The lower profile (Fig. 6.6B) demonstrates that the gas front on the left rises to meet the seafloor at the western edge of the trench. The relationship of the Central Trench with the subcrops of dipping Carboniferous reflectors has been illustrated above on Figure 4.5.

Figure 6.7 illustrates the seabed and sub-seabed morphology of the Harvey Trench located further to the east. All three profiles demonstrate that this trench possesses steep walls and an irregular seabed topography of apparently erosional origin. Some of the peaks appear to be sand waves, which show diffuse seabed reflections thus maybe implying a recent origin. Note that the Pinger profile (Fig. 6.7B) differs from the echosounder (Fig. 6.7A) and Sparker (Fig. 6.7C) on the right-hand side due to excessive “cable out” and differs elsewhere since it was acquired on an adjacent trackline. The lower Sparker profile (Fig. 6.7C) shows an apparent gas front reaching the seabed at the eastern edge of the trench.

Moreover, GeoChirp data from the Jones Trench, Peel Basin 1 and 2 sites and Lambay Deep (see Fig. 1.3 for location of sites) demonstrates the linkage of observed trench-like seabed morphology with changes in the depth of shallow gas fronts (see Fig. 5.7-5.10). Therefore, it is suggested that these seabed structures have been influenced by gas venting processes. The coincidence of some of the trench-like structures with smaller-scale gas escape features such as mud diapirs (e.g. Lambay Deep) and pockmarks (Peel Basin 2), adds credibility to this hypothesis.



**Figure 6.5:** The Western Trench: (A) Pinger–Seapro SBP 5.5kHz profile; (B) 1000J Sparker profile. Both profiles image a narrow depression, termed the “Western Trench”. The Western Trench possesses steep sides and irregular seabed morphology. The lower profile (B) illustrates that the trench occurs where the gas front reaches the surface; however, no gas is evident beneath the trench. See Figure 4.2 for location. (From Croker, 1994 (Fig. 14) with additional interpretation.)



**Figure 6.6:** The Central Trench: (A) Pinger–Seapro SBP 5.5kHz profile; (B) 1000J Sparker profile. Both profiles image the Central Trench located to the east of the Western Trench. The upper profile (A) shows the irregular seabed topography and suggests that major peaks have been created by seabed erosion. The lower profile (B) demonstrates that the gas front on the left rises to meet the seafloor at the edge of the trench. See Figure 4.2 for location. (From Croker, 1994 (Fig. 16) with additional interpretation.)

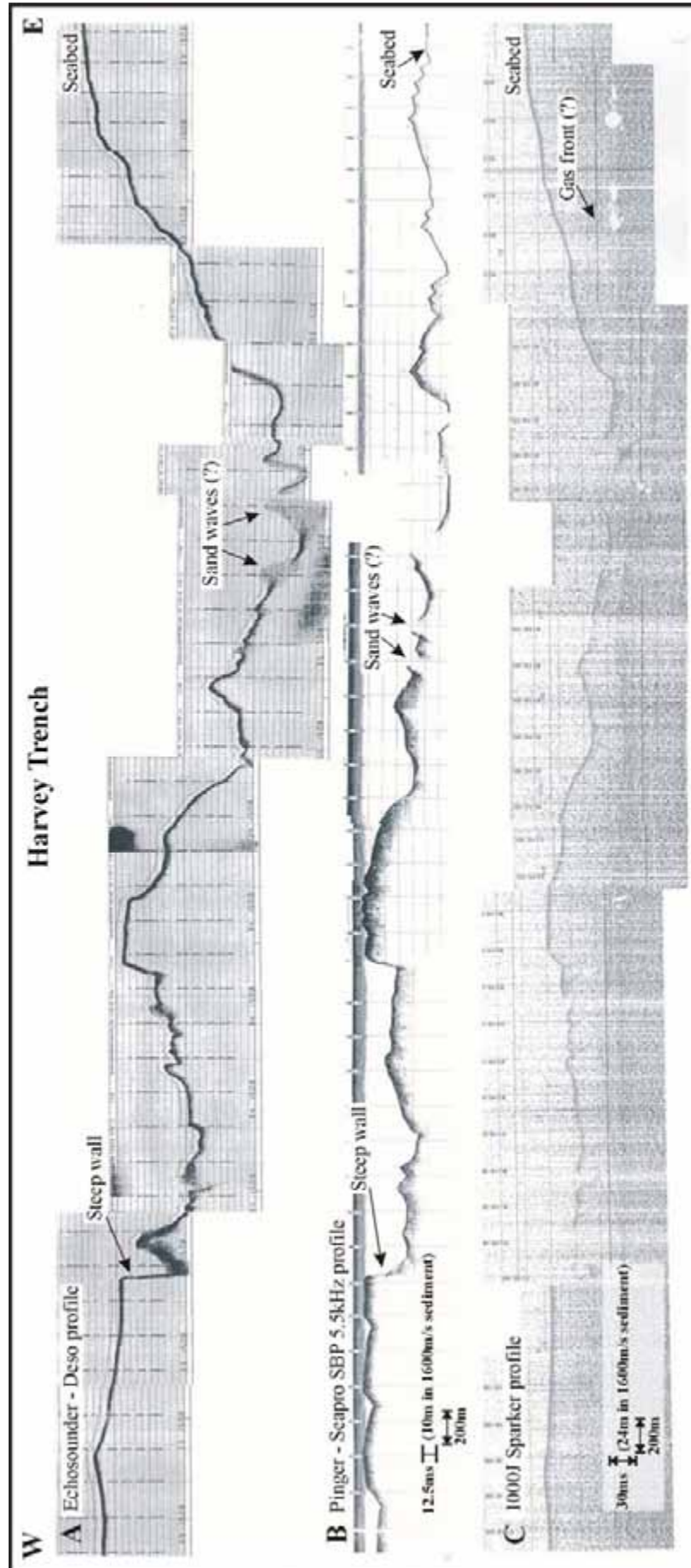


**Figure 6.7:** Harvey Trench: (A) Echosounder-Deso, (B) Pinger-Seapro SBP 5.5kHz, and (C) 1000J Sparker profiles. All three profiles cross the Harvey Trench located east of the Central Trench. The trench possesses steep walls and an irregular seabed topography apparently of erosional origin. Some of the peaks appear to be sand waves, which show diffuse seabed reflections thus maybe implying a recent origin. Note that the Pinger profile (B) differs from the echosounder (A) and Sparker (C) on the right-hand side due to excessive “cable out” and differs elsewhere since it was acquired on an adjacent track line. See Figure 4.2 for location. (From Croker, 1994 (Fig. 18) with added interpretation.)

### **6.6 Abnormal sand waves**

Abnormally high sand waves have been documented in the southern part of the IRL-SEA6 area. Figure 6.8 images one of these waves located in a hollow or shallow trench. The seafloor topography is apparent below the sand wave. The sand wave is broadly symmetrical, but deposition within the wave appears to be from south to north. Figure 6.9 shows the side-scan sonar image of the same wave in plan view. The wave possesses a very straight and regular crest and is surrounded with a moat or shallow trench. A seismic line run across the location of this feature shows a tentatively interpreted Jurassic reflector and faults extending to the surface in the proximity of the sand wave (Fig. 4.6).

Further south another area of abnormal sand waves has been documented (Fig. 6.10). The upper sparker profile (Fig. 6.10A) shows two high amplitude sand waves in a small depression in the centre of the section above a bedrock pinnacle. The sketched bedding on the lower profile based on the interpretation of high-resolution seismic line GH85-41-01 (Fig. 6.10B & Fig. 4.7) indicates the presence of a fault below the sand waves.

Thus the origin of these abnormal sand waves may be related to gas seepage processes, although this conclusion remains highly tentative at present.

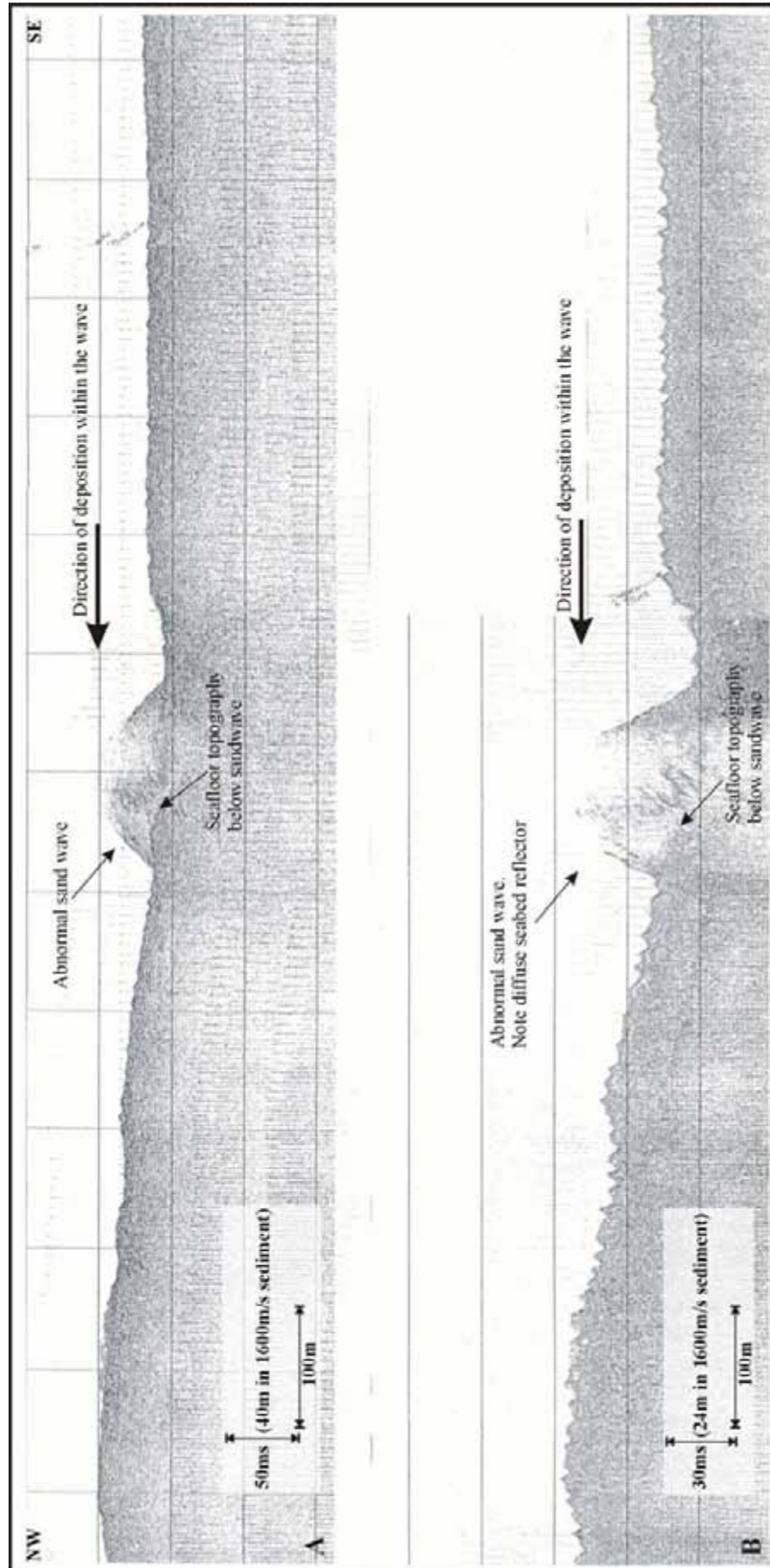


**Figure 6.8:** Abnormal sand wave: (A) 200J Boomer and (B) 3.5kHz Pinger profiles. This abnormally high sand wave is located in a hollow or shallow trench and there seems to be seafloor topography below the sand wave. The sand wave is broadly symmetrical, but deposition within the wave appears to be from south to north. See Figure 4.2 for location. (From Croker, 1994 (Fig. 22) with additional interpretation.)

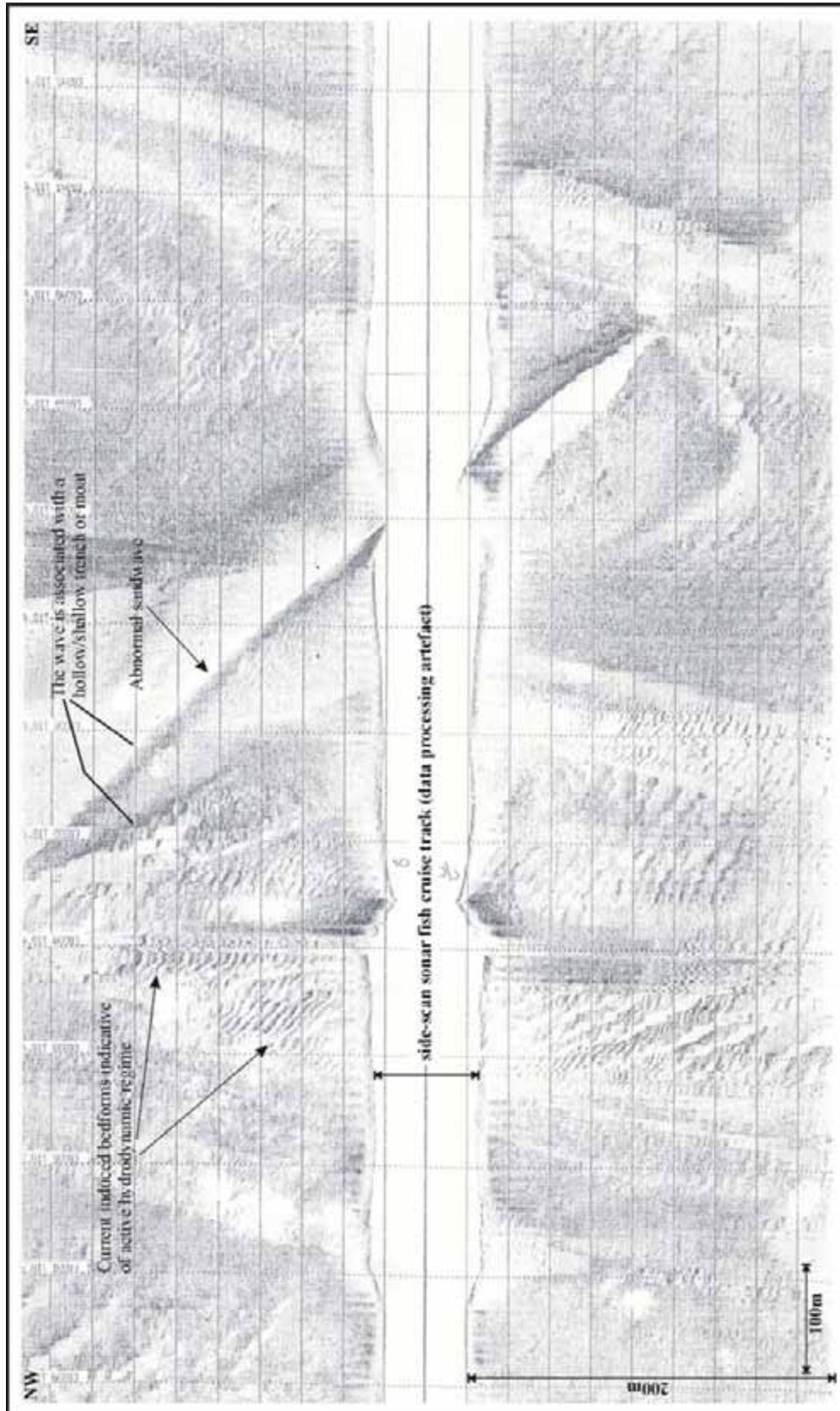


**Figure 6.9:** Side-scan sonar image showing one of the abnormal sand waves in plan view. The wave possesses a very straight and regular crest and is surrounded with a moat or shallow trench. See Figure 4.2 for location. (From Croker, 1994 (Fig. 23) with additional interpretation.)

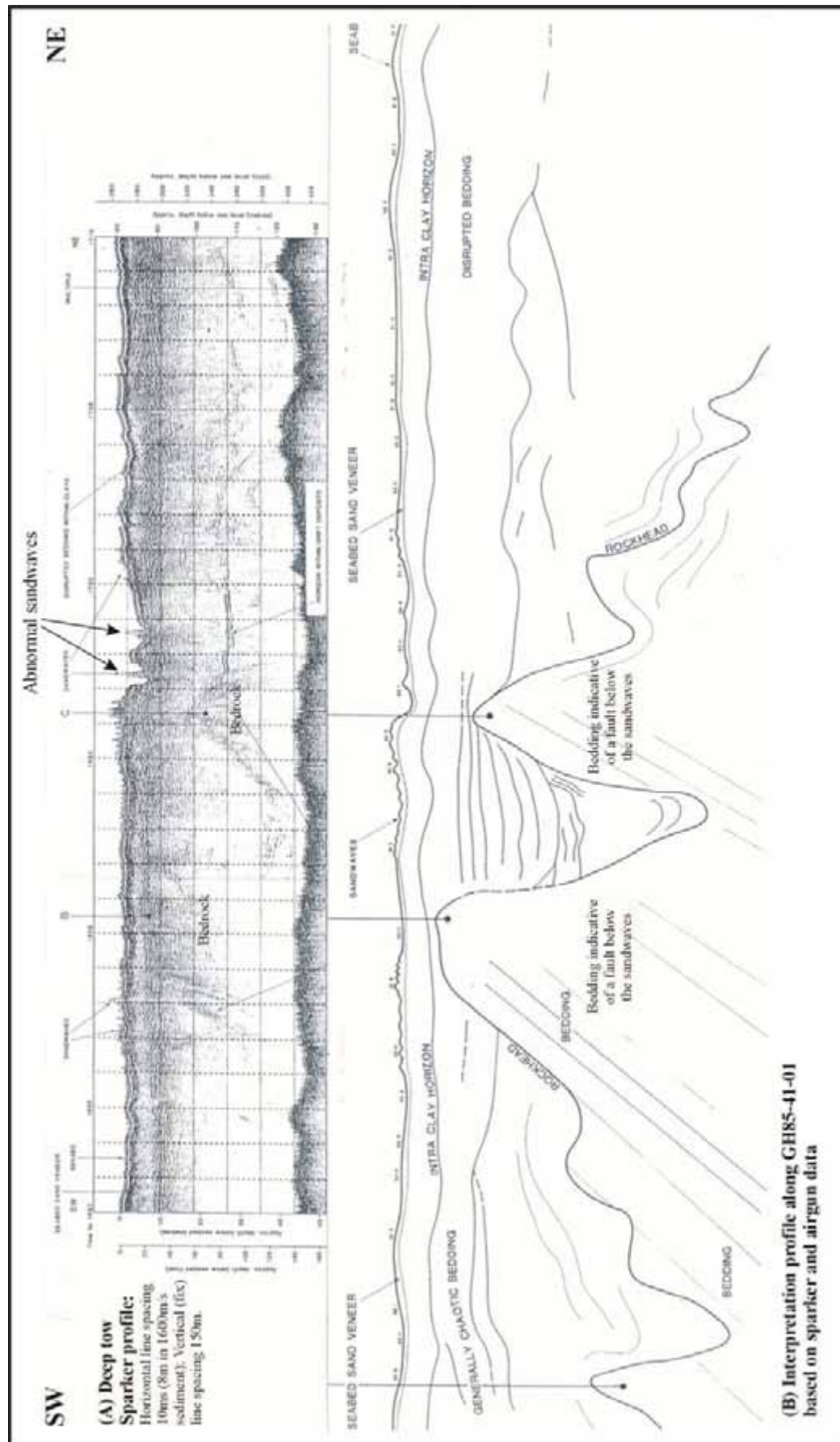


**Figure 6.10:** (A): Deep-tow Sparker profile. (B): Interpretation profile along GH85-41-01 based on Sparker and airgun data. The upper profile (A) shows two high amplitude sand waves in a small depression in the centre of the section above a bedrock pinnacle. The sketched bedding on the lower profile (B) indicates the presence of a fault below the sand waves. See Figure 4.2 for location. (From Croker, 1994 (Fig. 25) with additional interpretation.)

**6.7 Summary of distribution of gas accumulations and gas escape structures.**

The map shown on Figure 6.11 illustrates the distribution of all shallow gas accumulation, migration and gas escape features documented by this study, while Figure 6.12 shows the same distribution overlain on the solid geology map of the northern part of the IRL-SEA6 area.

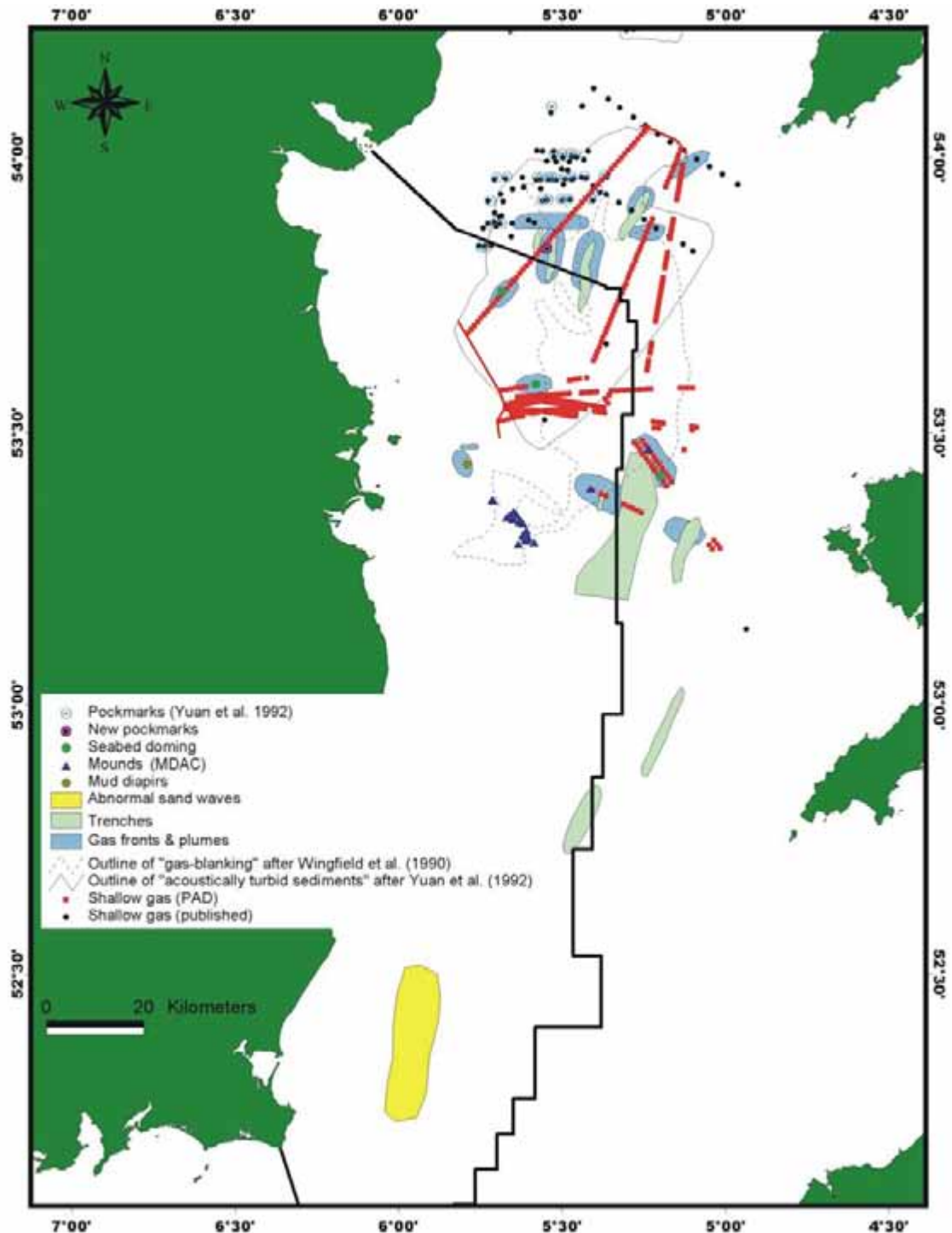


**Figure 6.11:** Distribution of gas accumulation, migration and escape features in the western Irish Sea.

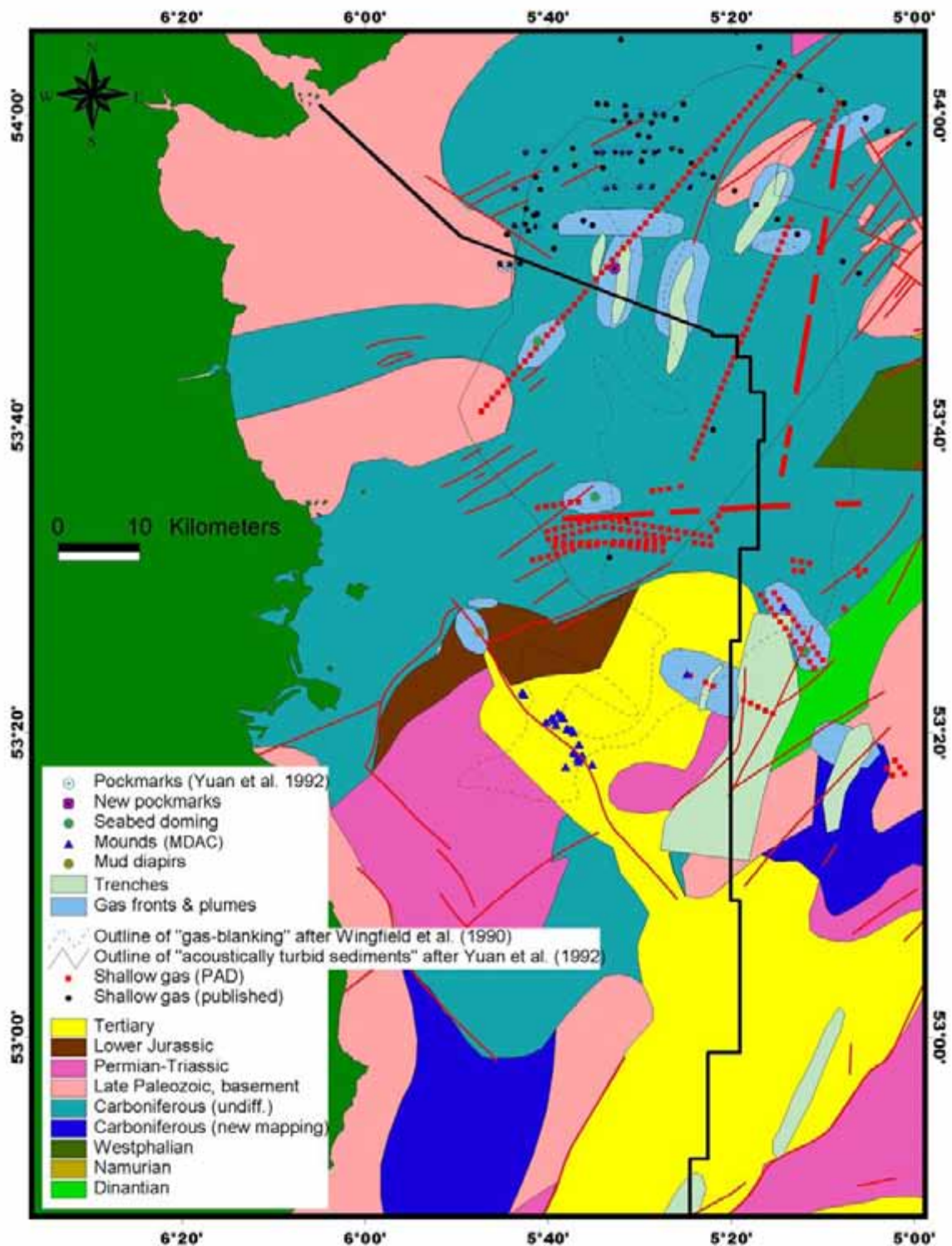


**Figure 6.12:** Solid geology of the northern part of the IRL-SEA6 sector and adjacent areas (courtesy of BGS with modifications by Croker & Power, 1996b). Carboniferous rocks represent the main known potential sources of methane in the area. The map also demonstrates the distribution of gas accumulation, migration and escape structures, which were documented where source rocks subcrop Quaternary deposits or where migration pathways (faults) are present.

## 7. Evidence of Gas Seepage

This section summarises the evidence for gas seepage in the IRL-SEA6 area. Some of the evidence implies that seepage is ongoing, while other evidence suggests that the seepage at least took place in the recent past or possibly occurs in pulses. Evidence of contemporary gas seepage has been summarised on Figure 7.1 and is described in more detail below. Figure 7.2 locates the investigated study sites.

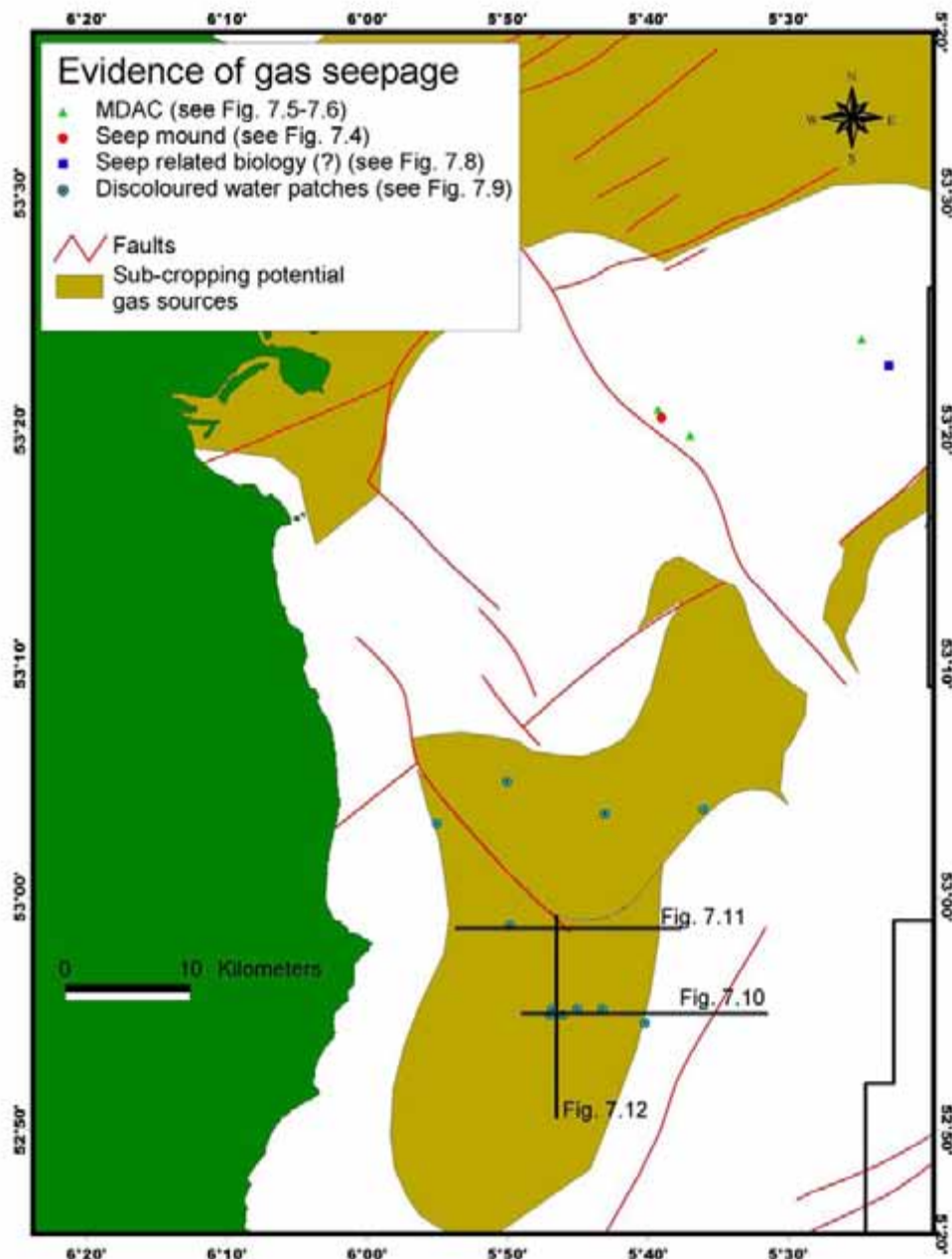


**Figure 7.1:** Summary map indicating evidence of contemporary gas seepage documented by this study. Also shown are the locations of seismic lines presented on Fig. 7.10-7.12.

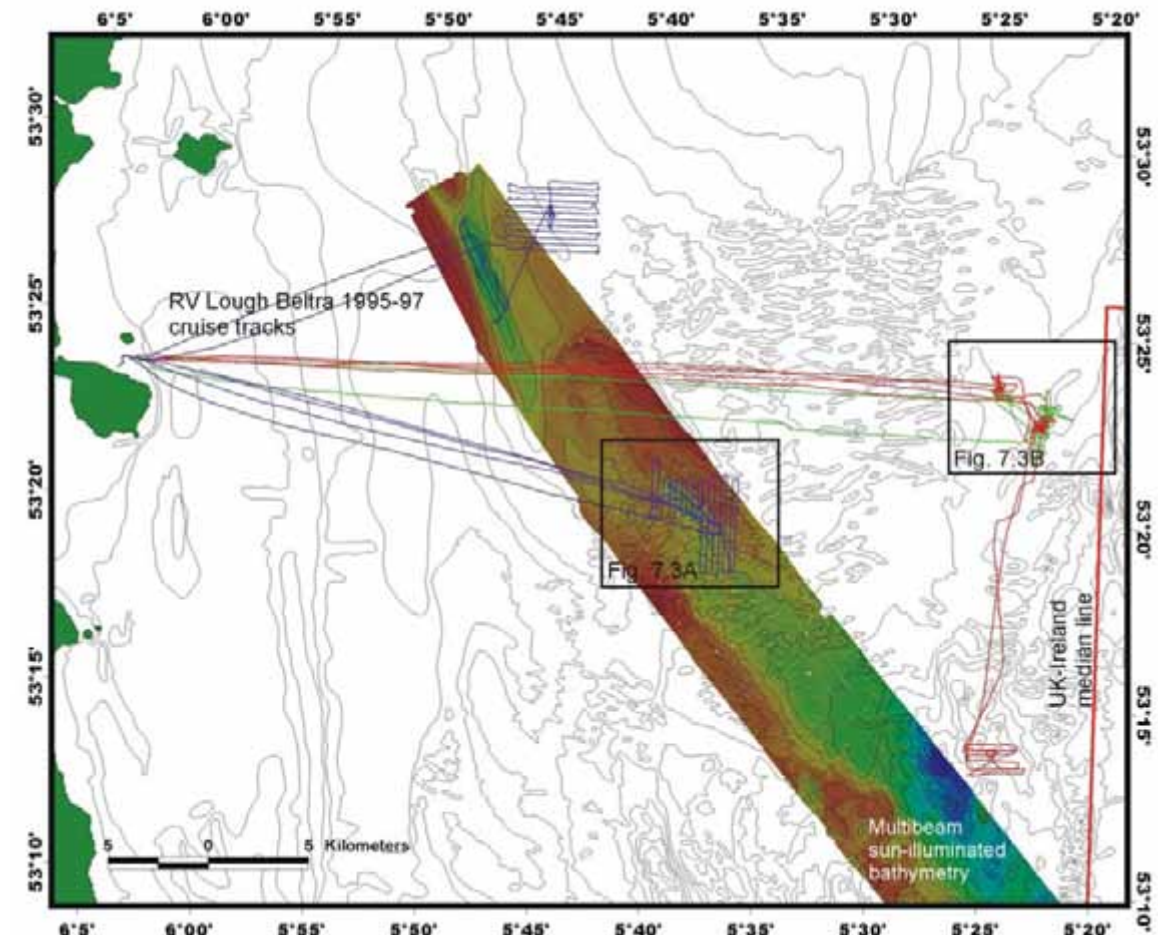


**Figure 7.2:** Map showing cruise tracks of RV Lough Beltra 1995, 1996 & 1997 cruises with indication of the ROV video survey sites. Cruise tracks are plotted on top of the sun-illuminated multibeam bathymetry acquired during RV Celtic Voyager 2001-2002 cruises. Bathymetric contours drawn at 10m intervals (courtesy of BGS). Location of Figures 7.3A & B are also shown.

### 7.1 Acoustic evidence

Acoustic evidence of contemporary gas seepage has been encountered in the IRL-SEA6 area on two separate occasions. In 1996, during the course of a site survey over the Finnegan prospect for Enterprise Oil (Britsurvey, 1996), gas was observed seeping into the water column (Figure 4.11B). In 2001 during the Celtic Voyager multibeam cruise, gas was recorded on the echosounder seeping from one of the mounds (Fig. 7.3, 7.4). The echosounder photograph shows twin plumes of gas bubbles rising into the water column. The plume height is approximately 35m and the plumes are being deflected in the direction of the tidal current.

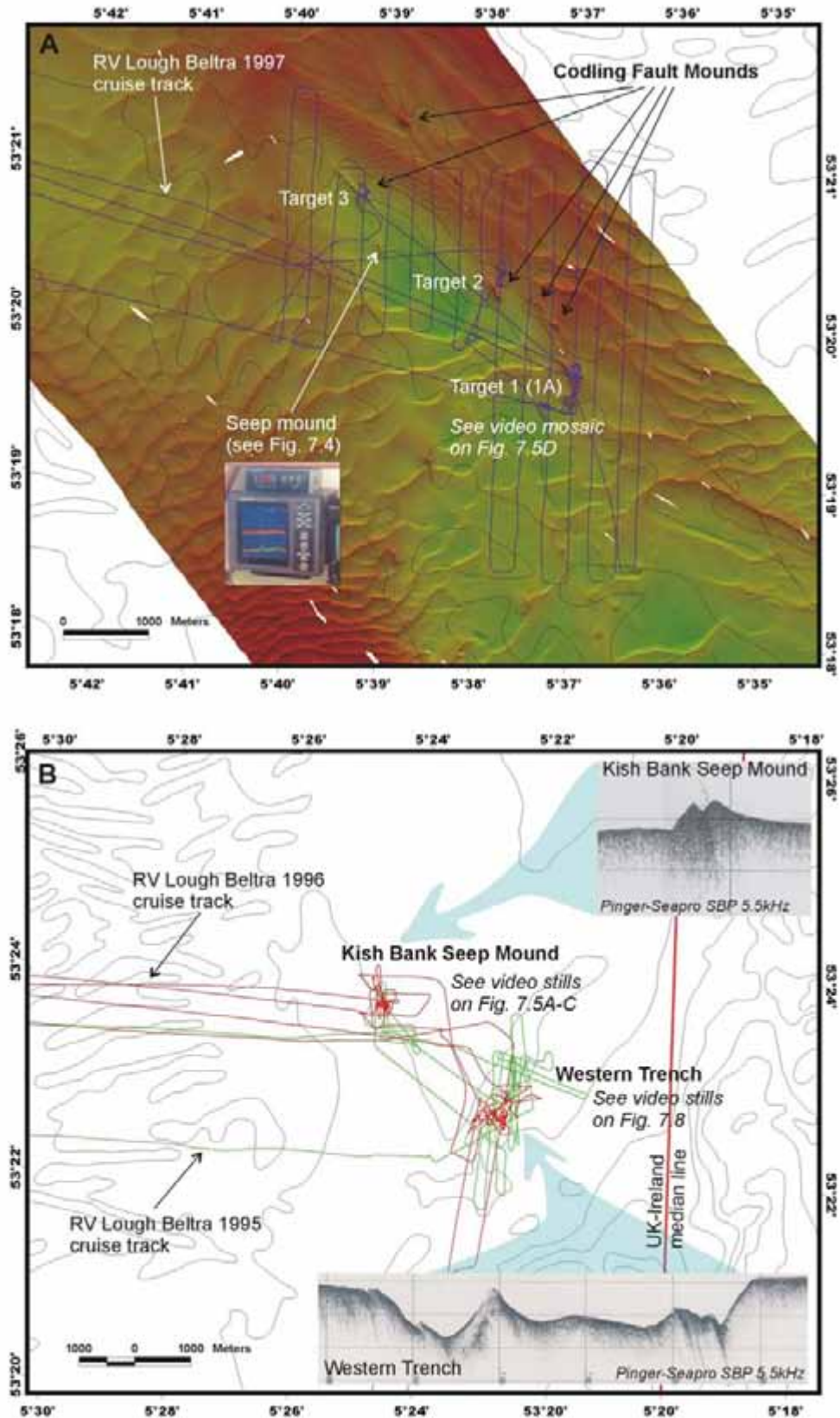


**Figure 7.3:** (A): Zoom image showing RV Lough Beltra 1997 cruise track over the Codling Fault mounds, and indicating location of the ROV video survey sites. Background image is represented with sun-illuminated multibeam bathymetry (RV Celtic Voyager 2001-2002). (B): Zoom image of the RV Lough Beltra 1995 & 1996 cruise tracks over the Kish Bank seep mound and Western Trench areas with indication of the ROV video survey sites. Insets from the Pinger-Seapro 5.5kHz profiles illustrate seabed morphologies of the surveyed sites.



**Figure 7.4:** Echosounder record acquired during RV Celtic Voyager 2001 cruise, showing gas plume rising from one of the mounds in the Codling Fault area. Plume height is approximately 35m. For location see Fig. 7.3A.

## **7.2 Ground-truthing evidence**

Ground-truthing surveys with the ROV provided visual information on the appearance of the seabed in the proximity of gas escape structures. Particularly, video imagery indicated the presence of methane-derived authigenic carbonates (MDAC) and possibly unusual benthic biology.

### ***7.2.1 Methane-derived Authigenic Carbonate (MDAC)***

General aspects of MDAC have been outlined above (see Ch. 1.2.4). The presence of MDAC does not necessarily imply that gas seepage is ongoing, but indicates that gas

seepage took place in the recent past and might be reinitiated in the near future if the seepage occurs in pulses.

#### 7.2.1.1 Video evidence

Video surveys with the ROV during the RV Lough Beltra 1996 cruise has indicated the presence of MDAC at 96m water depth at the Kish Bank (KBA) seep mound site (Fig. 7.3B). Figure 7.5A-C shows examples of what is interpreted as slabs of carbonate-cemented sediment crust. Similar crusts composed of carbonate-cemented sandstones were observed on the Codling Fault mounds surveyed during the RV Lough Beltra 1997 cruise (Fig. 7.3A). The mosaic of video stills from Target 1 (Fig. 7.3A) is presented on Figure 7.5D, and shows that the carbonate-cemented sandstones can have near-vertical relief.

#### 7.2.1.2 Seabed sample data

Carbonate-cemented sandstones were recovered from Target 3 in the Codling Fault area (Fig. 7.3A & Fig. 7.6). Fragments shown on Figure 7.6 (A & C) were initially part of one sample (approx. 60 x 35cm, hauled up on the anchor), which was broken up during sub-sampling. SEM analysis of one of these samples indicates that it is mainly composed of quartz grains (87%) and aragonite cement (6%). The aragonite occurs in the form of needle-type crystals typical of authigenic precipitation (Fig. 7.6E-F). Iron sulphide minerals are also present in the form of thin films coating quartz grains and showing a range of morphologies from near amorphous to well-developed framboidal pyrite (Fig. 7.6 G-H) (Croker et al., 2002).

#### 7.2.1.3 Evidence from fishermen

Useful information regarding the distribution and extent of MDAC can also be gleaned from anecdotal evidence from fishermen. Figure 7.7 shows part of a fishermen's chart of trawling areas and obstructions in an area within the Kish Bank Basin in the vicinity of the seep mounds referred to above (see Fig. 7.3A). This map is annotated with the words "concrete" and "coral". In the light of the findings from the research cruises it is plausible to assume that what the fishermen have termed in a non-scientific style as "concrete" might actually be carbonate-cemented sandstone (MDAC).

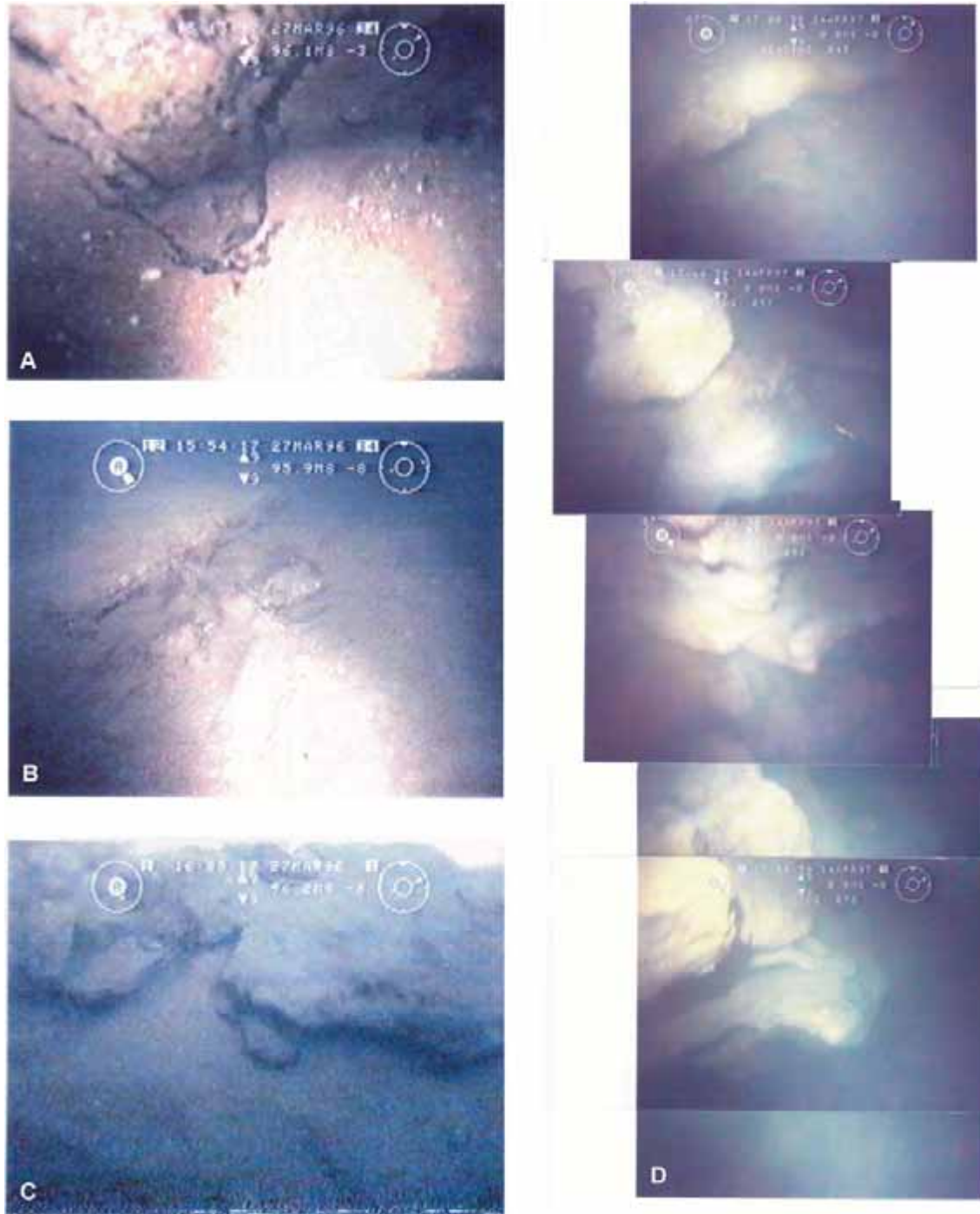


**Figure 7.5:** Stills from the ROV video imagery showing slabs of what is interpreted as carbonate-cemented sediment crust. (A-C): Stills from RV Lough Beltra 1996 ROV video, Kish Bank seep mound, water depth 96m (see Fig. 7.3B for location); (D): Mosaic of video stills taken on Target 1 (see Fig. 7.3A for location) during RV Lough Beltra 1997 ROV survey of the Codling Fault mounds. Note the considerable relief of the carbonate-cemented sandstones.

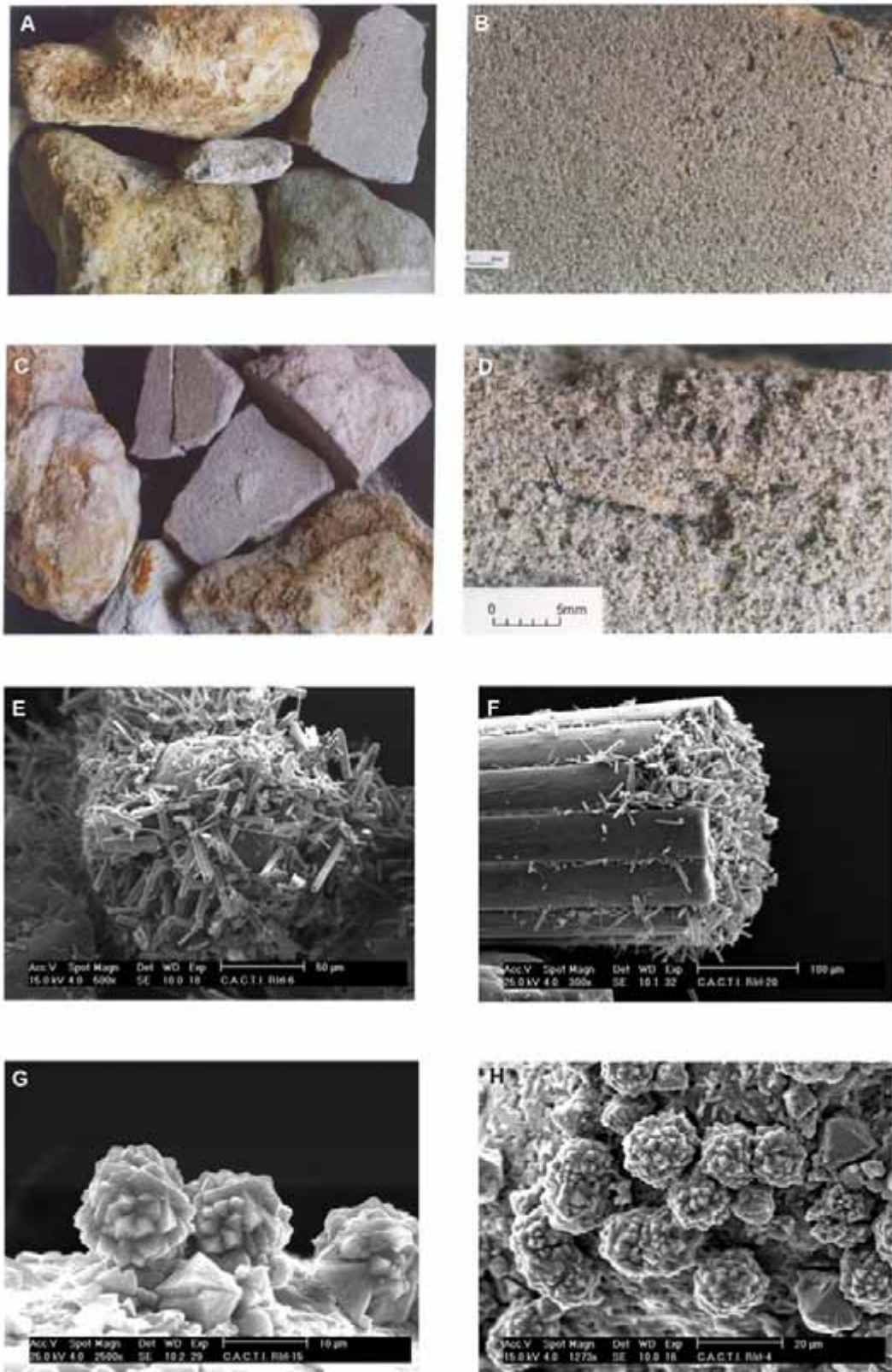


**Figure 7.6:** Anchor samples acquired during RV Lough Beltra 1997 cruise from target 3 located on Figure 7.3A. (A&C): Photographs of sample fragments showing both original and internal cut surfaces. (B&D): Close up photographs of the same samples at low (170% - B) and high (460% - D) magnification. Arrow represents the reference point. (E): SEM photograph imaging aragonite cemented sand grain. (F): SEM photograph imaging aragonite needles encrusting an echinoderm spine. (G&H): SEM photographs imaging Fe-sulphide minerals.

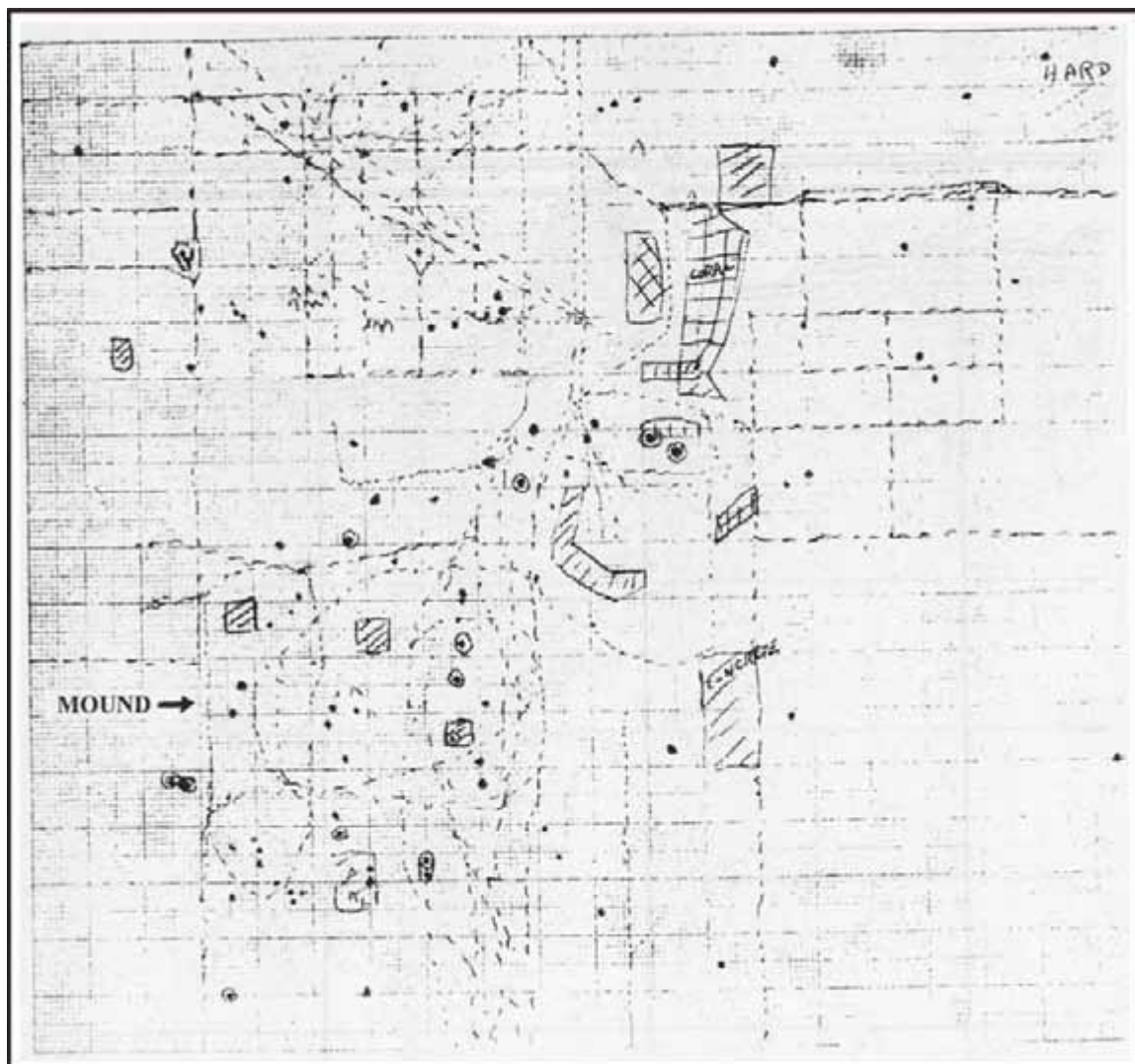


**Figure 7.7:** A fishermen's chart showing trawling areas and obstructions. Areas indicated as "concrete" might tentatively indicate distribution of carbonate-cemented sandstones.

### ***7.2.2 Unusual benthic biology***

Video surveys with the ROV indicated the presence of possibly unusual benthic biological assemblages at some of the sites. The Western Trench was surveyed in detail during ROV dives from the RV Lough Beltra in 1995 and 1996. The ROV surveys revealed that the seabed within the trench is often dominated by abnormal shelly concentrations and can also accommodate abundant *Sabellid* tube worms. Selected video stills from the Western Trench are shown on Figure 7.8. These somewhat unusual benthic bio-accumulations are suspected to be associated with methane seepage but this is a very tentative conclusion at present.

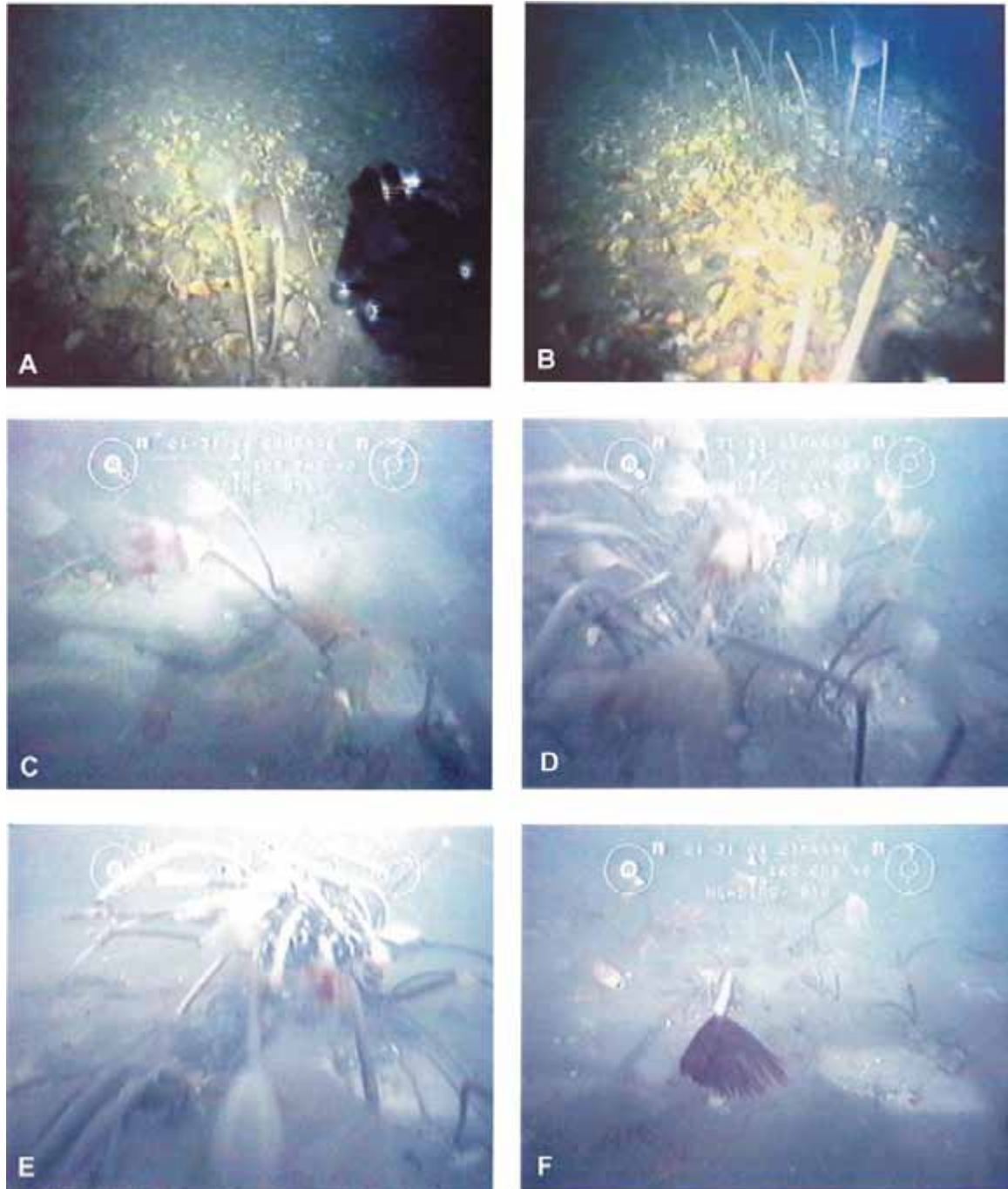


**Figure 7.8:** Selected stills from the Western Trench ROV video surveys conducted during RV Lough Beltra 1995 and 1996 cruises (see Fig. 7.3B for location). (A-B): Shelly concentrations and *Sabellid* tube worms, 115m water depth. (C-F): Tube worms, 123m water depth.

### **7.3 Evidence from aerial video survey**

Circular patches of discoloured water were reported and subsequently documented on the sea surface east of Wicklow Head by an aerial video survey in August 1995 (Croker & Power 1996b). The location of these events is indicated on Figure 7.1, and a video image

of one is presented on Figure 7.9. Analysis of water samples revealed that this discoloration was due to the presence of fine organic matter from the seafloor that was suspended in the water column. Similar patches in this area have been observed on a number of occasions from both surface vessels and civilian aircraft by the senior author.



**Figure 7.9:** Still from Air Corp video, taken 10 miles east of Wicklow Head, 2<sup>nd</sup> August 1995. Discoloured water patches possibly due to the effects of gas seepage and/or sediment suspension. See Fig. 7.1 for location. (From Croker & Power, 1996b: Fig. 10.)

Seismic lines from this area reveal that the sediment suspension plumes documented by the aerial video survey coincide with an area of Carboniferous subcrop. The location of these seismic lines is indicated on Figure 7.1 and the lines themselves are shown with interpretation as Figures 7.10-7.12. Arrows indicate the location of sediment suspension plumes. Figure 7.11 also demonstrates that the Carboniferous section is fractured with a number of faults.

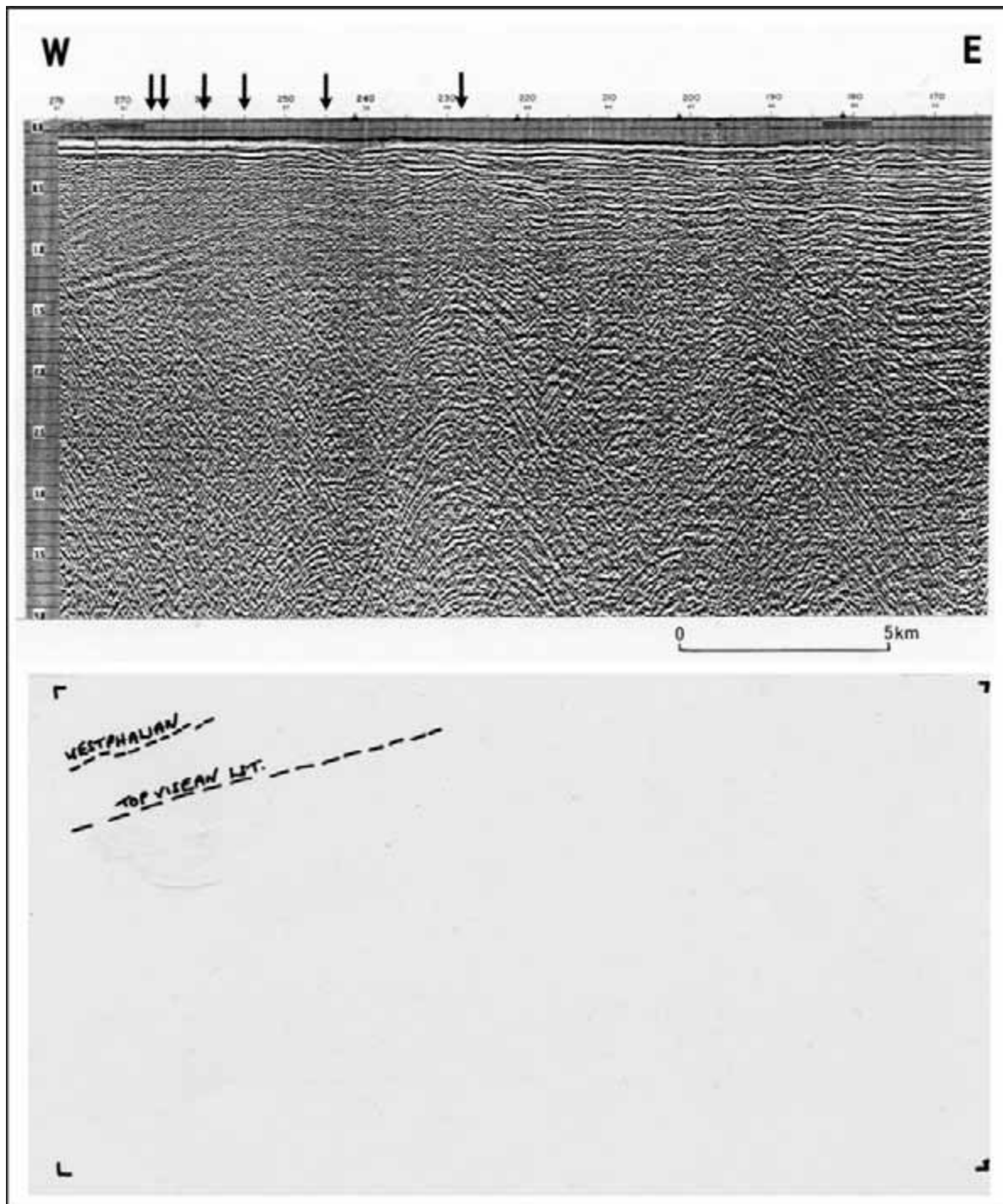


**Figure 7.10:** Seismic line EI-9 with interpretation overlay. Arrows indicate the location of sediment suspension plumes documented by 1995 aerial video survey. See Fig. 7.1 for location. (From Croker & Power, 1996b: Fig. 14.)

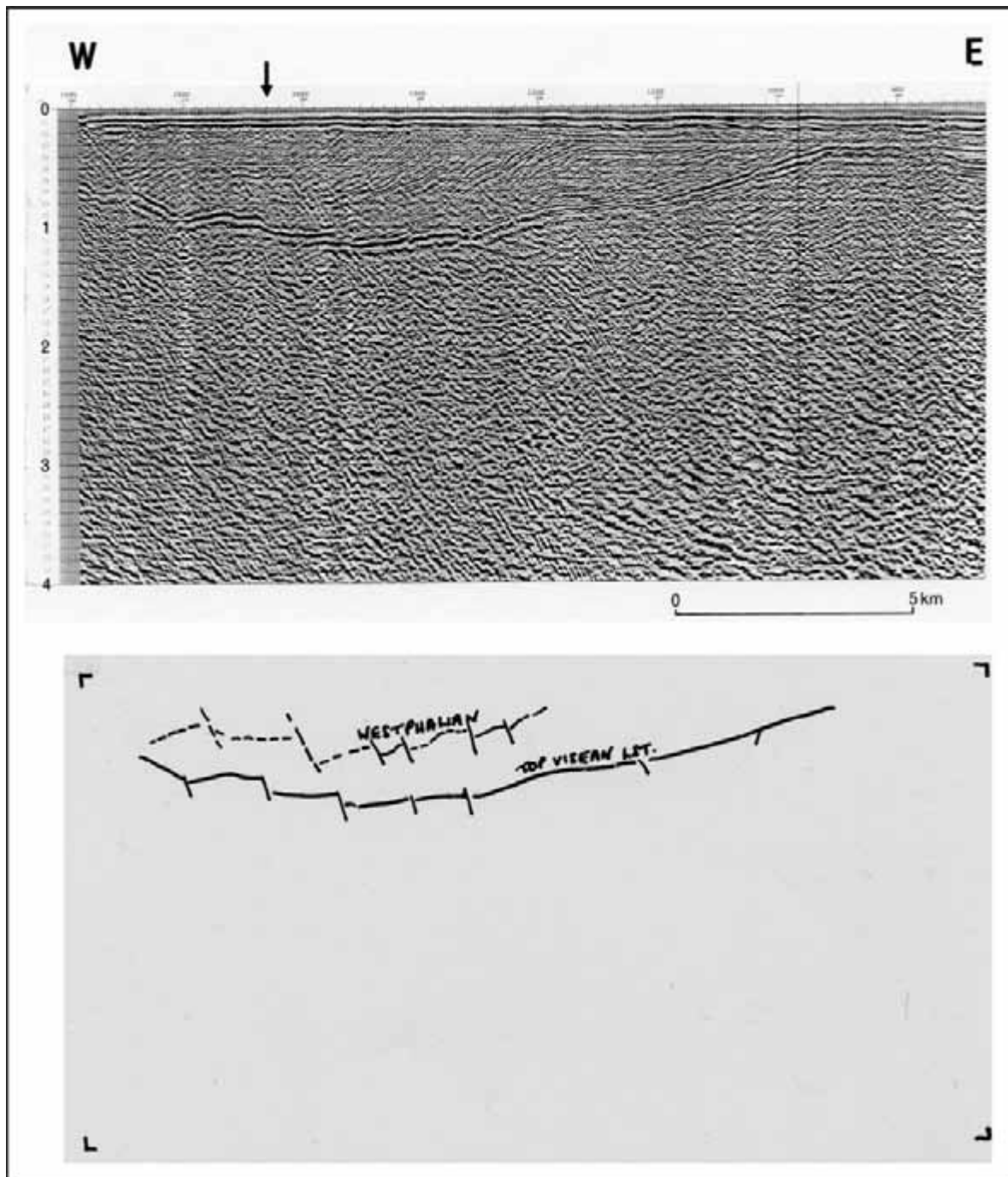


**Figure 7.11:** Seismic line IS-8 with interpretation overlay. Arrow indicates the location of sediment suspension plume documented by 1995 aerial video survey. See Fig. 7.1 for location. (From Croker & Power, 1996b: Fig. 15.)

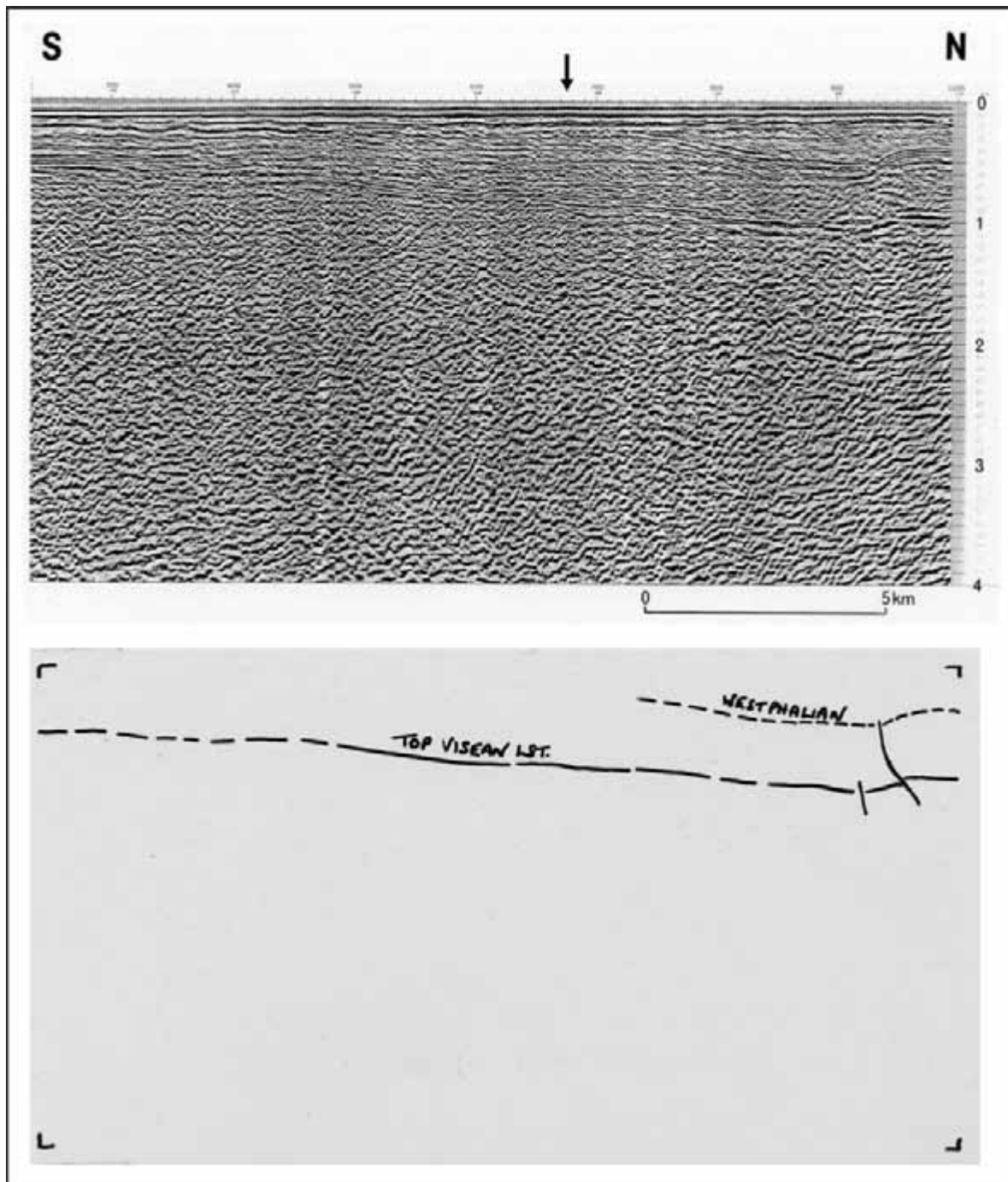


**Figure 7.12:** Seismic line IS-15 with interpretation overlay. Arrow indicates the location of sediment suspension plume documented by 1995 aerial video survey. See Fig. 7.1 for location. (From Croker & Power, 1996b: Fig. 16.)

The subcrop evidence might therefore suggest that the organic matter, which was detected to be a component of the discoloured water patches, may have been stirred up by shallow gas venting. However, it should also be noted that strong hydrodynamic conditions often resuspend sediment in the Irish Sea producing turbidity throughout the

entire water column even in water depths approaching 100m. Therefore, without other direct evidence, a gas-related hypothesis must be treated with some caution.

## **8. Discussion and Conclusions**

The data presented above with regards to the distribution and type of sub-surface gas accumulations and gas escape structures in the IRL-SEA6 area provide evidence in favour of a thermogenic origin for the gas since: the distribution of gas accumulations is not confined to any particular sediment type; gas blanking and acoustic turbidity are documented in both sandy and muddy areas; north of 53 degrees most of the gas accumulations and escape features occur where Carboniferous subcrops the Quaternary or where migration routes from the Carboniferous via faults are present. In the south, features related to gas seepage seem to occur where migration pathways, commonly represented by faults, exist from the Jurassic or possibly Carboniferous source rocks. Thus, it is probable that most of the documented gas-related features are facilitated by the escape of thermogenically-produced gas.

This report has described the distribution and type of gas accumulations and escape structures in the IRL-SEA6 sector of the Irish Sea using all available data. While accumulations of gas are not confined to any particular sediment type, the type of gas escape structure is largely a function of the lithological composition of seabed sediments. Pockmarks and mud diapirs are only present in the muddy areas of seabed with the Lambay Deep Mud Diapir investigated in detail. The association of this structure with the sub-surface gas front and its location on the trace of the Codling Fault implies that this diapir was formed due to a combination of gas-pressured sediments and fault dilation.

This study provides tentative evidence suggesting that the origin of some of the trench-type structures may be partially related to large-scale gas venting. Within the IRL-SEA6 area changes in the depth of shallow gas fronts were documented in association with the Peel Basin, Lambay Deep and Western trenches. Other gas escape structures, represented by pockmarks and seep mounds, were documented in close proximity to the trenches, and many trenches appear to be coincident with mapped faulting. Figure 8.1 shows the BGS solid geology mapped faults overlain on the 10m bathymetry. Apart from the obvious Codling Fault, note the apparent coincidence of faults with the Peel Basin 2 and Central Trench features, for example. At a more detailed scale, Figure 8.2 shows the same

bathymetry with faults mapped in the Central Irish Sea by Floodpage et al., (2001). The Block 42/8 trench appears to directly overlie one of the mapped faults. This trench and others, such as the Southern Trench (UK Block 106/4), remain to be investigated. Thus it is plausible to speculate that trenches may have a gas-related origin. However, the present day seabed morphology of the trenches suggests that they are also largely influenced by hydrodynamic activity.

Approximately 30 mound-like structures have been identified on remotely sensed imagery. All of the mounds occur in the sandy areas of the seabed in the Kish Bank Basin. Video surveys and seabed sampling revealed that the mounds are composed of slabs of carbonate-cemented sandstones (MDAC). Echosounder profiles showed that some of these mounds are actively seeping gas. However, the exact mode of formation of these mounds is still unclear. Simple cementation of the sands by MDAC doesn't explain how they grow to become features with a vertical relief of some 5-10m above the seabed.

Whereas the main concentration of MDAC mounds is along the Codling Fault with another isolated mound to the east (KBA), it has to be assumed that the occurrence of MDAC in the IRL-SEA6 area may be more widespread than documented here.

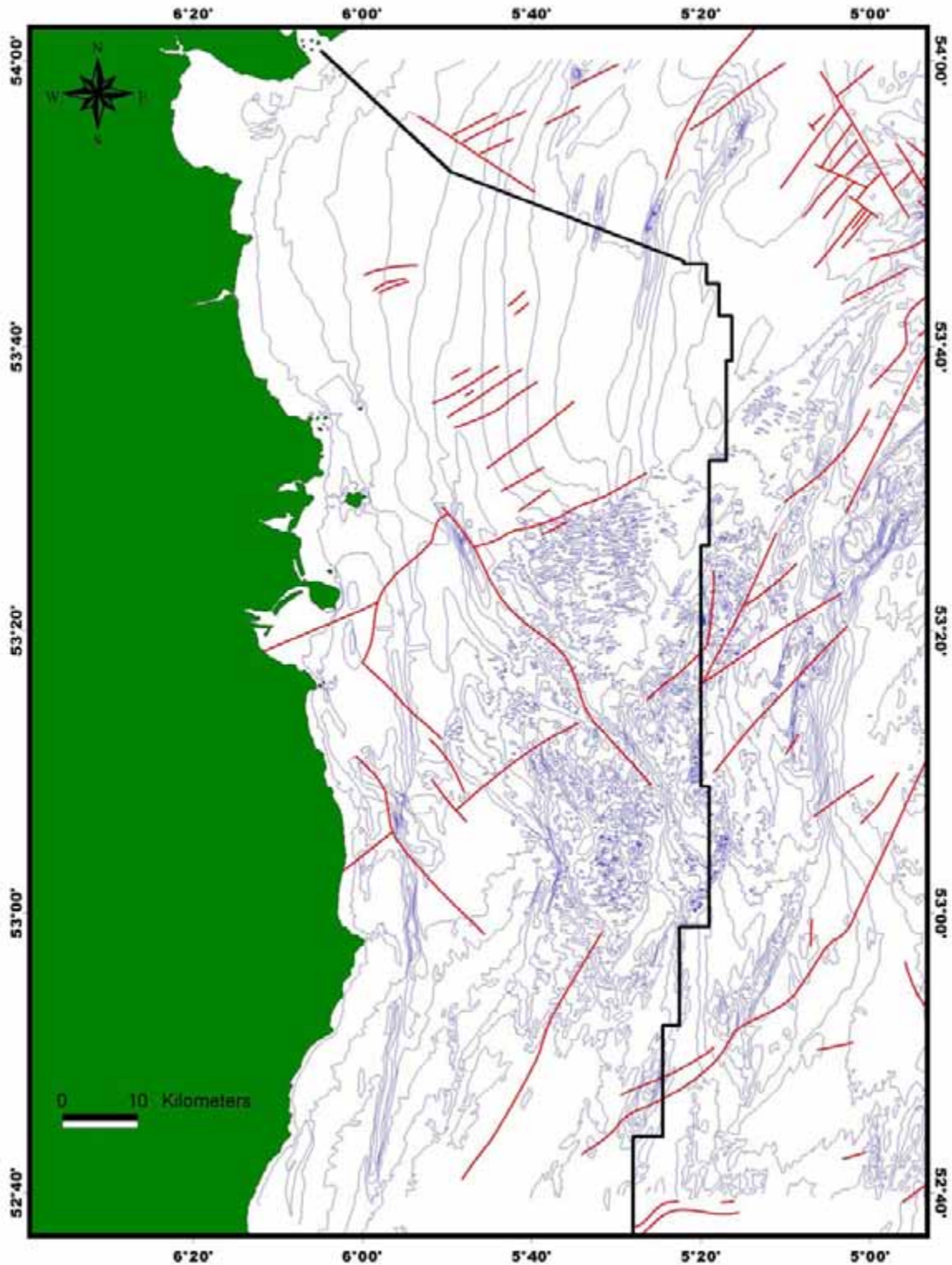


**Figure 8.1:** Bathymetry (BGS 10m contours) and faults from the BGS solid geology series. Note the apparent coincidence between faults and the Peel Basin 2 and Central Trench features, for example.

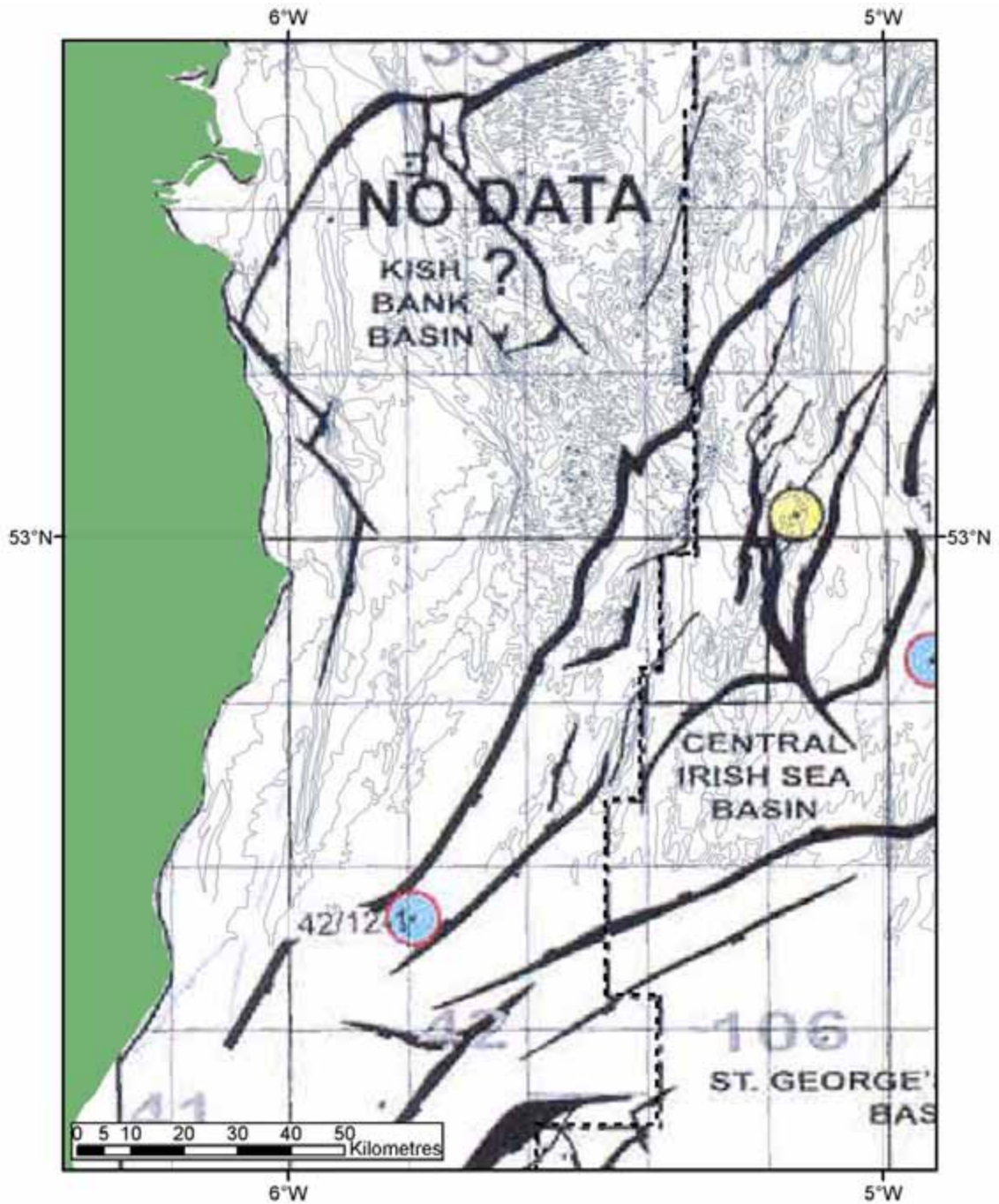


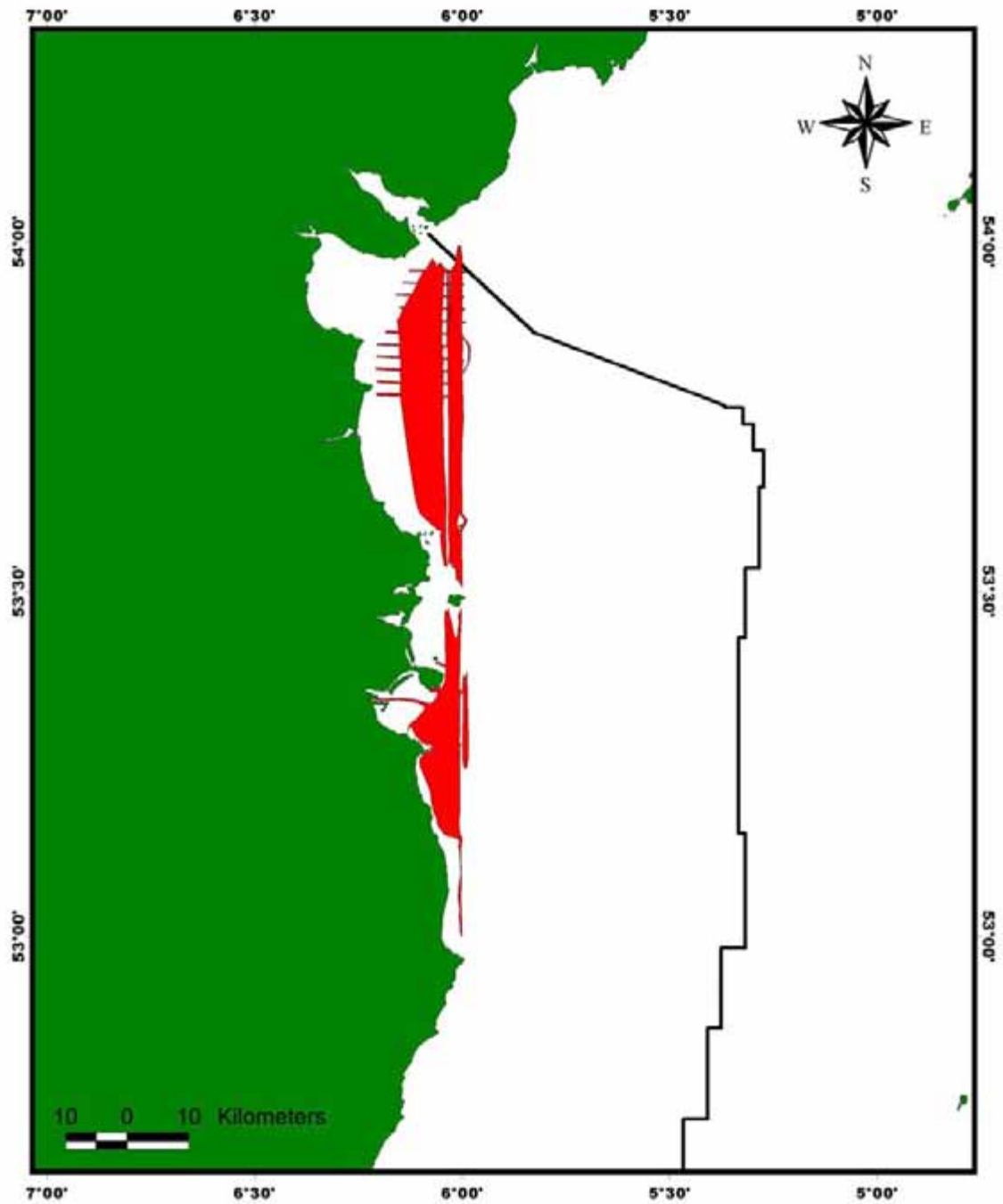
**Figure 8.2:** BGS 10m bathymetry contours and fault map of the Central Irish Sea Basin (from Floodpage et al., 2001, Figure 11). The Block 42/8 trench appears to directly overlie one of the mapped faults.

## **9. Recommendations for Further Work**

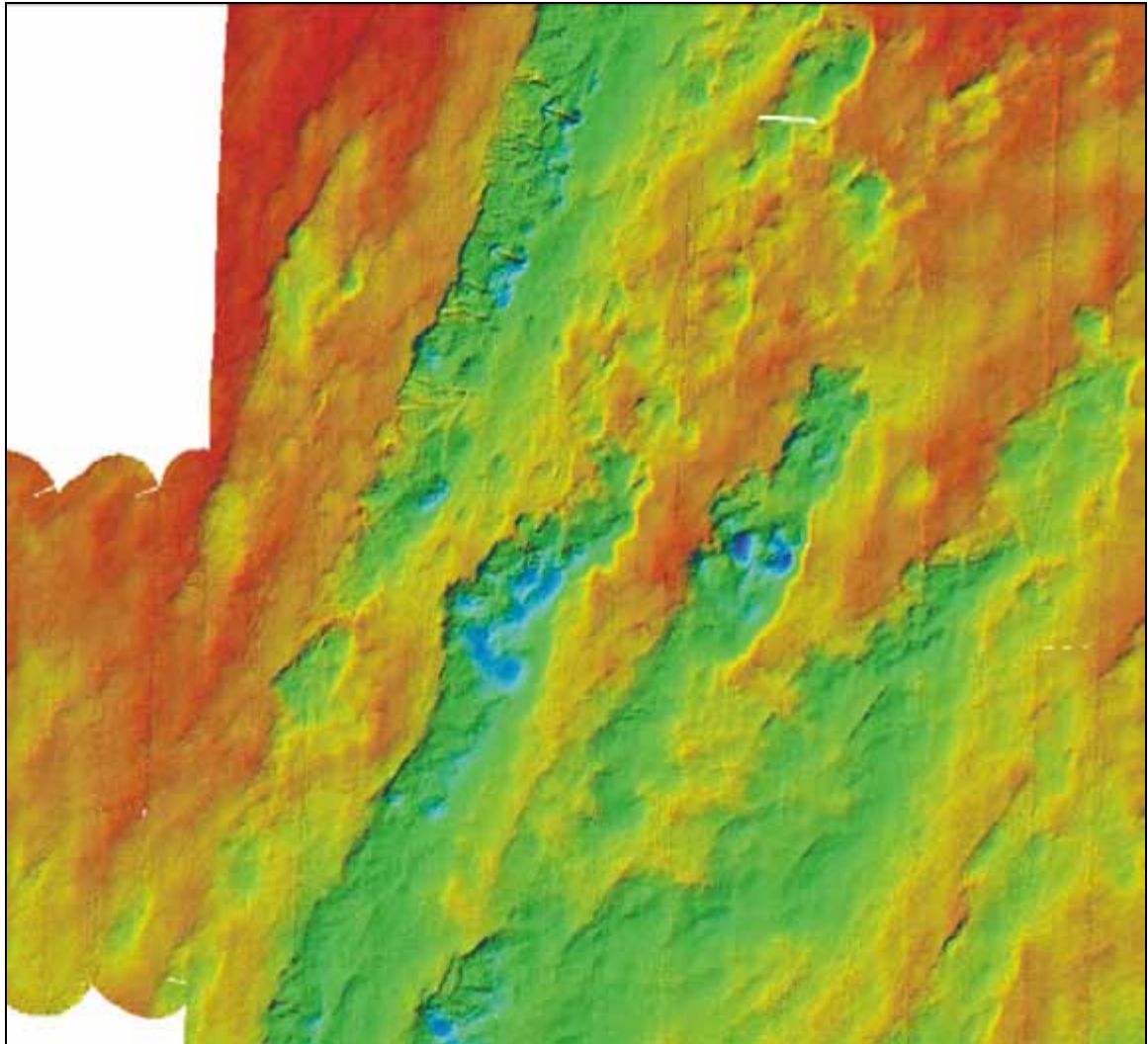
More remotely sensed and ground truthing surveys are required in order to accurately assess the distribution of methane derived authigenic carbonates within the IRL-SEA6 sector. Multibeam and side-scan sonar mapping should be used as a tool for the identification of potential targets for ground-truthing surveys. Video surveys using ROVs equipped with a sampling capability are recommended as the principal ground-truthing method. Further SEM and isotope analysis is recommended in order to fully understand the carbonate precipitation mechanisms.

Figure 9.1 shows the multibeam and sub-bottom profiler coverage in the western Irish Sea acquired as part of the Irish National Seabed Survey up to November 2004. This data should also be examined for gas-related seabed structures.

An intriguing multibeam dataset was recently collected by the SCALLOP project (Project Title: "Stock Assessment of Scallops on the South-East Coast of Ireland"; source of funding: An Bord Iascaigh Mhara (Irish Sea Fisheries Board)) in the southern part of the IRL-SEA6 area (courtesy of Gerry Sutton, CMRC). Figure 9.2 shows part of this multibeam coverage imaging trench-type structures which incorporate localised deeps and transverse sand waves. This area will be further investigated in conjunction with available seismic data to establish whether there is any relationship between the mapped structures and gas escape processes.



**Figure 9.1:** Irish National Seabed Survey multibeam and sub-bottom profiler coverage in the western Irish Sea acquired up to November 2004.



**Figure 9.2:** Fragment of the multibeam data collected by the SCALLOP project (Project Title: "Stock Assessment of Scallops on the South-East Coast of Ireland"; source of funding: An Bord Iascaigh Mhara (Irish Sea Fisheries Board)) in the southern part of the IRL-SEA6 area (courtesy of Gerry Sutton, CMRC).

## **10. References**

- Boe, R., Rise, L., Ottesen, D. (1998) Elongate depressions on the southern slope of the Norwegian Trench (Skagerrak): morphology and evolution. *Marine Geology*, 146, 191-203.
- Boetius, A., Ravenschlag, K., Schubert, C.J., Rickert, D., Widdel, F., Gieseke, A., Amann, R., Jorgensen, B.B., Witte, U., Pfannkuche, O. (2000) A marine microbial consortium apparently mediating anaerobic oxidation of methane. *Nature*, 407, 623-626.
- Britsurvey (1996) Enterprise Oil plc, Site Survey Block 33/22-A Offshore Ireland, 24/06/96-12/07/96, Final Report. (Report released by Petroleum Affairs Division, Dublin)
- Brooks, J.M., Bright, T.J., Bernard, B.B., Schwab, C.R. (1979) Chemical aspects of a brine pool at the East Flower Garden bank, northwestern Gulf of Mexico. *Limnology and Oceanography*, 24, 735-745.
- Corcoran, D, Clayton, G (1999) Interpretation of vitrinite reflectance profiles in the Central Irish Sea area: implications for the timing of organic maturation. *Journal of Petroleum Geology* 22(3), 261-286.
- Croker, P.F. (1994) Shallow gas in the Irish Sea and associated seafloor morphology. Paper presented as poster at 3rd International Conference on Gas in Marine Sediments, Texel, The Netherlands, 25-28 September, 1994.
- Croker, P.F. (1995) Shallow gas accumulation and migration in the western Irish Sea. In: Croker, P.F. & Shannon, P.M. (eds), *The Petroleum Geology of Ireland's Offshore Basins*, Geological Society Special Publication No 93, 41-58.
- Croker, P.F. (1997a) Carbonate-cemented sandstone mounds in the Kish Bank Basin. Oral presentation at the Annual Irish Geological Research Meeting, Queen's University Belfast, February 1997.
- Croker, P.F. (1997b) Lough Beltra Cruise Report - Irish Sea Investigations, 14th to 16th April 1997. Petroleum Affairs Division, Dublin, October 1997.
- Croker, P.F., Garcia-Gil, S., Monteys, X., O'Loughlin, O. (2002) A multibeam survey of the Codling Fault zone, western Irish Sea. Presentation at AIGRM, UCD, February 2002.
- Croker, P.F. & O'Loughlin, O. (1998) Celtic Voyager Cruise Report - Investigation of PB1, PB2, JT and Lambay Deep sites, 23rd April to 26th April 1998. Petroleum Affairs Division, Dublin, November 1998.
- Croker, P.F. & O'Loughlin, O. (1999a) Chirp high-resolution seismic profiling results and radionuclide stratigraphy in the western Irish Sea. (Annual Irish Geological Research Meeting, TCD, February 1999)
- Croker, P.F. & O'Loughlin, O. (1999b) Celtic Voyager Cruise Report - Investigation of Lambay Deep, Codling Fault and UCD/RPII monitoring sites, 10th to 12th June 1999. Petroleum Affairs Division, Dublin, December 1999.
- Croker, P.F. & O'Loughlin, O. (2000) Celtic Voyager Cruise Report - 11th to 13th April 2000. Petroleum Affairs Division, Dublin, May 2000.
- Croker, P.F. & O'Loughlin, O. (2001) Celtic Voyager Cruise Report – 18-19th April, 4-6th May 2001. Petroleum Affairs Division, Dublin, December 2001.
- Croker, P.F. and Power, K.T. (1995) Lough Beltra Cruise Report – Investigation of the Western Trench and Kish Bank Anomaly, Central Irish Sea, 23rd to 25th April 1995. Petroleum Affairs Division, Dublin, June 1995.

- Croker, P.F. and Power, K.T. (1996a) Revising the solid geology map of the western Irish Sea - evidence from shallow gas, seismic, bathymetry, gravity and high-resolution aeromagnetic data. (Annual Irish Geological Research Meeting, University College Dublin, February, 1996)
- Croker, P.F. and Power, K.T. (1996b) Lough Beltra Cruise Report – Investigation of the Western Trench, Central Trench and Kish Bank Anomaly, Central Irish Sea, 23rd to 27th March 1996. Petroleum Affairs Division, Dublin, May 1996.
- Croker, P.F., Whittington, R.J., and Dobson, M.R. (1982) Cardigan Bay (Sheet 52°N-06°W), Solid Geology, (1:250,000 Offshore Map Series). British Geological Survey.
- Cunningham, M.J.M., Phillips, A.W.E. & Densmore, A.L. (2004) Evidence for Cenozoic tectonic deformation in SE Ireland and near offshore. *Tectonics*, 23.
- Dando, P.R. (2001) A review of pockmarks in the UK part of the North Sea, with particular respect to their biology. Technical report produced for Strategic Environmental Assessment SEA2, Department of Trade and Industry, UK. Source: <http://www.offshoresea.org/>
- Dando, P. R., Austen, M. C., Burke, R. J., Kendall, M. A., Kennicutt, M. C., Judd, A. G., Moore, D. C., O'Hara, S. C. M., Schmaljohann, R. & Southward, A. J. (1991) Ecology of a North Sea pockmark with an active methane seep. *Mar. Ecol. Prog. Ser.*, 70, 49-63.
- Dando, P. R., Bussmann, I., Niven, S. J., O'Hara, S. C. M., Schmaljohann, R. & Taylor, L. J. (1994a) A methane seep area in the Skagerrak, the habitat of the Pogonophore, *Siboglinum poseidoni*, and the bivalve mollusc *Thyasira sarsi*. *Marine Ecology Progress Series*, 107, 157-167.
- Dando, P.R. & Hovland, M. (1992) Environmental effects of submarine seeping natural gas. *Continental Shelf Research*, 12, 1197-1207.
- Dando, P.R., O'Hara, S.C.M, Schuster, U., Taylor, L.J., Clayton, C.J., Baylis, S., Laier, T. (1994b) Gas seepage from a carbonate-cemented sandstone reef on the Kattegat coast of Denmark. *Marine and Petroleum Geology*, 11, 2, 182-189.
- Davis, A.M. (1992) Shallow gas: an overview. *Continental Shelf Research*, 12, 1077-1079.
- Dobson, M.R. & Whittington, R.J. (1979) The geology of the Kish Bank. *J. Geol. Soc. London*, 136, 243-249.
- Dunford, G.M., Dancer, P.N., Long, K.D. (2001) Hydrocarbon potential of the Kish Bank Basin: Integration within a regional model for the greater Irish Sea Basin. In: Shannon, P.M., Haughton, P.D.W. & Corcoran, D.V. (eds) *The Petroleum Exploration of Ireland's Offshore Basins*. Geological Society, London, Special Publications, 188, 135-154.
- European Commission (1997) Council Directive 97/62/EC of 27 October 1997 adapting to technical and scientific progress Directive 92/43/EEC on the conservation of natural habitats and of wild fauna and flora. *Official Journal L305* (8.11.1997), 42-65.
- Faber, E. & Stahl, W. (1984) Geochemical surface exploration for hydrocarbons in the North Sea. *American Association of Petroleum Geologists (Bulletin)*, 68, 363-386.
- Fannin, N.G.T. (1980) The use of regional geological surveys in the North Sea and adjacent areas in the recognition of offshore hazards. In: *Offshore site investigation*. Ards, D.A. (ed), Graham and Trotman, London, pp. 5-21.
- Floodgate, G.D. & Judd, A.G. (1992) The origins of shallow gas. *Continental Shelf Research*, 12, 1145-1156.

- Floodpage, J., Newman, P. & White, J. (2001) Hydrocarbon prospectivity in the Irish Sea area: insights from recent exploration of the Central Irish Sea, Peel and Solway basins. In: Shannon, P.M., Haughton, P.D.W. & Corcoran, D.V. (eds) *The Petroleum Exploration of Ireland's Offshore Basins*. Geological Society, London, Special Publications, 188, 107-134.
- Flügel, H.J. and Langhof, I. (1983) A new hermaphroditic pogonophore from the Skagerrak. *Sarsia*, 68, 131-138.
- García-Gil, S., Vilas, F. & García-García, A. (2002) Shallow gas features in incised-valley fills (Ría de Vigo, NW Spain): a case study. *Continental Shelf Research*, 22, 2303-2315.
- Grant, A.C., Levy, E.M., Lee, K., Moffat, J.D. (1986) Pisces IV research submersible finds oil on Baffin Shelf. *Current Research of the Geological Survey of Canada*, Part A, 65-69.
- Green, P.F., Duddy, I.R., Bray, R.J., Duncan, W.I. & Corcoran, D.V. (2001) The influence of thermal history on hydrocarbon prospectivity in the Central Irish Sea Basin. In: Shannon, P.M., Haughton, P.D.W. & Corcoran, D.V. (eds) *The Petroleum Exploration of Ireland's Offshore Basins*. Geological Society, London, Special Publications, 188, 171-188.
- Hatton, R. (1997) Seabed geochemical survey, blocks 33/16, 33/17, 33/18 & 33/22, offshore Ireland, final interpretation report prepared for Enterprise Oil plc.
- Hovland, M. (1990) Suspected gas-associated clay diapirism on the seabed off Mid Norway. *Marine and Petroleum Geology*, 7, 267-276.
- Hovland, M. (1992) Pockmarks and gas-charged sediments in the eastern Skagerrak. *Continental Shelf Research*, 12, 1111-1119.
- Hovland, M. (1993) Submarine gas seepage in the North Sea and adjacent areas. In: Parker, J.R. (ed.) *Petroleum Geology of Northwest Europe: Proceedings of the 4th Conference*. The Geological Society, London, 1333-1338.
- Hovland, M. (2002) On the self-sealing nature of marine seeps. *Continental Shelf Research*, 22, 2387-2394.
- Hovland, M. & Curzi, A.G. (1989) Gas seepage and assumed mud diapirism in the Italian central Adriatic Sea. *Marine and Petroleum Geology*, 6, 161-169.
- Hovland, M., Gardner, J.V. & Judd, A.G. (2003) The significance of pockmarks to understanding fluid flow processes and geohazards. *Geofluids* 2 (2), 127-136.
- Hovland, M., & Judd, A. (1988) Seabed pockmarks and seepages: impact on geology, biology, and the marine environment. *Graham & Trotman*, London, 293pp.
- Hovland, M., & Judd, A.G. (1992) The global production of methane from shallow submarine sources. *Continental Shelf Research*, 12, 1231-1238.
- Hovland, M. & Thomsen, E. (1989) Hydrocarbon-based communities in the North Sea? *Sarsia*, 74, 29-40.
- Izatt, C., Maingarm, S. & Racey, A. (2001) Fault distribution and timing in the Central Irish Sea Basin. In: Shannon, P.M., Haughton, P.D.W. & Corcoran, D.V. (eds) *The Petroleum Exploration of Ireland's Offshore Basins*. Geological Society, London, Special Publications, 188, 155-169.
- Jackson, D.I., Jackson, A.A., Evans, D., Wingfield, R.T.R., Barnes, R.P., Arthur, M.J. (1995) *The geology of the Irish Sea: United Kingdom Offshore Regional Report*. HMSO, London.
- Jackson, D.I. & Mulholland, P. (1993) Tectonic and stratigraphic aspects of the East Irish Sea Basin and adjacent areas: contrasts in their post-Carboniferous structural styles. In: Parker, J.R. (ed.) *Petroleum Geology of Northwest Europe: Proceedings of the 4th Conference*. The Geological Society, London, 791-808.

- Jacob, A.W.B. (1993) Seismic hazard in Ireland. In: The practice of earthquake hazard assessment. (ed: McGuire, R.K.) International Association of Seismology and Physics of the Earth's Interior and European Seismological Commission, 150-152.
- James, J.W.C. (1988) Cardigan Bay (Sheet 52°N-06°W), Sea Bed Sediments, (1:250,000 Offshore Map Series). British Geological Survey.
- James, J.W.C. (1990) Anglesey (Sheet 53°N-06°W), Sea Bed Sediments, (1:250,000 Offshore Map Series). British Geological Survey.
- Jenner, J.K. (1981) The structure and stratigraphy of the Kish Bank Basin. In: Illing, L.V. & Hobson, G.D. (eds) Petroleum Geology of the Continental Shelf of North-West Europe. Heyden & Son Ltd, London, 426-431.
- Jones, G.B., Floodgate, G.D. & Bennell, J.D. (1986) Chemical and microbiological aspects of acoustically turbid sediments: preliminary investigations. Marine Geotechnology, 6, 315-332.
- Jørgensen, N.O. (1992) Methane-derived carbonate cementation of Holocene marine sediments from Kattegat, Denmark. Continental Shelf Research, 12, 1209-1218.
- Judd, A.G. (2001) Pockmarks in the UK sector of the North Sea. Technical report produced for Strategic Environmental Assessment SEA2. Department of Trade and Industry, UK. Source: <http://www.offshoresea.org/>
- Judd, A.G. (2005) The distribution and extent of 'submarine structures formed by leaking gas': SEA6 Strategic Environmental Assessment of the Irish Sea. Department of Trade and Industry, UK.
- Judd, A.G. & Hovland, M. (1992) The evidence of shallow gas in marine sediments. Continental Shelf Research, 12, 1081-1095.
- Maddox, S.J., Blow, R. & Hardman, M. (1995) Hydrocarbon prospectivity of the Central Irish Sea Basin with reference to Block 42/12, offshore Ireland. In: Croker, P.F. & Shannon, P.M. (eds), The Petroleum Geology of Ireland's Offshore Basins, Geological Society Special Publication No 93, 57-77.
- Maingarm, S., Izatt, C., Whittington, R.J., Fitches, W.R. (1999) Tectonic evolution of the Southern-Central Irish Sea Basin. Journal of Petroleum Geology 22(3), 287-304.
- Marathon Oil U.K., Ltd. (2004) Dragon Appraisal Well in Block 103/1. Early Consultation Document, November 2004.
- Martindale, W., Dobson, M.R. & Whittington, R.J. (1982) Anglesey (Sheet 53°N-06°W), Solid Geology, (1:250,000 Offshore Map Series). British Geological Survey.
- Masson, D.G., Bett, B.J., Billett, D.S.M., Jacobs, C.L., Wheeler, A.J., Wynn, R.B. (2003) The origin of deep-water, coral-topped mounds in the northern Rockall Trough, Northeast Atlantic. Marine Geology, 194, 159-180.
- Mitchell, P.I., Condren, O.M., Vintro, L.L., McMahon, C.A. (1999) Trends in plutonium, americium and radiocaesium accumulation and long-term bioavailability in the western Irish Sea mud basin. Journal of Environmental Radioactivity 44(3), 223-251.
- Naylor, D., Haughey, N., Clayton, G. & Graham, J.R. (1993) The Kish Bank Basin, offshore Ireland. In: Parker, J.R. (ed.) Petroleum Geology of Northwest Europe: Proceedings of the 4th Conference. The Geological Society, London, 845-855.
- Naylor, D. & Shannon, P.M. (1982) Geology of offshore Ireland and West Britain. Graham & Trotman Ltd., London, 161pp.
- Orford, J.D. (1988) A review of tides, currents and waves in the Irish Sea. In: Sweeney, J.C. (ed) The Irish Sea: A Resource at Risk. Geographical Society of Ireland Special Publications No. 3.
- Premchitt, J., Rad, N.S., To, P., Shaw, R. and James, J.W.C. (1992) A study of gas in marine sediments in Hong Kong. Continental Shelf Research, 12, 1251-1264.

- Ransome, C.R. (1982) Isle of Man (Sheet 54N 06W), Solid Geology, (1:250,000 Offshore Map Series). British Geological Survey.
- Readman, P.W., O'Reilly, B.M., Edwards, J.W.F. & Sankey, M.J. (1995) A gravity map of Ireland and surrounding waters. In: Croker, P.F. & Shannon, P.M. (eds), The Petroleum Geology of Ireland's Offshore Basins, Geological Society London Special Publication No 93, 9-16.
- Schmaljohann, R. and Flugel, H. (1987) Methane oxidising bacteria in Pogonophora. *Sarsia*, 72, 91-98.
- Schoell, M. (1980) The hydrocarbon and carbon isotope composition of methane from natural gases of various origins. *Geochemica et Cosmochimica Acta*, 44, 649-662.
- Schubel, J.R. (1974) Gas bubbles and the acoustically impermeable or turbid character of some estuarine sediments. In: Natural gases in marine sediments, I.R. Kaplan (ed), Plenum Press, New York, 324pp.
- Söderberg, P. & Flodén, T. (1992) Gas seepages, gas eruptions and degassing structures in the seafloor along the Strömman tectonic lineament in the crystalline Stockholm Archipelago, east Sweden. *Continental Shelf Research*, 12, 1157-1171.
- Southward, E.C. (1987) Contribution of symbiotic chemoautotrophs to the nutrition of benthic invertebrates. In: Sletgh, M. (ed). *Microbes in the sea*. Ellis Horwood Ltd, Chichester, 83-118.
- Spies, R.B. and Davis, P.H. (1979) The infaunal benthos of a natural oil seep in the Santa Barbara Channel. *Marine Biology*, 50, 227-237.
- Tappin, D.R. and Croker, P.F. (1999) New South Irish Sea geology map. In: "The Petroleum Exploration of Ireland's Offshore Basins" conference, Dublin, 29-30th April, 1999: Extended Abstracts. (Eds: Croker, P.F.; O'Loughlin, O.), 188.
- Taylor, D.I. (1992) Nearshore shallow gas around the U.K. coast. *Continental Shelf Research*, 12, 1135-1144.
- Wheeler, A. J., Walshe, J. & Sutton, G.D. (2001) Seabed Mapping and Seafloor Processes in the Kish, Burford, Bray and Fraser Banks Area, Southwestern Irish Sea. *Irish Geography*, 34(2), 194-211.
- Whiticar, M.J. (1999) Carbon and hydrogen isotope systematics of bacterial formation and oxidation of methane. *Chemical Geology*, 161, 291-314.
- Whiticar, M.J. (2002) Diagenetic relationships of methanogenesis, nutrients, acoustic turbidity, pockmarks and freshwater seepages in Eckenförde Bay. *Marine Geology*, 182, 29-53.
- Wingfield, R.T.R. (1987) Giant sand waves and relict periglacial features on the sea bed west of Anglesey. *Proceedings of the Geologists' Association* 98(4), 400-404.
- Wingfield, R.T.R., Hession, M.A. & Whittington, R.J. (1990a) Anglesey (Sheet 53°N-06°W), Quaternary Geology, (1:250,000 Offshore Map Series). British Geological Survey.
- Wingfield, R.T.R., Hession, M.A. & Whittington, R.J. (1990b) Cardigan Bay (Sheet 52°N-06°W), Quaternary Geology, (1:250,000 Offshore Map Series). British Geological Survey.
- Yuan, F., Bennell, J. D., Davis, A.M. (1992) Acoustic and physical characteristics of gassy sediments in the western Irish Sea. *Continental Shelf Research*, 12, 1121-1134.